

THE
BEARING CAPACITY AND SETTLEMENT
OF
GRAVEL PILES IN CLAY

A Thesis presented to the
DEPARTMENT OF CIVIL ENGINEERING
UNIVERSITY OF CAPE TOWN

In partial fulfilment of the requirements for the
degree of Master of Science in Engineering.

by

D. L. JONES

1980

The University of Cape Town has been given
the right to reproduce this thesis in whole
or in part. Copyright is held by the author.

The copyright of this thesis vests in the author. No quotation from it or information derived from it is to be published without full acknowledgement of the source. The thesis is to be used for private study or non-commercial research purposes only.

Published by the University of Cape Town (UCT) in terms of the non-exclusive license granted to UCT by the author.

DECLARATION

The writer hereby declares the following work, with the exception of quoted sources, is his own work and has not been submitted to any other university.

Signed by candidate

D. L. Jones.

The writer has successfully completed course work to the value of 32 credits towards the M.Sc. degree. This thesis therefore represents approximately 1/4 of the requirements for the degree.

ACKNOWLEDGEMENTS

The writer wishes to express his appreciation to the following individuals for their assistance in the preparation of this thesis. Professor A.D.W. Sparks is to be thanked for his guidance and numerous helpful suggestions made during the course of this study.

The writer also wishes to thank Debbie Lewis for tracing the various diagrams and to Robert Leslie and Partners for the use of triaxial equipment at their laboratory. Finally, the writer is indebted to his wife for undertaking all the typing.

CONTENTS

	<u>Page</u>
Chapter 1 : Thesis outline	1.1
1.1 Introduction	1.1
1.2 Aims of thesis	1.1
1.3 Chapter summary	1.2
Chapter 2: Historical background & uses of gravel piles	2.1
2.1 Introduction	2.1
2.2 Historical development	2.1
2.3 Column formation	2.4
2.4 Column performance	2.4
2.5 Summary	2.5
Chapter 3: Consolidation theory	3.1
3.1 Summary	3.1
3.2 The three dimensional theory of Biot & Terzaghi	3.1
3.3 Derivation of Terzaghi's three dimensional equations.	3.3
3.4 The finite difference method of solving the consolidation equation.	3.7
3.5 Rate of consolidation	3.9
3.6 Drain wells	3.9
3.7 Smear zone	3.10
3.8 Summary	3.10
Chapter 4: Stress-strain properties of sand	4.1
4.1 Introduction	4.1
4.2 Particulate and continuum systems for soils	4.1
4.3 Failure criteria	4.1
4.4 Stress-strain relationship	4.4
4.5 Non-linearity in soils	4.4
4.6 Friction angle	4.7

4.7	Stress dilatancy	4.8
4.8	Summary	4.13
Chapter 5: Critical state theory		5.1
5.1	Introduction	5.1
5.2	The normal consolidation line	5.1
5.3	The critical state line	5.3
5.4	The Roscoe surface	5.3
5.5	The Hvorslev surface	5.4
5.6	Cam-clay model	5.4
5.7	Comparisons with other failure criteria	5.6
5.8	Other non-linear methods	5.7
5.9	Summary	5.7
Chapter 6: Laboratory testing of sands		6.1
6.1	Introduction	6.1
6.2	Testing methods	6.1
6.3	Stress-strain curves	6.5
6.4	Stress paths and friction angles	6.9
6.5	Influence of void ratio	6.11
6.6	Radial strain	6.14
6.7	Radial stress	6.14
6.8	Non-dimensional relationships between stress and strain	6.17
6.9	Summary	6.20
Chapter 7: The interaction of a raft-pile system		7.1
7.1	Introduction	7.1
7.2	Rigid design method	7.1
7.3	Simplified elastic method	7.2
7.4	Truly elastic foundation	7.2
7.5	Raft and gravel piles	7.3
7.6	Influence of the structure	7.3
7.7	Summary	7.3

Chapter 8: Current design practice	8.1
8.1 Introduction	8.1
8.2 Earth pressure method	8.1
8.3 Pressuremeter analogy	8.3
8.4 Elastic design method	8.7
8.5 Summary	8.13
Chapter 9: Alternative design method based upon model tests	9.1
9.1 Introduction	9.1
9.2 Ultimate column load	9.1
9.3 Load-settlement relationship	9.2
9.4 Time-settlement relationship	9.5
9.5 Design method using Cam-clay theory	9.8
9.6 Summary	9.8
Chapter 10: Conclusion	10.1
10.1 Introduction	10.1
10.2 Achievement of objectives	10.1
10.3 Developed interests	10.2
References	i
Appendix	ix

CHAPTER 1

THESIS OUTLINE

1.1 INTRODUCTION

The purpose of this chapter is to explain why the topic was chosen and to briefly outline each chapter.

1.2 AIMS OF THESIS

The writer has been interested in the subject of gravel piles for a number of years and has been surprised at the lack of rational design methods. When the piles are inserted in sand their purpose is mainly one of densification and their effectiveness is usually measured by a Dutch Cone Penetrometer with an increase in cone resistance as the sand is densified. For clays the above method is clearly not applicable and a conservative approach has generally been adopted with regard to the pile length and spacing.

There appears to be only one paper which is often quoted as a design method (Hughes and Withers 1974) and at least one contractor used this method as a basis for design (Cementation 1977). The State of the Art was advanced in 1976 when a symposium on ground treatment was held. Again the basic design philosophy adopted was that of Hughes and Withers, and numerous case histories appeared to back up the design approach.

The writer was therefore interested in formulating a new design method which could act as a check on the traditional method. Also, it was felt that an understanding of the stress-strain behaviour of the pile was needed to fully appreciate the implications of any design method. However, prior to the submission of the thesis the writer was made aware of work undertaken in Australia (Balaam and Booker 1979) which used elastic methods to establish the stress-strain behaviour of a pile. This approach is valuable as the sensitivity of design to various parameter changes can quickly be checked by reference to the numerous graphs presented. As this work is little known the relevant graphs have

been reproduced in Ch. 8 of this thesis.

It is intended that this thesis will act as a concise guide to column behaviour and design, as well as to the uses to which they may be put. Also, a new design method is proposed which has been developed from a basic understanding of the stress-strain behaviour of a pile. The sequential approach used in developing this thesis is outlined in the next section.

1.3

CHAPTER SUMMARY

Chapter 2:- traces the developments of gravel piles and the uses to which they have been put. The mode of formation is also discussed.

Chapter 3 - deals with three-dimensional consolidation and compares the theories of Biot and Terzaghi. That due to Terzaghi is derived from first principles. Methods of solving the equations are also given.

Chapter 4 - looks at the stress-strain properties of sands. Various failure criteria are examined as well as such aspects as non-linearity, stress dilatancy and the influence of void ratio. The chapter serves as a guide to results expected during laboratory testing.

Chapter 5 - briefly examines some aspects of critical state theory. The main purpose of the chapter is to show the inter-relationship between such variables as stresses, strains and void ratio.

Chapter 6 - lists the various laboratory tests undertaken on sands and gravels. The results obtained are used to formulate a new design method as detailed in Chapter 9.

Chapter 7 - is intended to show the complex relationship that exists between a raft-pile-soil system. The subject is not dealt with in depth, but should be sufficient to make the reader aware of the complexities involved.

Chapter 8 - can be considered as a State of the Art chapter and outlines three design methods which can be used for gravel piles.

Chapter 9 - presents a new design method based largely upon the laboratory testing as described in Chapter 6.

Chapter 10 - concludes the thesis and states what benefit the writer has gained in undertaking this work.

CHAPTER 2

HISTORICAL BACKGROUND AND USES OF GRAVEL PILES

2.1 INTRODUCTION

Gravel piles or stone columns have been used to improve the bearing capacity and settlement characteristics of land fill, sands and clays. The columns consist of compacted granular material introduced into the ground by large vibrating pokers or the tamping effect of a heavy weight.

This chapter deals with the history and development of stone columns and the uses to which they have been employed. Comment is also made on the efficiency of such columns and current thinking on the usefulness of columns.

2.2 HISTORICAL DEVELOPMENT

The first recorded use of stone columns for the reinforcing of ground occurred in 1830 (Hughes and Withers 1974). The columns were used to reduce the settlements of foundations at an artillery arsenal in Bayonne, France. The columns were constructed by driving stakes into the soft estuarine deposits. These were then withdrawn and the hole backfilled with crushed limestone. It is reported that the columns, which supported a load of 10 kN each, reduced the anticipated settlements by a factor of four.

There are two principle methods of forming stone columns, one being with a powerful vibrator termed a vibroflot and the other by punching stone into the ground by dropping a heavy weight.

In the 1930's in Germany the firm of Johann Keller developed the technique which is now known as vibroflotation (Keller 1967) and in 1937 Keller carried out vibroflotation for a building in Berlin on 7.5m depth of loose sand (Greenwood 1976). The process involved the in-situ compaction of the ground to form compacted sand columns. The surrounding soil provided the backfill for the crater formed during the compaction process.

Compaction of sand by vibroflotation continued and led to the development of various other methods such as the Terra-Probe for the compaction of sands (Brown and Glenn (1970), James (1973)). A State of the Art of various methods of treating foundations is given by Mitchell (1970) for which various systems can be compared, whilst an exercise comparing the merits of vibroflotation and compaction piles was carried out by Basoro and Boitano (1969).

Once experience had been gained in the compaction of sands the field of application expanded from pure sands through to stiff sands and clayey sands. (Grimes and Cantley (1965), Greenwood (1965)). In South Africa the technique became widely used in the Durban area, notably for the sugar industry (Anon 1965, 1964). In Durban the soil treated typically consisted of three types, fine sand with up to 10% clay, fine silty sands with 10% to 20% clay and clayey sands containing 20% to 30% clay. (Webb and Hall 1969). During the execution of such work it was found that best results were obtained if the backfill consisted of material having a coarser grain size than that of the ground being treated. Stone columns were thus being used in sands.

Vibroflotation does not densify a clay as it does a sand, due to the damping effect of the clay. However, compacted stone columns can be introduced into the ground by use of the vibroflot machine in a process known as vibro-replacement (see 2.3). Many examples exist in the literature of their use which range from treatment of ground for oil tanks (Anon 1965, Bratchell, Leggatt and Simons 1975) to the stabilization of earth embankments (Cementation 1977, McKenna, Eyre and Wolstenhome 1976).

As an alternative to the formation of columns by vibroflotation the dynamic consolidation method has also been used (Kruger et al, 1980, Menard 1979). In a process known as dynamic substitution stone columns were punched into the ground by dropping a weight on to selected ground. The process was used to stabilize the foundation of an embankment for a freeway to be built on compressible subsoil.

In Sweden instead of forming stone columns use is made of lime

THE FORMATION OF STONE COLUMNS BY THE
VIBRO - REPLACEMENT PROCESS

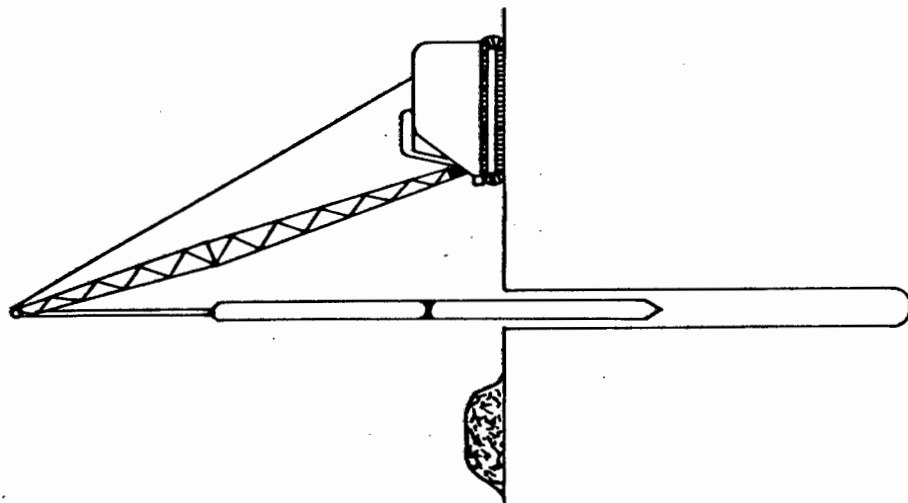


FIG. 2.1 FORMATION OF HOLE

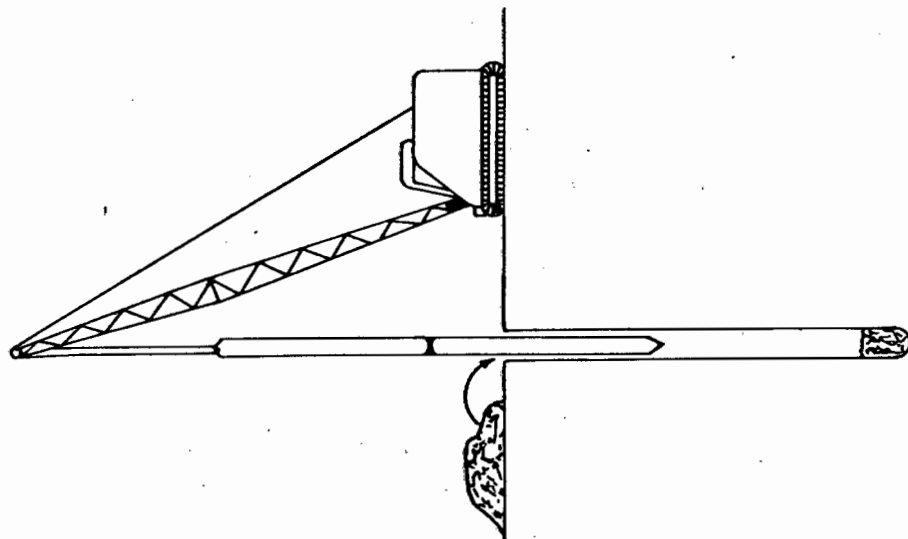


FIG. 2.2 INFILLING OF HOLE

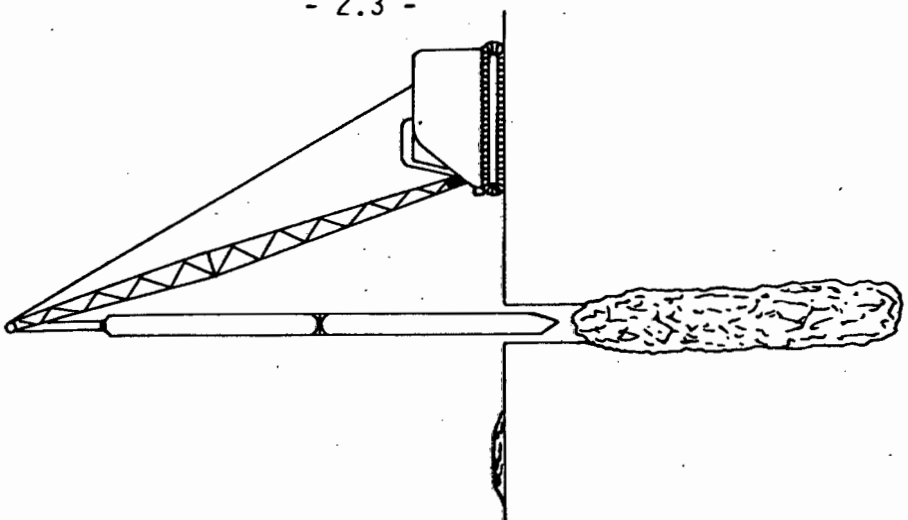


FIG. 2.3 COMPACTION OF HOLE

to form lime columns (Browns and Boman 1979), in which the powdered unslaked lime is mixed in situ with soft clay using an auger to form columns up to 10,0m long. The design principles used appear to be similar to that used for stone columns as well as to the claims for increased bearing capacity and reduction in settlement.

2.3 COLUMN FORMATION

The formation of a stone column by the vibro-replacement process can be seen in the diagrams (Fig. 2.1, 2.2 and 2.3). The vibroflot is essentially a long thin walled steel tube which is suspended from a crane. The tube contains a set of eccentric weights and a drive motor to produce the vibrations which are frequently of the order of 50 Hertz. Water or air can be jetted out of the tube and so assist in the penetration into the ground.

In Figure 2.1 the vibrator is lowered into the ground and radially displaces the surrounding soil. The water jetting is not needed in soft clays but is used in sand to liquefy the ground and so enable the vibrator to penetrate under its own weight. When the vibrator is removed the hole remains open. A stone backfill is poured into the hole and by a surging action of the vibrator the stone is displaced both radially and downwards into the soil until a maximum compaction of the stone is achieved. This process is continued until the column reaches the surface.

2.4 COLUMN PERFORMANCE

As detailed in later sections, a loaded column bulges and develops the passive resistance of the soil for its support. Also, the columns act as large sand drains and hasten the consolidation of the soil. (Typical bearing volumes for columns in clay are 150 kN/m^2). However, it has been suggested that the actual improvement of the ground by the introduction of the columns is not as great as made out in the technical literature. The reasons are that the action of the vibroflot can cause considerable remoulding of the soil which results in lower shear strengths as well as pro-

ducing a smear zone around the column so causing a reduction in the efficiency of such columns as sand drains.

2.5

SUMMARY

1. Stone columns have been used since 1830, but it is only since the 1930's that the techniques used today were developed.
2. Stone columns have been used for a variety of foundation problems as well as stabilizing earth embankments.
3. Columns are generally formed by the process of vibro-replacement, although dynamic techniques also exist.
4. Typical column loads are 150 kN/m^2 .

CHAPTER 3

CONSOLIDATION THEORY

3.1 SUMMARY

It has long been recognised that both the rate and amount of settlement predicted by conventional laboratory tests differs from that actually occurring in practice. The reason is that a lateral as well as vertical pore pressure dissipation occurs. This is particularly so if vertical sand drains, or gravel piles, are used which have the effect of rapidly increasing the rate of settlement. The one dimensional consolidation theory is clearly not applicable to such a case.

This chapter derives the three dimensional equations of consolidation as proposed by Terzaghi and compares it with the more mathematically correct method of Biot. The equations can be solved by using finite difference methods which are especially useful for irregular boundary conditions. Alternatively, it is perhaps quicker and easier to use the consolidation curves derived by Barron.

3.2 THE THREE DIMENSIONAL THEORIES OF BIOT AND TERZAGHI.

Terzaghi has shown that one dimensional consolidation is governed by the following relationship:

$$\frac{\partial u}{\partial t} = C_v \frac{\partial^2 u}{\partial z^2} \quad (3.1)$$

However, in practice it is found that the rate of consolidation is usually greater than that derived from the above eqn. Horizontal as well as vertical pore pressure distribution must therefore have taken place. This has been established by field trials in which differing coefficients of consolidation have been measured in the horizontal and vertical directions (Murray 1976).

A more realistic approach would therefore be to use a three dimensional method. This is especially so for gravel piles and

sand drains where the horizontal drainage is greater than the vertical drainage.

Three dimensional theories for consolidation have been developed by both Terzaghi (1925, 1944) and Biot (1941). That due to Terzaghi is a simple diffusion approach later developed by Rendulic (1936) and an extension of the one dimensional theory, whilst that of Biot relates displacements to pore water pressures.

A comparison of the two theories has been carried out by Cryer (1963) who shows that for a sphere of soil hydrostatically loaded the two theories predict qualitatively similar volume changes, but the prediction for the water pressure at the centre of the sphere differ considerably. Terzaghi's theory predicts that the water pressure will initially decrease, while the Biot theory predicts that the water pressure will increase initially. The pore pressure rise has been termed the Mandel-Cryer effect after Mandel (1957) and Cryer (1963) and experiments have confirmed that the effect does occur for over-consolidated soils. For this reason it has been deemed more accurate to use the equations due to Biot (Christian 1977, Davis and Poulos 1972, Barron 1972); although it is mathematically more complex. For most purposes however, the diffusion approach based upon the Terzaghi-Rendulic equations has proved adequate (Gibson and McNamee 1963, Murray 1974).

3.3

DERIVATION OF TERZAGHI'S THREE DIMENSIONAL EQUATIONS.

In deriving the three dimensional equations of consolidation the same basic assumptions as the one dimensional case apply, viz:

1. The soil is fully saturated.
2. The water and soil particles are incompressible.
3. The volume change is small compared with the initial volume of the soil.
4. Darcy's law is valid and can be extended to anisotropic soils.

5. The permeabilities k_x , k_y and k_z are constant over the relevant ranges of effective stress in each direction.

Consider the element as shown in Fig. 3.1, where the flow has different velocities in the x , y and z directions. Thus v_x , v_y and v_z are the velocity components at $dx/2$, $dy/2$ and $dz/2$ from the point with coordinates x , y , z .

The flow per unit of time into the element is:

$$q = \left\{ v_x - \frac{\partial v_x}{\partial x} \frac{dx}{2} \right\} dy dz + \left\{ v_y - \frac{\partial v_y}{\partial y} \frac{dy}{2} \right\} dx dz + \left\{ v_z - \frac{\partial v_z}{\partial z} \frac{dz}{2} \right\} dx dy \quad (3.2)$$

and flow out of the element is:

$$q' = \left\{ v_x + \frac{\partial v_x}{\partial x} \frac{dx}{2} \right\} dy dz + \left\{ v_y + \frac{\partial v_y}{\partial y} \frac{dy}{2} \right\} dx dz + \left\{ v_z + \frac{\partial v_z}{\partial z} \frac{dz}{2} \right\} dx dz \quad (3.3)$$

The change of volume is the difference between the flow into and out of the element, $q' - q$.

As the volume change is small:

$$\frac{\partial V}{\partial t} = \left\{ \frac{\partial v_x}{\partial x} + \frac{\partial v_y}{\partial y} + \frac{\partial v_z}{\partial z} \right\} dx dy dz \quad (3.4)$$

If V_s = total volume of the solid particles

V = volume of soil

e = void ratio

$$\text{then } V = V_s(1 + e) = dx dy dz \quad (3.5)$$

Differentiating with respect to t gives :

$$\frac{\partial V}{\partial t} = V_s \frac{\partial e}{\partial t} \quad (3.6)$$

$$\text{Now, } V_s = \text{constant} = \frac{1}{1+e} dx dy dz \quad (3.7)$$

Thus, combining eqns. (3.6) and (3.7), the rate of volume change is:

$$\frac{\partial V}{\partial t} = \frac{1}{1+e} \frac{\partial e}{\partial t} dx dy dz \quad (3.8)$$

Equating eqna. (3.4) and (3.8):

$$\frac{\partial e}{\partial t} = \{ (1+e) \left(\frac{\partial v_x}{\partial x} + \frac{\partial v_y}{\partial y} + \frac{\partial v_z}{\partial z} \right) \} \quad (3.9)$$

From the assumption that Darcy's law is valid for anisotropic soils:

$$v_x = \frac{k_x}{\gamma_w} \frac{\partial u}{\partial x}$$

$$v_y = \frac{k_y}{\gamma_w} \frac{\partial u}{\partial y} \quad (3.10)$$

$$v_z = \frac{k_z}{\gamma_w} \frac{\partial u}{\partial z}$$

Differentiating eqn. (3.10) with respect to x, y and z and substituting in eqn. (3.9) gives:

$$\frac{\partial e}{\partial t} = \frac{(1+e)}{\gamma_w} \left\{ k_x \frac{\partial^2 u}{\partial x^2} + k_y \frac{\partial^2 u}{\partial y^2} + k_z \frac{\partial^2 u}{\partial z^2} \right\} \quad (3.11)$$

$$\text{Now, } \sigma_0' + \mu_0 = \sigma_0 + \mu$$

$$\text{or } \sigma' = \sigma_0' + \mu_0 - \mu \quad (3.12)$$

where σ_0' is the initial value of effective stress

σ' is the effective stress at time t

μ is the neutral stress at time t

If a total stress increment is applied instantaneously, μ_0 is independent of time.

Differentiating eqn. (3.12) with respect to t gives:

$$\frac{\partial \sigma'}{\partial t} = - \frac{\partial \mu}{\partial t} \quad (3.13)$$

As an increase in σ will give rise to an equal decrease in μ :

$$\frac{\partial e}{\partial \sigma'} = - \frac{\partial e}{\partial \mu} \quad (3.14)$$

$$\text{Also, } a_v = m_v (1 + e) = - \frac{\partial e}{\partial \sigma'}$$

where a_v = coefficient of compressibility

m_v = coefficient of volume change.

and substituting into eqn. (3.14) :

$$a_v = \frac{\partial e}{\partial \mu}$$

$$\text{Since } \frac{\partial e}{\partial t} = \frac{\partial e}{\partial \mu} \frac{\partial \mu}{\partial t} \quad (3.15)$$

$$\text{then } \frac{\partial e}{\partial t} = a_v \frac{\partial \mu}{\partial t} = m_v (1 + e) \frac{\partial \mu}{\partial t} \quad (3.16)$$

Combining eqns. (3.11) and (3.16) gives:

$$\frac{\partial \mu}{\partial t} = \frac{1}{m_v \gamma_w} \left\{ k_x \frac{\partial^2 \mu}{\partial x^2} + k_y \frac{\partial^2 \mu}{\partial y^2} + k_z \frac{\partial^2 \mu}{\partial z^2} \right\} \quad (3.17)$$

Replacing $\frac{k}{m_v \gamma_w}$ by the coefficient of consolidation C_v gives:

$$\frac{\partial \mu}{\partial t} = C_{vx} \frac{\partial^2 \mu}{\partial x^2} + C_{vy} \frac{\partial^2 \mu}{\partial y^2} + C_{vz} \frac{\partial^2 \mu}{\partial z^2} \quad (3.18)$$

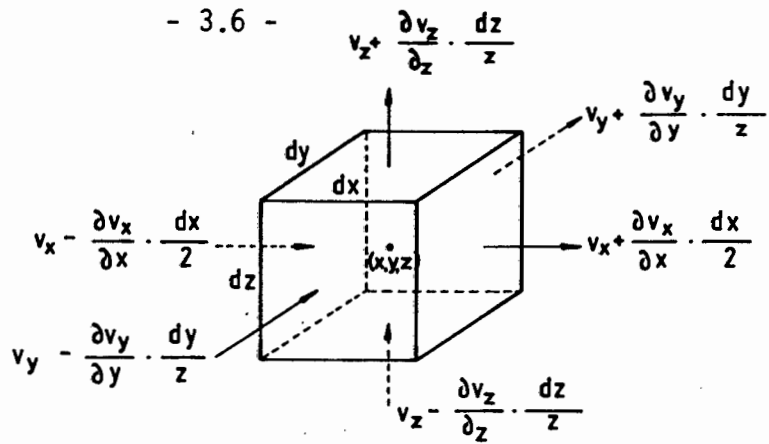


FIG. 3.1 SEEPAGE VELOCITIES ON THE SIDES OF AN ELEMENTAL CUBE

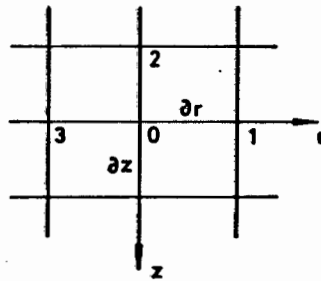


FIG. 3.2 FINITE DIFFERENCE NETWORK FOR CYLINDRICAL CO-ORDINATES

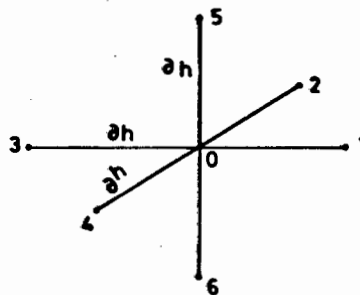


FIG. 3.3 FINITE DIFFERENCE NETWORK FOR CARTESIAN CO-ORDINATES

3.4

THE FINITE DIFFERENCE METHOD OF SOLVING THE CONSOLIDATION EQUATION.

The consolidation equations of Biot are more readily solved using finite element methods, whilst that due to Terzaghi readily lends itself to a solution by finite differences (Gibson and Lumb 1953). For a gravel pile the domain of influence can be considered to be circular (Balaam and Booker 1979) and can be likened to a cylinder permitted to drain freely from all its surfaces.

Eqn. (3.17) can therefore be rewritten in cylindrical coordinates to give:

$$\frac{\partial \mu}{\partial t} = C_v \left\{ \frac{\partial^2 \mu}{\partial r^2} + \frac{1}{r} \frac{\partial \mu}{\partial r} + \frac{\partial^2 \mu}{\partial z^2} \right\} \quad (3.19)$$

Values of pore water assigned to each node of the finite difference network are shown in Fig. 3.2, with coordinates r and z occupying the plane of the paper.

The finite difference equations can be derived as follows:

Using forward difference at time t_0

$$\frac{\partial \mu}{\partial t} = \frac{u_0 t_0 + t - u_0 t_0}{t} \quad (3.20)$$

Using central difference:

$$\frac{\partial^2 \mu}{\partial r^2} = \frac{u_3 - u_0 + u_1}{h^2} \quad (3.21)$$

$$\frac{\partial^2 \mu}{\partial z^2} = \frac{u_2 - 2u_0 + u_4}{h^2} \quad (3.22)$$

$$\frac{\partial \mu}{\partial r} = \frac{u_1 - u_3}{2h} \quad (3.23)$$

If $p = \frac{r}{\partial r}$, $\beta = \frac{C_v t}{h^2}$ and $\partial r = \partial z = h$

Then eqn. (3.19) can be rewritten to give:

$$u_0 t_0 + t = \beta \{ u_1 + u_2 + u_3 + u_4 - 4u_0 t + \frac{(u_1 - u_3)}{2p} \} + u_0 t_0 \quad (3.24)$$

This can be further simplified (Ross 1954) if β is made equal to $1/4$, so eliminating the $u_0 t_0$ term. The pore pressure can thus be found at any point within the clay mass.

Eqn. (3.24) will apply for piles under the centre of the raft where the drainage is assumed to be equal for each pile. However, at the edge of a raft supported by piles the boundary conditions change. This can be overcome by using a system of Cartesian coordinates in three dimensions as shown in Fig. 3.3.

The finite difference equations for Cartesian coordinates have previously been derived (Jones 1978) to give:

$$u_0 t_0 + t = \beta (u_1 + u_2 + u_3 + u_4 + u_5 + u_6 - 6u_0) + u_0 \quad (3.25)$$

where $\beta = 1/6$ to eliminate the u_0 term.

Equations (3.24) and (3.25) have been applied to an isotropic soil which is rarely the case in practice but these can easily be extended to anisotropic soils where $C_{vx} = C_{vy} \neq C_{vz}$

The above equations become unstable if the value of t is too large and convergence is not reached. It is often convenient to use a value of t such that $\frac{z^2}{C_v t} = 2$.

3.5

RATE OF CONSOLIDATION

The rate of consolidation is found by using the relevant time factor T_v and T_r , where:

$$T_v = \frac{C_v t}{H^2} \quad \text{and} \quad T_r = \frac{C_r t}{R^2}$$

which is equated with the pore pressure dissipation $U_v\%$ and $U_r\%$ respectively. The accuracy will depend upon the intervals into which the sample has been divided. A series of curves can thus be drawn up for the time factor against the degree of consolidation and the time for radial or vertical consolidation found in the usual way (Terzaghi and Peck 1967).

It has been shown by Carrillo (1942) that the average degree of consolidation \bar{U} is given by:

$$\bar{U} = 1 - (1 - \bar{U}_r)(1 - \bar{U}_v) \quad (3.26)$$

3.6

DRAIN WELLS

A gravel pile can be considered to be an enlarged sand drain so the above computations can be minimized if recourse is made to the work of Barron (1948), where a series of curves relating consolidation rates and time factors have been produced. The graphs have been derived using the Terzaghi - Rendulic equations, although not using finite-difference methods. The writer has previously shown that good agreement exists between the degree of consolidation obtained from the finite-difference method and that due to Barron (Jones 1978).

For most practical purposes it is thus more convenient to use the work of Barron, although the finite-difference method is especially useful where the boundary conditions are irregular such as the edge points under a raft supported by piles.

The thickness of the half layer H being drained has an influence on the efficiency of such drains with the effectiveness of vert-

ical drainage being greater when H is smaller. Thus, drain efficiency increases as the vertical thickness increases and Christie (1959) showed that their presence is only really justified where H is greater than 5 metres. Also, Richart (1957) has shown that drain spacing is more important than drain diameter in determining the rate of consolidation.

Barron has used two approaches in deriving his solutions, namely that of free strain and equal vertical strain. For equal vertical strain the assumption is made that the load is uniform over the area of influence, with differential settlements having no effect on the redistribution of stresses due to arching. For free strain it is accepted that the soil closest to the drain consolidates faster than that further away and so develops shear strains within the soil and results in a surface differential settlement and a redistribution of load. For a rigid raft the free strain approach is in closer agreement with the Biot theory than the equal strain approach (Balaam and Booker 1979), as shown in Figs. 8.7 to 8.11.

3.7

SMEAR ZONE

Barron has made allowances for the effects of smear on the interface between the sand drain and clay. Such an effect will also occur in gravel piles as the soil undergoes considerable remoulding during the insertion of the gravel and thus reduces the rate of consolidation. Also, attention should be paid to the grading of the gravel so that the pile does not readily get blocked and so cease to function as a drain.

3.8

SUMMARY

1. The Biot theory of consolidation is a more accurate method than that of Terzaghi.
2. For most practical purposes the Terzaghi method is adequate.
3. The Terzaghi three dimensional equations can be derived from an extension of the method used for the one dimensional case.

4. The finite difference method can readily be used to solve the consolidation equations.
5. The degree of consolidation is found in a similar way to that used for one dimensional consolidation.
6. It is generally more convenient to use the work of Barron (1948) for calculating the degree of consolidation than use the finite-difference method which is very time consuming.
7. A smear zone is usually developed at the drain-clay interface which affects the radial consolidation.

CHAPTER 4

STRESS - STRAIN PROPERTIES OF SAND

4.1 INTRODUCTION

An understanding of the stress - strain relationship of stone columns can be had if the fundamental behaviour of sands is appreciated. This chapter looks at such behaviour and examines failure criteria, stress dilatancy and the non-linear behaviour of sands. Consideration is also given to soil as a particulate system as well as the choice of testing method which has an influence on the soil behaviour.

4.2 PARTICULATE AND CONTINUUM SYSTEMS FOR SOILS

In the true sense of the word soils are particulate materials, although for the majority of purposes they can be considered as a continuum. For a particulate system stresses and strains between individual particles need to be considered, and such stresses can vary enormously for different particles within a soil mass. For the same overall applied stress, the inter-particle stress is governed to some extent by the particle size (Lambe and Whitman 1969). The overall applied stress acting as a continuous stress distribution could thus be thought of as a statistically mean value averaged over a sufficiently large area.

The high contact stresses can cause particle breakage and consequent change in gradation. The redistribution of stress that then occurs can have an affect on the strength of the material, as shown by the flattening of the Mohr - Coulomb envelope at high stresses. This is of particluar importance in earth dams.

4.3 FAILURE CRITERIA

The three principle failure criteria as described below, have been closely examined by Bishop (1966, 1971). The major,

intermediate and minor effective principle stresses are given by σ_1' , σ_2' and σ_3' .

The three criteria are:

Mohr - Coulomb:

$$\sigma_1' - \sigma_3' = \sin \phi' (\sigma_1' + \sigma_3') \quad (4.1)$$

Extended Tresca:

$$\sigma_1' - \sigma_3' = \alpha \left\{ \frac{\sigma_1' + \sigma_2' + \sigma_3'}{3} \right\} \quad (4.2)$$

Extended von Mises:

$$\begin{aligned} (\sigma_1' - \sigma_2')^2 + (\sigma_2' - \sigma_3')^2 + (\sigma_3' - \sigma_1')^2 \\ = 2\alpha^2 \left\{ \frac{\sigma_1' + \sigma_2' + \sigma_3'}{3} \right\}^2 \end{aligned} \quad (4.3)$$

It should be noted that in axial compression where $\sigma_2' = \sigma_3'$ the extended Tresca and extended von Mises both reduce to:

$$\sigma_1' - \sigma_3' = \alpha \left\{ \frac{\sigma_1' + 2\sigma_3'}{3} \right\} \quad (4.4)$$

and in extension where $\sigma_2' = \sigma_1'$:

$$\sigma_1' - \sigma_3' = \alpha \left\{ \frac{2\sigma_1' + \sigma_3'}{3} \right\} \quad (4.5)$$

since α is equal in both cases.

The validity or otherwise of each of the above criteria has clearly been demonstrated (Bishop and Green 1969), whereby the influence of the intermediate principle stress is plotted against friction angle (Fig. 4.1). It can be seen that the extended von Mises and extended Tresca have very limited range for which the criteria are valid, whilst that of the Mohr - Coulomb is in very close agreement.

The validity of the Mohr - Coulomb criteria is again seen by plotting all three in principle stress space (Fig. 4.2). Both the extended von Mises and extended Tresca pass into negative

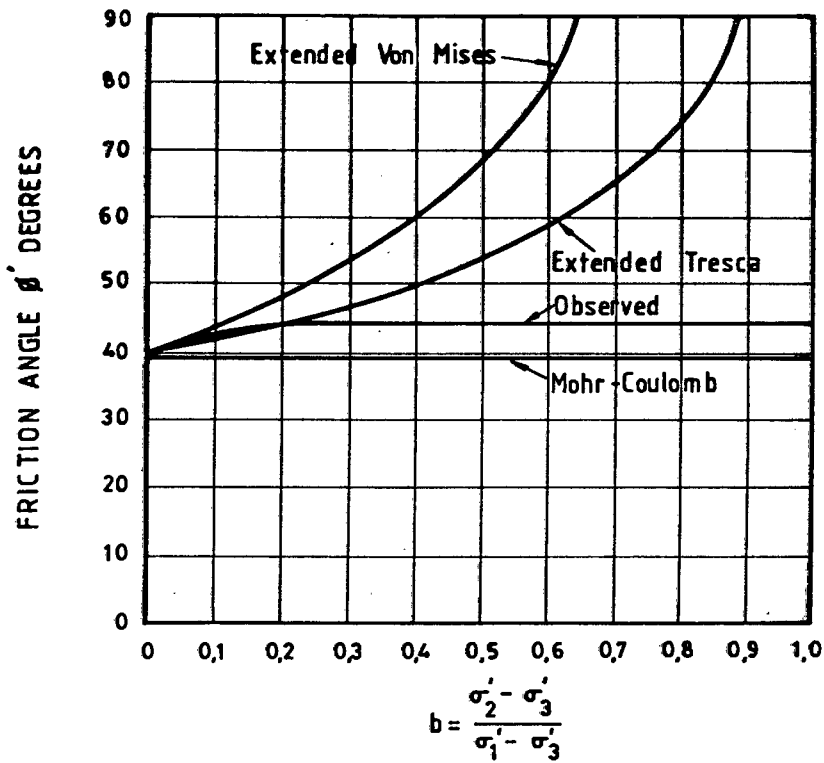


FIG. 4.1 OBSERVED AND PREDICTED VALUES OF ϕ' USING THE THREE FAILURE CRITERIA. (AFTER BISHOP AND GREEN 1969)

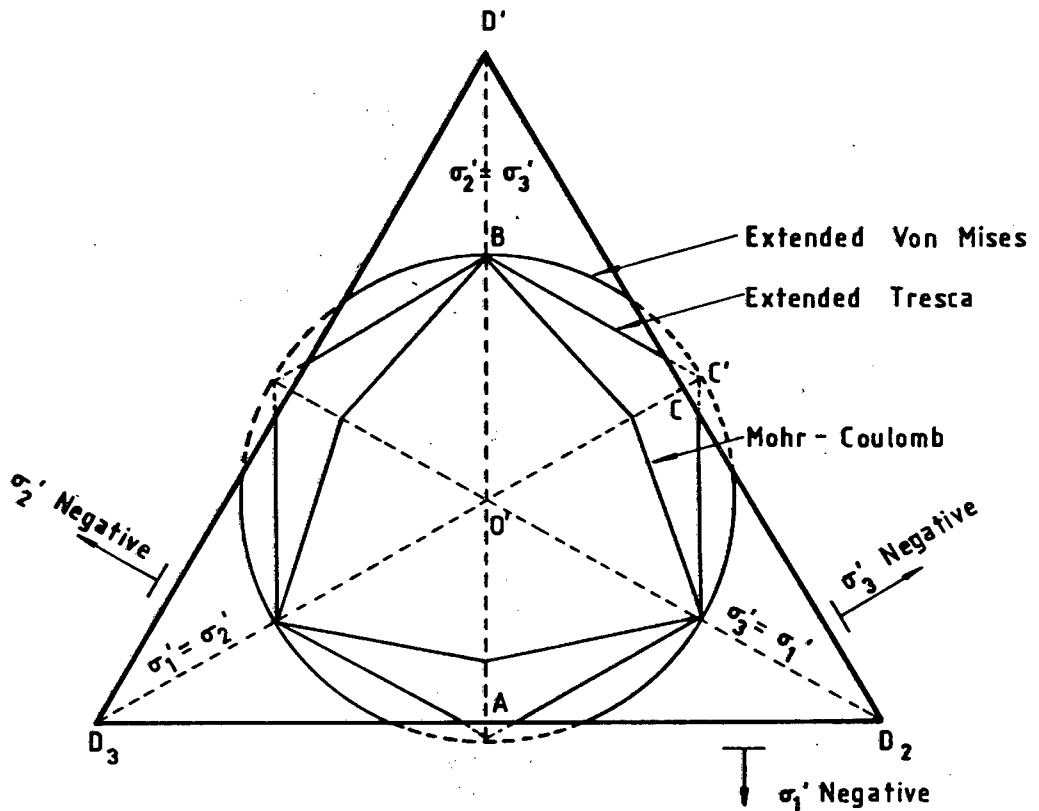


FIG. 4.2 THE THREE FAILURE CRITERIA IN PRINCIPLE EFFECTIVE STRESS SPACE (AFTER BISHOP 1966)

effective stress space, which indicates tension which is not possible for a cohesionless soil.

From a consideration of the above it is clear that the Mohr - Coulomb gives the best representation of soil behaviour.

4.4

STRESS - STRAIN RELATIONSHIP

A consideration of the results of drained triaxial tests on both dense and loose sands shows noticeable differences in behaviour (Bishop and Henkel 1957). Dense sands exhibit high strengths at relatively low axial strains and show a distinct peak stress, with a marked decrease in stress with increasing strain until a residual value is reached at large strains. For loose sands a well defined failure point is not reached, with the stress remaining essentially constant with increased strain once the maximum stress value is reached (Fig. 4.3). It is noticeable that the residual value of stress is approximately the same for both loose and dense samples of the same sand.

In a drained triaxial test a dense sample of sand expands in volume whereas a loose sand initially decreases in volume only to later expand to a volume equal to that of its initial volume.

For a drained test the shape of the stress - strain curves are essentially the same as that of undrained tests, but negative pore pressures are developed in the dense sample as it dilates (see 4.7), whilst positive pore pressures are developed in the loose samples.

The above patterns of behaviour bear a strong resemblance to that of clays with the dense samples corresponding with that of overconsolidated clays, and the loose samples with that of normally consolidated clays.

4.5

NON-LINEARITY IN SOILS

The stress - strain curves as described in paragraph 4.4 show that the soil is linear for only a limited portion of the curve,

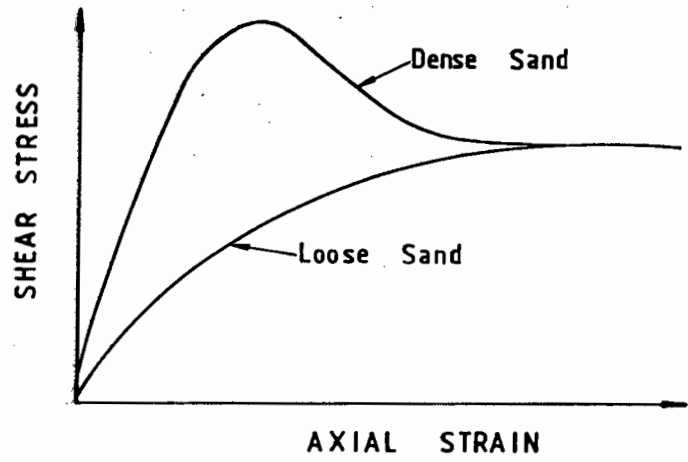
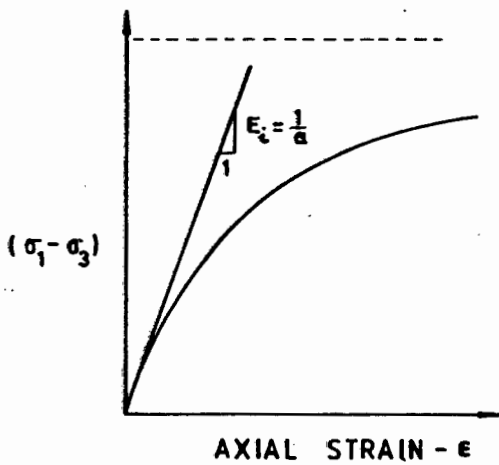
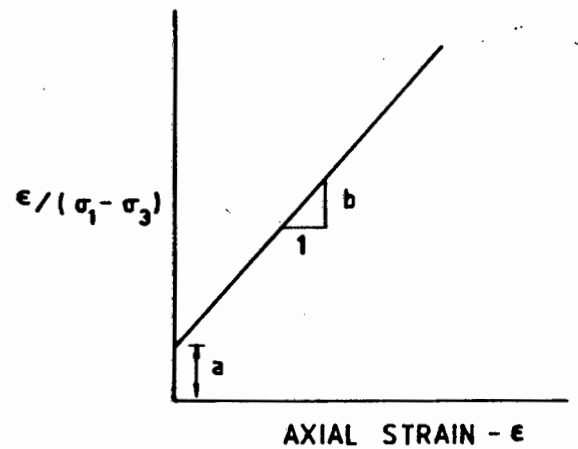


FIG. 4.3 STRESS STRAIN BEHAVIOR OF LOOSE AND DENSE SANDS



a) Hyperbolic Stress - Strain Curve



b) Transformed Hyperbolic Stress - Strain Curve

FIG. 4.4 HYPERBOLIC REPRESENTATION OF STRESS STRAIN CURVES
DEVELOPED BY KONDNER

although it has often been idealised as linearly elastic, notably in problems of stress distribution. A simplified non-linear relationship has been given by Duncan and Chang (1970) based on work by Kondner(1963) who found that the stress - strain curves of both clay and sand can be approximated by hyperbolae which have the following equation:

$$(\sigma_1 - \sigma_3) = \frac{\epsilon}{a + b\epsilon} \quad (4.6)$$

where σ_1 and σ_3 are the major and minor principle stresses
 ϵ is the axial strain
 a and b are constants.

The values of 'a' and 'b' are obtained as shown in Fig. 4.4. The parameter 'a' is the reciprocal of the initial tangent modulus E_i , whilst 'b' is the reciprocal of the asymptotic stress difference which the stress - strain curve approaches at infinite strain.

The asymptotic value of $(\sigma_1 - \sigma_3)$ is larger than the compressive stress at failure with the two values being related by a common factor R_f where:

$$R_f = \frac{(\sigma_1 - \sigma_3)_{\text{failure}}}{(\sigma_1 - \sigma_3)_{\text{ultimate}}} \quad (4.7)$$

Typical values obtained by Duncan and Chang are between 0,75 and 1,0 which compare with $\pm 0,89$ for a sand and $\pm 0,93$ for a gravel as tested by the author.

Equation (4.6) can now be rewritten to give:

$$(\sigma_1 - \sigma_3)_f = \frac{\epsilon}{\frac{1}{E_i} + \frac{\epsilon R_f}{(\sigma_1 - \sigma_3)_{\text{ult}}}} \quad (4.8)$$

The initial tangent modulus E_i has been related to the confining pressure by Janbu to give:

$$E_i = K. p_a \left(\frac{\sigma}{p_a} \right)^n \quad (4.9)$$

where K = a modulus number

p_a = atmospheric pressure

n = exponent determining the rate of variation of E_t
with σ_3 .

Values of K and n are found by plotting E_t against σ_3 on a log. - log. scale, and obtaining a best fit straight line to give:

K = intercept on E_t axis

$n = \log_{\sigma_3} \left(\frac{E_t}{K} \right)$ where E_t corresponds to stress level σ_3 .

(N.B. it is convenient to choose $\sigma_3 = 10$)

It was found by the author that a minimum of four points need to be plotted to give a degree of confidence to the results.

The Mohr-Coulomb failure criteria can also be incorporated to give:

$$(\sigma_1 - \sigma_3)_f = \frac{2c \cos \phi + 2\sigma_3 \sin \phi}{1 - \sin \phi} \quad (4.10)$$

A more general model can be developed which involves the tangent modulus E_t at any stress condition, thus:

$$E_t = 1 - \frac{R_f (1 - \sin \phi) (\sigma_1 - \sigma_3)^2}{2c \cos \phi + 2\sigma_3 \sin \phi} \left(\frac{K p_a (\sigma_3)}{p_a} \right)^n \quad (4.11)$$

The tangent modulus is obtained from a multilinear model by using an incremental rather than a bi-linear approach (Desai and Christian 1977), but this does mean that a simulation past the peak stress values results in a negative value of modulus.

4.6

FRICTION ANGLE

The friction angle obtained is very much dependent upon the testing method used to establish it, as shown by the fact that

sands tested in plane strain exhibit different friction angles from those tested triaxially (Cornforth 1964, Rowe 1969). Although the triaxial testing apparatus is perhaps the most widely used testing equipment the test has its shortcomings (Parry 1956) and Roscoe (1970) pointed out that the knowledge of stress - strain behaviour of soils would be restricted if work was only confined to axi-symmetrical triaxial test.

The work of Parry concerned the testing of two identical samples of clay. In one test the cell pressure was kept constant whilst the axial pressure increased and in the other test the axial stress was kept constant while the cell pressure was reduced. Both samples had the same peak stress ratio at failure and hence the same friction angle, but this was developed at vastly different values of strain (Fig. 4.5a).

A similar occurrence has been reported by Lade (1978) who showed that, depending upon the shape of the effective stress path, the maximum deviator stress could either be reached before or after the principle stress ratio. Bishop (1971) using data from Castro (1969), showed that for a saturated loose sand an effective friction angle of 16.1° was calculated on the basis of maximum deviator stress, but a value of 30° obtained using the maximum principle stress ratio (Fig. 4.5b).

The test method used to establish the working value of friction angle must be relevant to the project in hand to obtain consistent results.

4.7

STRESS DILATANCY

It has already been shown that loose and dense samples of the same sand behave differently during shear. The expansion of a dense sand when sheared was first observed by Osbourne Reynolds in 1885 (Rowe 1969), and he applied the name dilatant to such behaviour. This phenomena has since been extensively studied (Taylor 1948, Bishop 1950, Rowe 1962) and expressions have been derived which separate the frictional and dilatancy components.

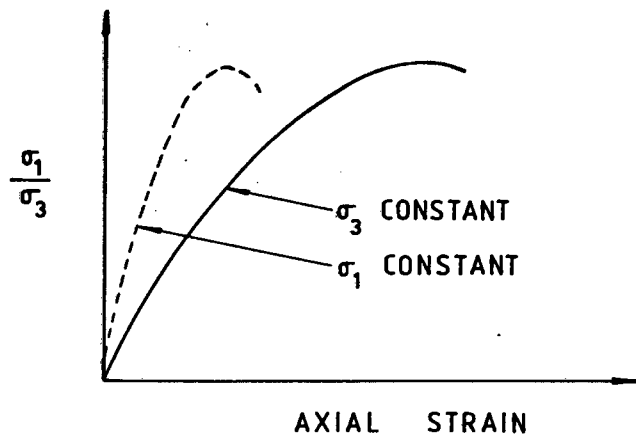


FIG. 4.5a INFLUENCE OF STRESS PATH ON STRAINS TO DEVELOP PEAK STRESS RATIO ON IDENTICAL CLAY SAMPLES

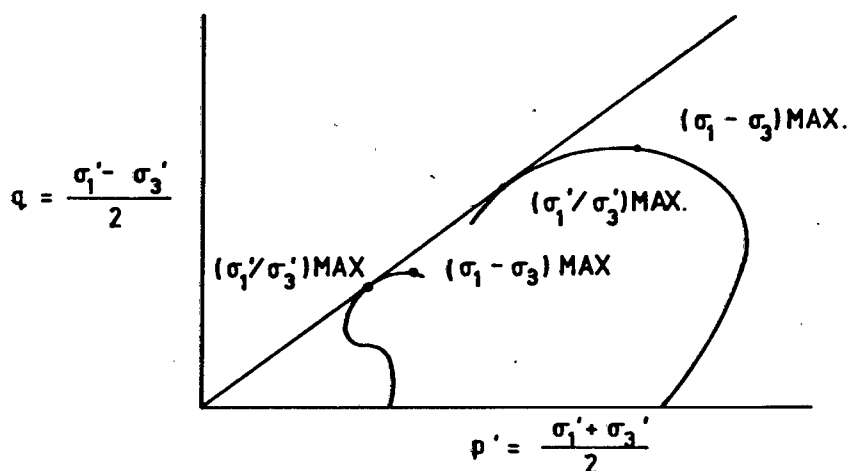


FIG. 4.5b VARIANCE BETWEEN THE MAXIMUM DEVIATOR STRESS \$(\sigma_1 - \sigma_3)\$ MAX. AND PRINCIPLE STRESS RATIO FOR DIFFERING STRESS PATHS

The principle of dilation can be understood by considering the following analogy as detailed by Atkinson and Bransby (1978). This considers a block resting on a rough plane acted upon by a vertical force P and a sideways force Q . For sliding to occur, Q must be increased to μP (where μ is the coefficient of friction).

If the block is considered to be a block of sand, then

$$\tau' = \mu' \sigma \quad (4.12)$$

and if it is now assumed to be serrated, the horizontal force will cause a small horizontal movement δu and a vertical movement δv , where $\delta v / \delta u = \tan \phi$ (Fig. 4.6).

The relationship between P and Q during sliding is obtained by summing the normal forces N and shear forces S on the planes of contact to give :

$$N = P \cos \alpha + Q \sin \alpha \quad (4.13)$$

$$S = -P \sin \alpha + Q \cos \alpha$$

since $S = \mu N$

$$Q - P \tan \alpha = \mu P + \mu Q \tan \alpha \quad (4.14)$$

substituting for $\tan \alpha$

$$\frac{Q}{P} = \frac{\mu + (\delta v / \delta u)}{1 - \mu (\delta v / \delta u)} \quad (4.15)$$

If a stack of serrated blocks of total height H are now considered to be acted upon by a shear force $\tau' A$ and a normal force $\sigma' A$, the ratio $\delta v / H$ is equal to the vertical strain in the sand, which in turn, is equal to the volumetric strain $\delta \epsilon_v$ since the horizontal strain is zero. Also, the shear strain $\delta u / \delta H$ is equal to the shear strain $\delta \gamma_{yx}$.

By substituting:

$$\frac{\tau'_{yx}}{\sigma'_y} = \mu - \frac{(\delta \epsilon_v / \delta \gamma_{yx})}{1 + \mu(\delta \epsilon_v / \delta \gamma_{yx})} \quad (4.16)$$

which relates shear and normal stresses to a frictional constant and volumetric and shear strains.

From a consideration of the work done to the system by a horizontal displacement of δu , the net work involved is:

$$\tau'_{yx} A \delta u - \sigma'_y A \delta v \quad (4.17)$$

If it is assumed that this work is dissipated in friction, and is proportional to the frictional constant μ , the normal force $\sigma'_y A$ and the shear displacement δu , then:

$$\tau'_{yx} A \delta u - \sigma'_y A \delta v = \mu \sigma'_y A \delta u \quad (4.18)$$

$$\text{or } \tau'_{yx} / \sigma'_y = \mu + (\delta v / \delta u)$$

The above equations show that during shear, work is done in overcoming both friction and volume change. As the ratio τ'_{yx} / σ'_y increases the greater will be the dilation of the sample. This explains the behaviour of dense sand with a high degree of interlocking (c.f. serrated block model), where more work is required for the system to shear, thus resulting in high values of τ'_{yx} / σ'_y and hence higher dilation values.

A practical implication of the effects of dilation can be gained by considering the stress dilatancy equation for compression as given by Rowe (1969):

$$R = DK \quad (4.19)$$

where $R = \sigma'_1 / \sigma'_3$

$D = (1 - dv/d\epsilon)$ and v is the volume decrease per unit volume.

ϵ is the major principle compressive strain.

$$K = \tan^2 (45 + \phi_f/2)$$

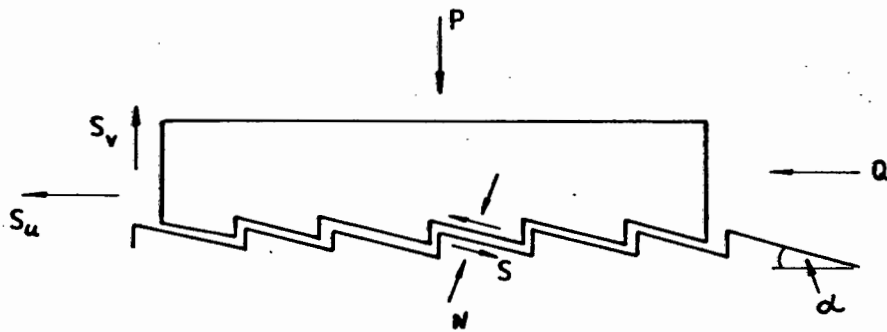


FIG. 4.6 SERRATED BLOCK ANALOGY ILLUSTRATING DILATANCY

$$\frac{\tau'_{yx}}{\sigma'_y} = \mu - \frac{(\delta \epsilon v / \delta \gamma_{yx})}{1 + \mu(\delta \epsilon v / \delta \gamma_{yx})} \quad (4.16)$$

which relates shear and normal stresses to a frictional constant and volumetric and shear strains.

From a consideration of the work done to the system by a horizontal displacement of δu , the net work involved is:

$$\tau'_{yx} A \delta u - \sigma'_y A \delta v \quad (4.17)$$

If it is assumed that this work is dissipated in friction, and is proportional to the frictional constant μ , the normal force $\sigma'_y A$ and the shear displacement δu , then:

$$\tau'_{yx} A \delta u - \sigma'_y A \delta v = \mu \sigma'_y A \delta u \quad (4.18)$$

$$\text{or } \tau'_{yx} / \sigma'_y = \mu + (\delta v / \delta u)$$

The above equations show that during shear, work is done in overcoming both friction and volume change. As the ratio τ'_{yx} / σ'_y increases the greater will be the dilation of the sample. This explains the behaviour of dense sand with a high degree of interlocking (c.f. serrated block model), where more work is required for the system to shear, thus resulting in high values of τ'_{yx} / σ'_y and hence higher dilation values.

A practical implication of the effects of dilation can be gained by considering the stress dilatancy equation for compression as given by Rowe (1969):

$$R = DK \quad (4.19)$$

where $R = \sigma'_1 / \sigma'_3$

$D = (1 - dv/d\epsilon)$ and v is the volume decrease per unit volume.

ϵ is the major principle compressive strain.

$$K = \tan^2 (45 + \phi_f / 2)$$

Horne (1965) showed that for triaxial compression

$$1 \leq D \leq 2$$

The upper limit for sand in its densest state is thus:

$$\sigma'_1/\sigma'_3 = 2 \tan^2 (45 + \phi_u/2) \quad (4.20)$$

and the lower limit

$$\sigma'_1/\sigma'_3 = \tan^2 (45 + \phi_{cv}/2) \quad (4.21)$$

The value of ϕ_f varies between a lower value of ϕ_u , the friction angle between mineral particles and an upper value ϕ_{cv} at the critical state, but for the densest state at the peak stress ratio $\phi_f = \phi_u$.

By rearranging eqn. 4.20, the vertical stress that can be sustained by a sample is thus:

$$\sigma'_1 = 2\sigma'_3 \tan^2 (45 + \phi_f/2) \quad (4.22)$$

The applicability of the above to stone column design is obvious.

4.8

SUMMARY

1. Although particulate in nature, sands can be considered to be a continuum.
2. The Mohr-Coulomb failure criteria best represents the failure condition of sands.
3. Dense sands dilate during shear and generate negative pore pressures, whilst loose sands compress and develop positive pore pressures. The behaviour of sands can thus be likened to that of clays.
4. The non-linear behaviour of soils can be approximated by a hyperbolic relationship.

5. Values of friction angle obtained in plane strain or triaxial tests differ. The method of test and the stress path followed during a test influences the value of friction angle obtained.
6. The dilatant behaviour of sand can be modelled by analogies with sliding blocks. The work done during shear is dissipated in both friction and in overcoming dilatancy.

CHAPTER 5

CRITICAL STATE THEORY

5.1 INTRODUCTION

Non-linearity was dealt with in Chapter 4. The aim of this chapter is to serve as a brief introduction to critical state theory, an alternative way of looking at non-linearity in soils. An appreciation of the critical state theory gives as insight into the interdependence of such variables as void ratio, volumetric strain, total and effective stresses, and should thus give a better understanding of the deformation behaviour of a stone column under load.

It is not intended to outline the theory and derivation of equations in detail as this has been adequately covered in the definitive work on the subject by Scholfield and Wroth (1968) and more succinctly by Atkinson and Bransby (1978).

5.2. THE NORMAL CONSOLIDATION LINE

If a sample of clay is isotropically compressed and the specific volume v is plotted against $\ln p'$ where $p' = \frac{1}{3}(\sigma_1 + \sigma_2 + \sigma_3)$ and $\sigma_1 = \sigma_2 = \sigma_3$ then the curve will follow the line AB in Fig. 5.1. Upon unloading the swelling line BD is followed. If the sample is again compressed to a higher loading than previously and again unloaded, the path will follow the swelling line DB until point B is reached, continue to point C and then swell along line CE.

It can be seen that line AC acts as a boundary line between possible and impossible states and can be termed a state boundary surface. Also, the swelling lines DB and CE are parallel. AC is the normal consolidation line whilst those of DB and CE are overconsolidation lines.

The above can be expressed mathematically to give :

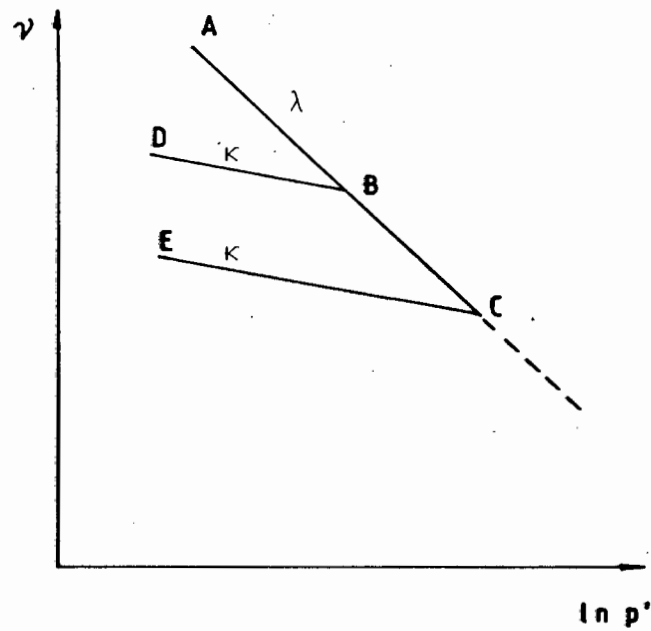
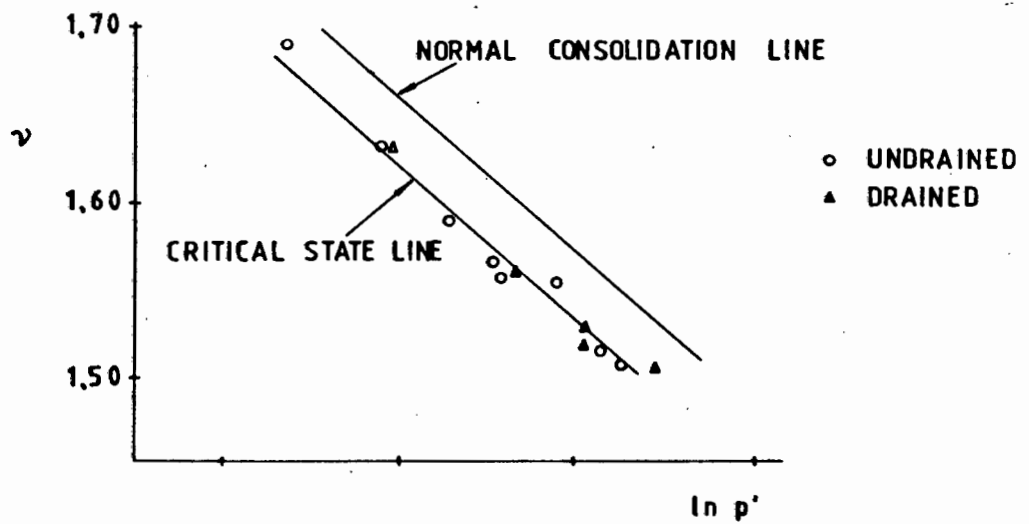


Fig. 5.1 Normal and overconsolidation lines for isotropically compressed clay.

Fig. 5.2 The critical state line in $v: \ln p'$ space. (Atkinson and Bransby 1978)



For AC,
$$v = N - \lambda \ln p' \quad (5.1)$$

and DB
$$v = v_K - \kappa \ln p' \quad (5.2)$$

where N is the specific volume of a normally consolidated soil when $p' = 1,0 \text{ kN/m}^2$ and

v_K is the specific volume of an overconsolidated soil at $p' = 1,0 \text{ kN/m}^2$.

It should be noted that for sands both λ and κ are very small and thus difficult to measure. Also, the normal consolidation line is only reached at relatively high stress levels so that most sands are generally overconsolidated at normal engineering stress levels.

5.3 THE CRITICAL STATE LINE

It has been shown by Parry (1960) that for isotropically compressed samples of Weald clay, the failure points of both drained and undrained samples lie on the same line when plotted on a $q':p'$ diagram $q' = \frac{1}{2}(\sigma_1 - \sigma_3)$ and on a line parallel to the normal consolidation line when plotted in $v:p'$ space. (Fig. 5.2) Such a line is termed the critical state line and is a function of q' , p' and v .

If projected onto the $q':p'$ plane the equation of the line is

$$q' = Mp' \quad (5.3)$$

where M is the gradient.

and on the $v: \ln p'$ plane:

$$v = \Gamma - \lambda \ln p' \quad (5.4)$$

5.4 THE ROSCOE SURFACE

The Roscoe surface is a state boundary surface forming a unique curved surface between the normal consolidation line and the critical state line when plotted in the three dimensional $q':p':v$ space. Thus, a sample starting from the normal consolidation line will travel along the Roscoe surface before terminating at the

critical state line, irrespective of the stress path followed.

5.5

THE HVORSLEV SURFACE

The Hvorslev surface can be thought of as a state boundary surface for overconsolidated samples similar to the Roscoe surface for normally consolidated samples. The existence of such a surface can again be seen by plotting data from Parry in $q'/p'_e : p'/p'_e$ space, where p'_e is the equivalent stress at any specific volume and is equal to $\exp\{(N - v)/\lambda\}$. This is shown in Fig. 5.3, as is the line of tensile failure of slope 3 which intersects the Hvorslev surface.

The complete state boundary surface is shown diagrammatically in $q':p':v$ space in Fig. 5.4.

5.6

CAM-CLAY MODEL

Two important mathematical models were developed at Cambridge, notably that of Granta-gravel and Cam-clay. Granta-gravel is a conceptual model of an ideal rigid /plastic continuum whilst that of Cam-clay is perhaps a more useable model in that it is an ideal elastic/plastic continuum. In fact, it can be shown that Granta-gravel is just a special case of Cam-clay.

Two types of strains occur upon loading a sample, elastic strains which are wholly recoverable and plastic strains which are non-recoverable. If strains are elastic only, then deformations tend to be small whilst deformations are significant if plastic strains occur. Using the critical state model and the concepts of state boundary surfaces it has been found that plastic deformations only occur whilst the state boundary surface is being traversed, and below the state boundary surface only elastic strains occur.

For the Cam-clay model the state boundary surface is given by

$$q' = \frac{Mp'}{\lambda - \kappa} (\Gamma + \lambda - \kappa - v - \lambda \ln p') \quad (5.5)$$

which can be rewritten to give

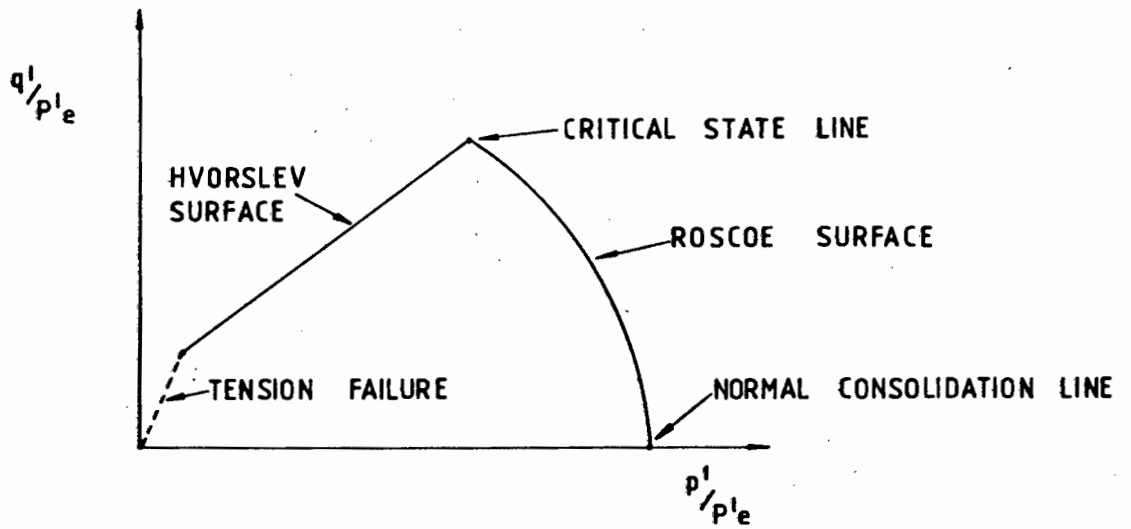


Fig. 5.3 The Hvorslev Surface in $q'/p'_e : p'/p'_e$ space.

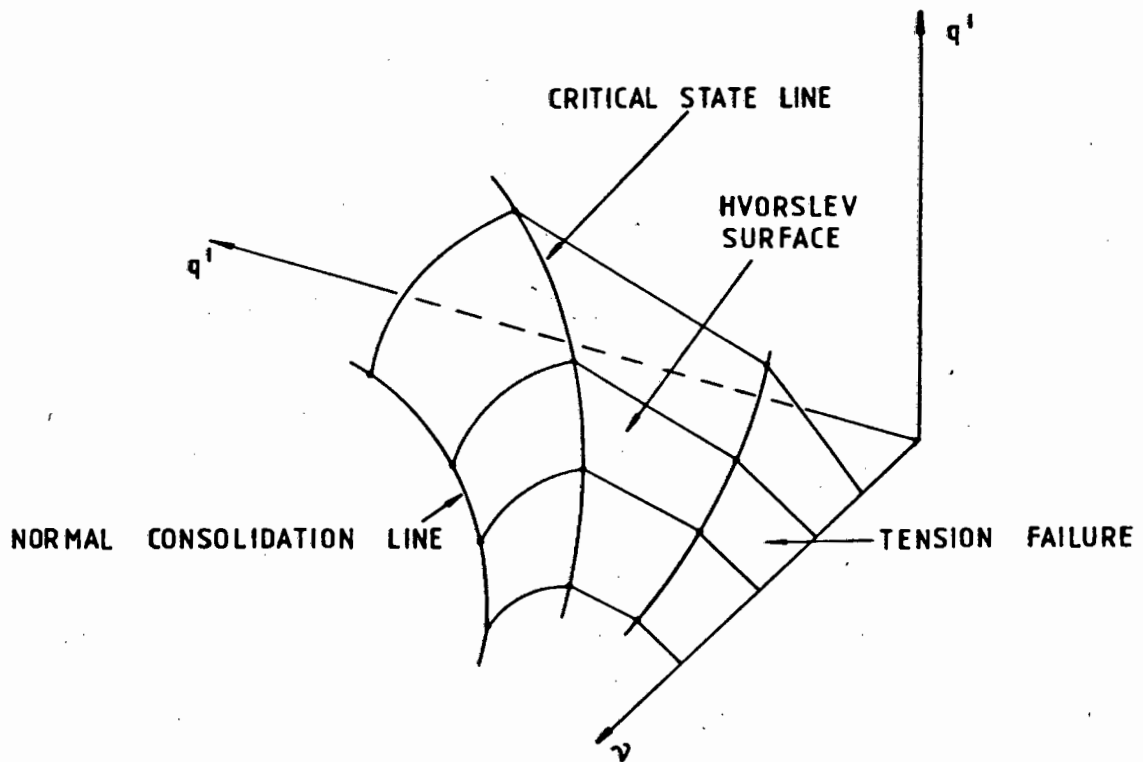


Fig. 5.4 The complete state boundary surface in $q':p':v$ space.

$$v = \Gamma + \lambda - \kappa - \lambda \ln p' - \frac{(\lambda - \kappa)q'}{Mp'} \quad (5.6)$$

which on differentiating gives:

$$\delta v = \lambda \frac{\delta p'}{p'} - \frac{(\lambda - \kappa)}{Mp'} \delta q' + \frac{(\lambda - \kappa)q'}{Mp'^2} \delta p' \quad (5.7)$$

The change in specific volume δv is made up of both the elastic and plastic change δv^e and δv^p respectively.

The elastic change of volume is:

$$\delta v^e = -\kappa(\delta p'/p') \quad (5.8)$$

hence the plastic change of specific volume is

$$\delta v^p = \frac{\lambda - \kappa}{Mp'} M - \frac{q'}{p'} \delta p' + \delta q' \quad (5.9)$$

and the plastic volumetric strain is thus

$$\delta \epsilon_V^p = -\frac{\delta v^p}{v} \quad (5.10)$$

and the elastic volumetric strain is

$$\delta \epsilon_V^e = \frac{\kappa \delta p'}{v p'} \quad (5.11)$$

The use of the Cam-clay theory gives a complete relationship for any soil and allows stresses, strains and pore pressures to be calculated at any point during the stress history of the soil.

5.7 COMPARISONS WITH OTHER FAILURE CRITERIA

Although valuable as a means of understanding the behaviour of soils, serious doubts have been expressed about the validity of some of the basic equations, notably eqn. 5.3, as this suggests a similarity with the extended Tresca failure criteria. It has

previously been shown in Chapter 4 that this can result in a failure surface passing into negative effective stress space which is impossible for a cohesionless material.

5.8 OTHER NON-LINEAR METHODS

A mathematical soil model has been proposed by Prevost (1979) which again allows for the plasticity of the soil. In this case the yield surfaces plot as ellipses, with failure occurring only when the yield condition reaches its ultimate limit state. Although differing in concept from that of critical state there are strong similarities in the logic of both systems. It is interesting to note that Prevost's model has remarkable agreement between theory and measured results, although it is based upon the transformed von Mises failure criteria.

5.9 SUMMARY

1. The normal consolidation line, the critical state line, the Roscoe surface and the Hvorslev surface can be combined to form a complete state boundary surface.
2. Plastic strains only occur whilst the state boundary surface is being traversed. Elastic strains occur at all points below this.
3. The Cam-clay model provides a means of calculating volumetric strains at any stress level.
4. Some aspects of the critical state theory are akin to the extended Tresca failure criteria.
5. A non-linear method posed by Prevost shows good agreement between theory and practice.

CHAPTER 6

LABORATORY TESTING OF SANDS

6.1 INTRODUCTION

Chapter 4 looked at the general stress-strain properties of sands and the various failure criteria which have been used to explain their behaviour. This chapter has concentrated on the laboratory testing of sands and gravels pertaining to this thesis, and concentrates on such aspects as stress paths, radial stress and strain and the significance of void ratio upon behaviour. A new dimensionless relationship between stress and strain is also established.

6.2 TESTING METHODS

The tests were carried out using conventional triaxial testing apparatus, and relate to the use of a 1,5 ins (37,5 mm) triaxial cell. A slight modification was used for one series of tests in which a special plunger was used to enable a static load to be applied vertically, rather than using the load frame of the triaxial machine.

Three types of tests were carried out viz. (a) Isotropic Compression, (b) Failing the sample by reducing cell pressure σ_3 , and (c) Failing the sample by increasing the deviator stress. In each case two materials were used, a well rounded uniform density sand, & a fine angular gravel of size $>4,75\text{mm}$ and $<6,7\text{ mm}$.

The sand presented few difficulties, and it was relatively easy to produce samples of approximately the same void ratio. The gravel, however proved more difficult due to the non-uniformity of particle shape, whilst the extreme angularity of the particles frequently resulted in puncturing of the rubber membranes even at modest values of stress and strain.

The main types of test performed are described below. Where applicable discussion of the results obtained is dealt with under a separate heading.

6.2(a) Isotropic Compression

A cylinder of sand encased in a rubber membrane was subjected to triaxial stresses by incrementally, increasing the cell pressure. At each increment of stress, after a suitable time had elapsed, the volumetric strain was measured by means of the volume change device. Due correction had to be made for the expansion of the triaxial cell with increasing cell pressure. The procedure was repeated for the gravel.

The specific volume v was plotted against the logarithm of p_1

$$\begin{aligned} \text{where } v &= 1 + e \\ \text{and } \ln p &= 1/3 (\sigma_1 + \sigma_2 + \sigma_3) \text{ (but } \sigma_1 = \sigma_2 = \sigma_3) \end{aligned} \quad (6.1)$$

and the results are shown graphically in Figure 6.1

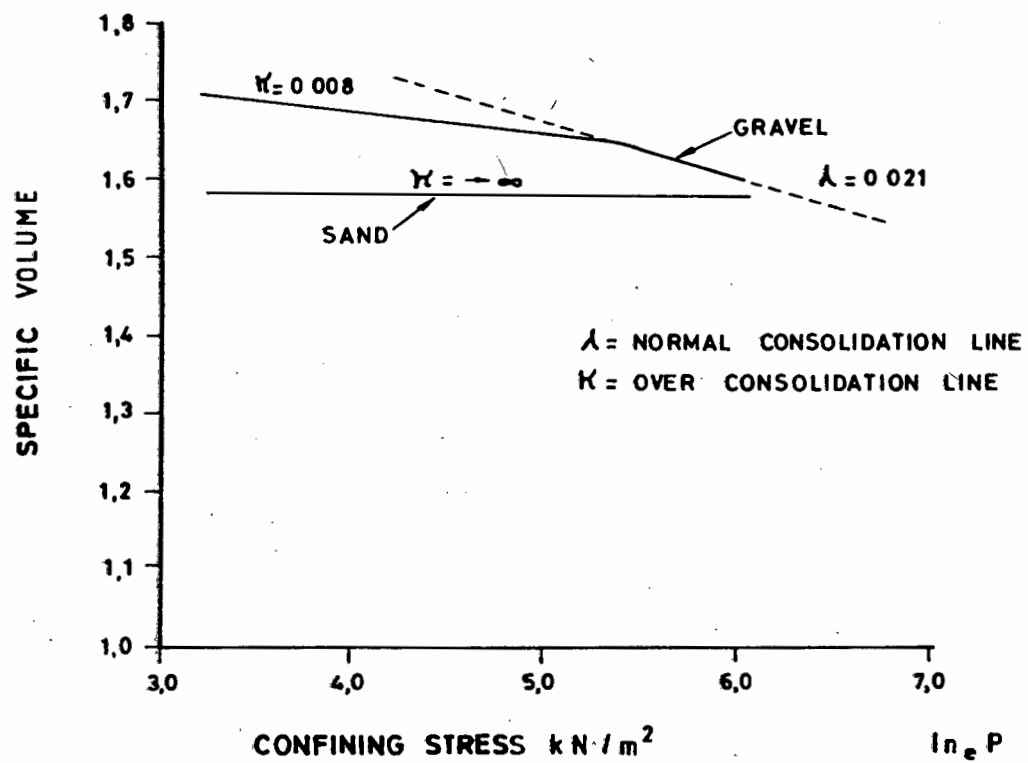
The difference between the two samples is clearly seen. The sand has a flat curve parallel to the $\ln p$ axis whilst that of the gravel has a gentle downward concave slope.

By applying the critical state parameters of λ for the normal consolidation line and κ for the swelling line we have.

$$\begin{aligned} \text{For the gravel : } \kappa &= 0,008 & \text{For the sand } \kappa &= \rightarrow \infty \\ \lambda &= 0,021 & \lambda &= < \kappa \end{aligned}$$

It is of course realized that the swelling line will vary in position, but be of constant slope, depending upon the initial specific volume of the sample.

If one compares the above results with that of Vesic and Clough (1968), it shows that for sands at stress levels normally encountered within engineering usage (ie $< 700 \text{ kN/m}^2$), loose and dense sands can be regarded as heavily overconsolidated as they lie well to the left of the normal consolidation line. The results obtained for the gravel are suprising as it appears as if one is approaching the normal consolidation line at comparatively low stress levels. Again, this could be a function of particle shape as a higher degree of compression



(AS TESTED BY THE WRITER FOR THIS THESIS)

FIG. 6.1 ISOTROPIC COMPRESSION OF SAND AND GRAVEL

would be possible due to particle breakage and consequent repacking of the grains. If the curves obtained are a true representation of the gravel compression characteristics it offers interesting possibilities for a possible design method for gravel piles. This will be discussed in a later chapter.

6.2(b) Failure by reducing cell pressure σ_3

An attempt was made to measure the radial and horizontal strain characteristics of a sand cylinder by maintaining a constant vertical load whilst incrementally reducing the confining pressure σ_3 . A constant load was obtained by using a specially adapted loading ram which enabled surcharge weights to be added to the ram. A simple screw device ensured that the load was not transferred to the sample until the screw was loosened.

Radial strain was measured by a somewhat crude device consisting of graduated silver foil which was wrapped around the cylinder. The foil was secured to the cylinder by using very weak rubber bands.

The procedure adopted during the test was to apply a constant horizontal stress to the sample by increasing the cell pressure. With the plunger in contact, but the screw thread tightened, a dead load was applied to the plunger. The screw was released and measurements of radial and horizontal strain taken. The cell pressure was reduced and the procedure repeated.

Unfortunately the above procedure did not work too well as a sudden failure occurred only when the cell pressure had been reduced to a very low value. It was thus impossible to take any meaningful measurements as both the horizontal and vertical strains were virtually immeasurable right up to the point of failure.

The experiment did however show that a sand cylinder can sustain very high vertical stresses even with low confining stresses, but when failure occurs it is sudden and occurs with little warning.

To overcome the above, a modified testing procedure was adopted by using a conventional triaxial testing load frame. The sample was prepared as before and the required cell pressure obtained. An axial load was then applied manually, using the conventional gearing of the machine, until a noticeable radial expansion had taken place. At this point the loading was terminated and the system allowed to come into equilibrium. Readings of volume change, radial and horizontal strain and loading were then recorded. The confining cell pressure was then reduced in stages and the relevant measurements taken as before.

In the above method the reducing of the cell pressure increased the radial strain and hence the vertical strain. This had the effect of reducing the applied load due to the stress relief experienced by the load proving ring. The principal stress ratio σ_3/σ_1 was plotted against the horizontal strain (Fig 6.10) and the vertical strain was plotted against the radial strain (Fig 6.9). An assessment of the results is made under separate headings later in the chapter.

6.2(c) Failure by increasing the deviator stress ($\sigma_1 - \sigma_3$)

Failure was also brought about in the conventional manner by carrying out a series of consolidated drained triaxial tests, to investigate stress path, behaviour, shape of the stress-strain curves, and the proportion of stress at failure related to the proportion of strain at failure. A more detailed discussion of the observations made during the tests now follows.

6.3 STRESS-STRAIN CURVES

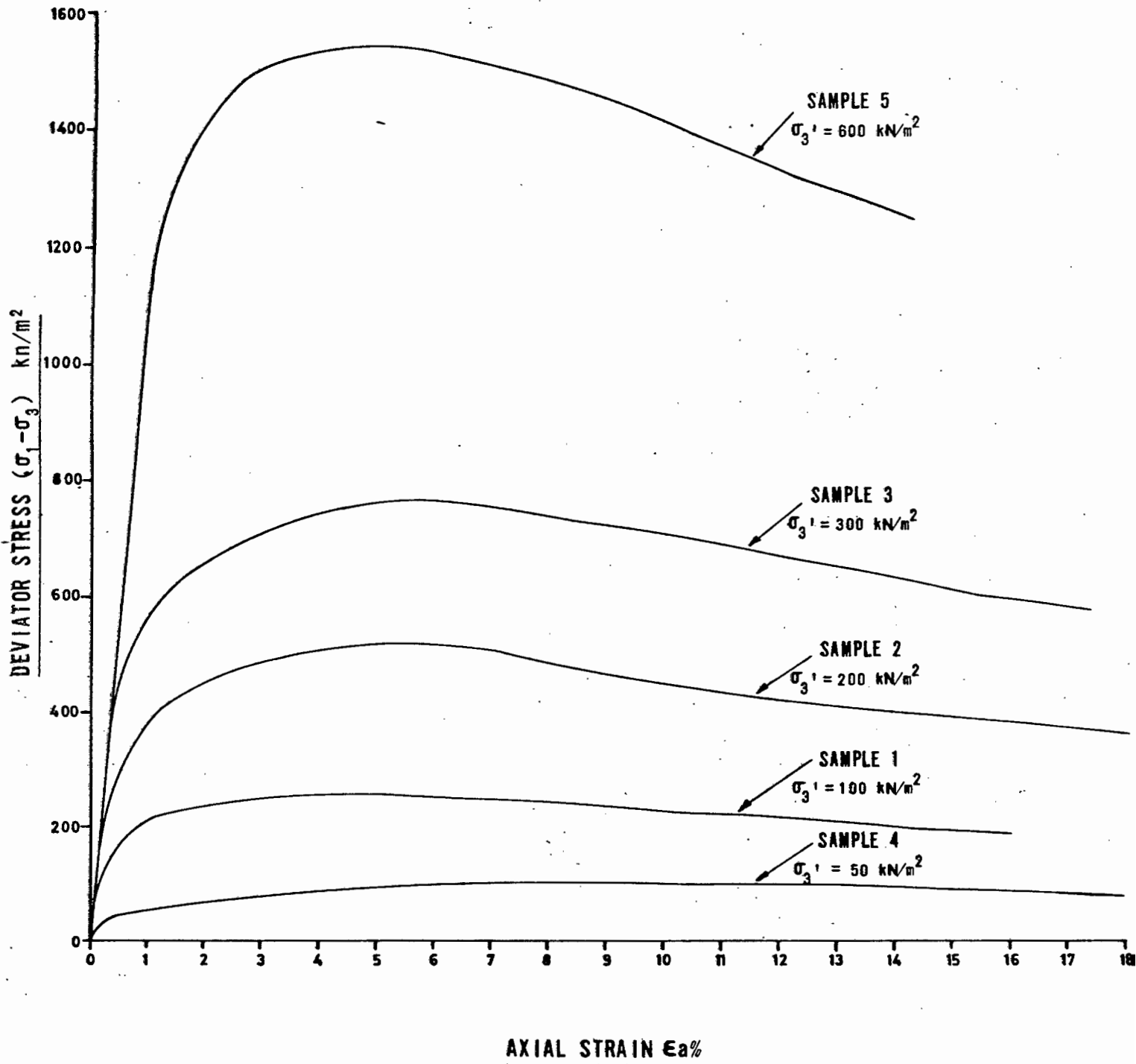
There are distinct differences in behaviour between the sand and the gravel, with the sand having very smooth curves with ill defined maximum stress levels. For the gravel the curves tend to be more erratic due to the particles physically breaking down during shear, a process which is clearly audible during the test. The stress strain curves are shown in Fig 6.2 and Fig 6.3 respectively.

If one first considers the sand, the curves follow the three stages in the straining process, as discussed by Lambe (1969) v.i v.i.z.

Fig 6.2

STRESS - STRAIN CURVES

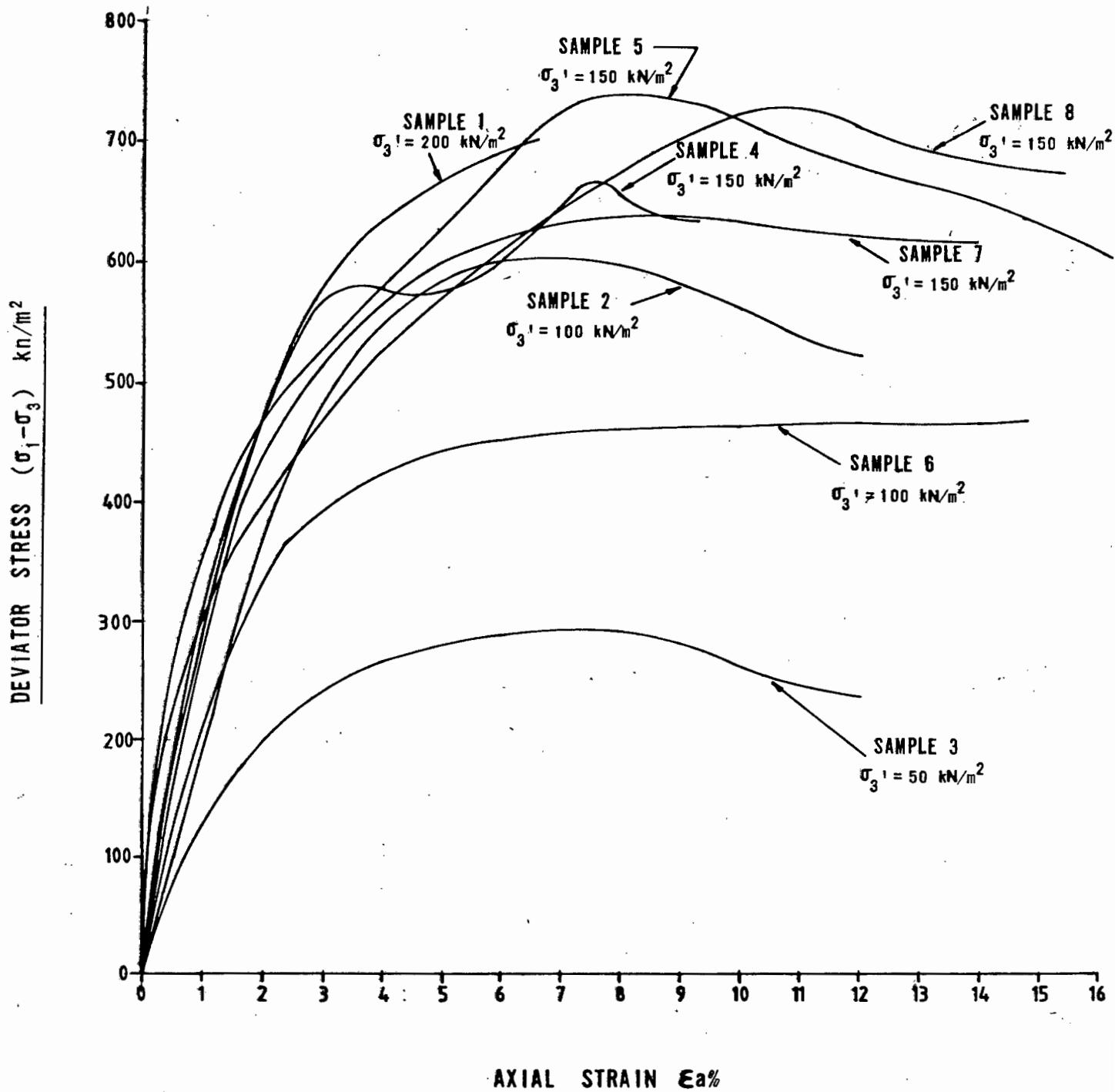
Density Sand



(AS TESTED BY THE WRITER FOR THIS THESIS)

Fig 6.3

STRESS - STRAIN CURVES
Fine Crusher - Run Gravel



(AS TESTED BY THE WRITER FOR THIS THESIS)

Note : Test terminated for Sample 1 due to membrane being punctured.

- (1) An initial stage during which the strains are small
- (2) A range which begins when the specimen begins to yield and which includes the peak of the curve and the gradual decrease of resistance past the peak.
- (3) A final range during which the resistance is constant with further straining, called the ultimate condition.

The shape of the curves suggest that the sand can be considered to be loose rather than dense as there is little difference between the peak stress and ultimate stress. It is surprising though, that the samples do not appear to be heading for a common ultimate condition, corresponding to that of the critical void ratio, even though testing has continued for large values of strain.

The gravel samples were tested at varying initial void ratio's and values of confining stress, which is reflected in the differing shapes of the curves. It is immediately apparent that the shape of the gravel curves are not as regular as that of the sand. (The curves represent a 'best fit' approach, and individual values are frequently scattered about the curve), but that the values of stress sustained by the sample are considerably higher for comparable values of confining pressure, than that of the sand.

The shape of the gravel curves suggest that the gravel can be considered to be medium dense, even though an attempt was made to obtain initial densities as high as possible in some cases. This indicates that the poor grading characteristics of the gravel will only allow a packing density within certain bounds irrespective of the externally applied compaction. This has relevance for stone column formation.

In the case of the gravel there is evidence to suggest that some of the samples are tending towards a common ultimate value.

6.4 STRESS PATHS AND FRICTION ANGLE

Stress paths were plotted, using the method adopted by Lambe (1967) rather than that of Schofield and Wroth (1968). As the tests were consolidated drained triaxial tests the stress paths followed were straight lines which were parallel to each other due to no pore pressures being developed. The stress paths for the sand are given in Fig 6.4, and that of the gravel in Fig 6.5.

The stress path for the sand terminate at a well defined failure line (Kf line) but this is not well defined for the gravel. This is to be expected after consideration of the form of the stress strain curves. It is thus somewhat difficult to establish a Kf line, and hence a consistent value for the friction angle. An observation made on the gravel though was that the stress paths commencing from the same point 'q', but at different initial void ratios will follow exactly the same path with only the length of the path altering in each case.

As the Kf line is not well established for the gravel, the friction angle ϕ' can be established directly for each sample using the maximum values of stress reached in each case and applying the Mohr-Coulomb failure which states

$$\sigma_1' - \sigma_3' = \sin \phi' (\sigma_1' + \sigma_3') \quad (6.2)$$

Table 6.1 shows the value of ϕ' calculated in each case, as well as the void ratio at failure.

TABLE 6.1
SAND

q_f	P_f	e_f	ϕ'°
50	100	0,3444	30,0
125	225	0,3531	33,7
254	454	0,2876	34,0
374	674	0,3007	33,6
767	1367	0,5573	34,1

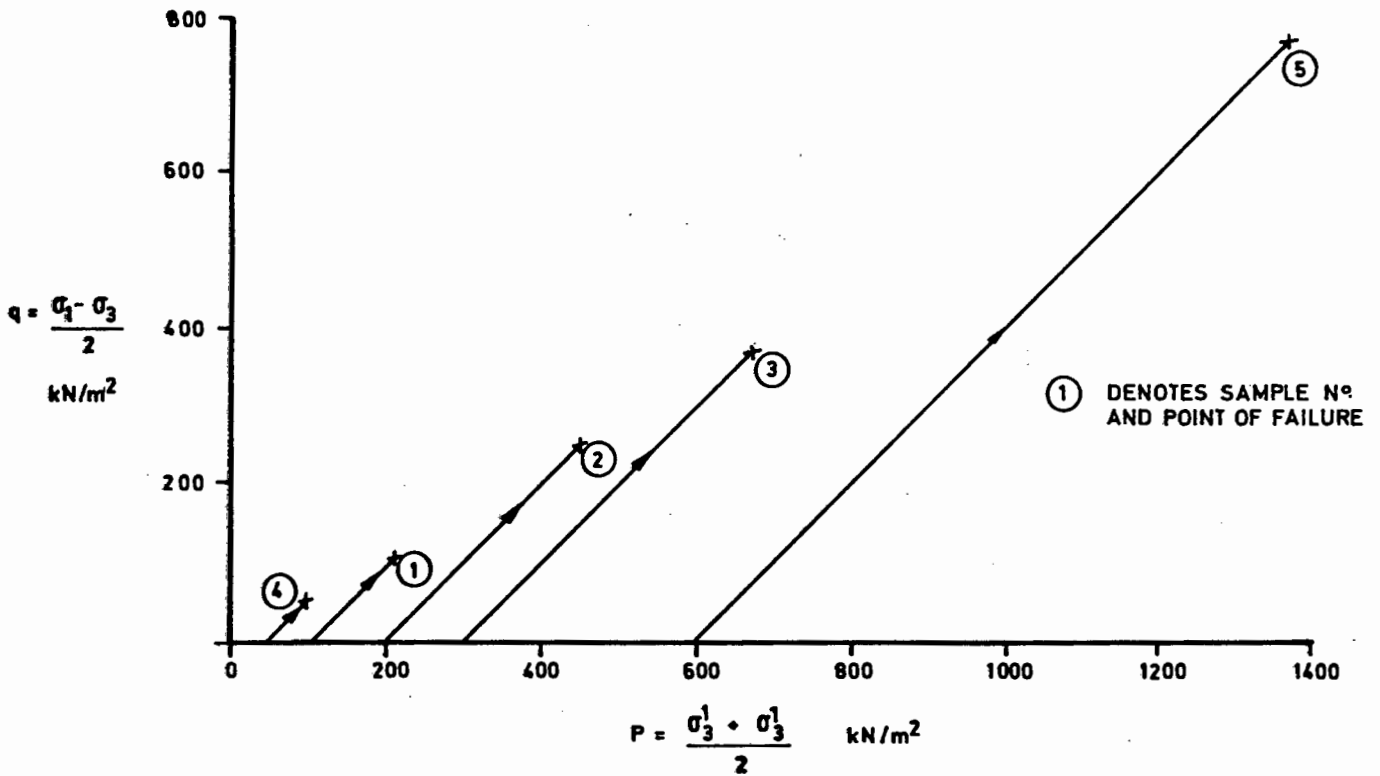


FIG. 6.4 EFFECTIVE STRESS PATHS FOR DENSITY SAND

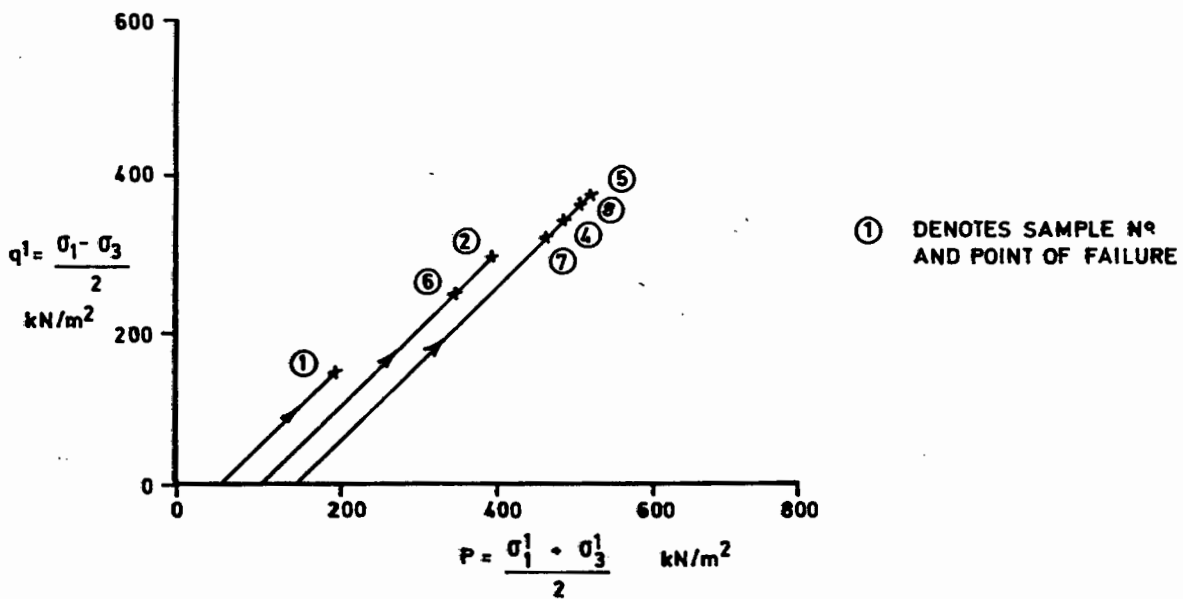


FIG. 6.5 EFFECTIVE STRESS PATHS FOR CRUSHER RUN GRAVEL

(AS TESTED BY THE WRITER FOR THIS THESIS)

q_f	p_f	e_f	ϕ°
146	196	0,8263	48,2
250	350	0,8700	45,6
302	402	0,7198	48,7
319	469	0,7177	42,9
339	489	0,7126	43,9
365	515	0,7320	45,1
369	519	0,7078	45,3

The calculated friction angles obtained show that the more angular gravel has a high degree of interlocking, so resulting in higher friction values. It is therefore clear that an angular gravel should preferably be used for the formation of stone columns, rather than well rounded material such as river gravels.

6.5 INFLUENCE OF VOID RATIO

Cornforth (1964) showed that the angle of shearing resistance decreased as the porosity increased. With reference to Table 6.1 and Fig 6.6 it can be seen that for the limited range of initial void ratios (and hence porosity) considered, this relationship is not well established.

The influence of the void ratio at failure on the stress ratio q/p is demonstrated in Fig. 6.7. The general trend is of decreasing stress ratio with increasing void ratio.

The strain at failure is also strongly linked to void ratio, with higher strain values corresponding to larger values of void ratio, as shown in Fig. 6.8. This is to be expected as it is known that dense sands with a low void ratio fail at relatively low strains whilst loose sands undergo a great deal of compression before failure is reached, as shown in Chapter 4.

- 6.12 -

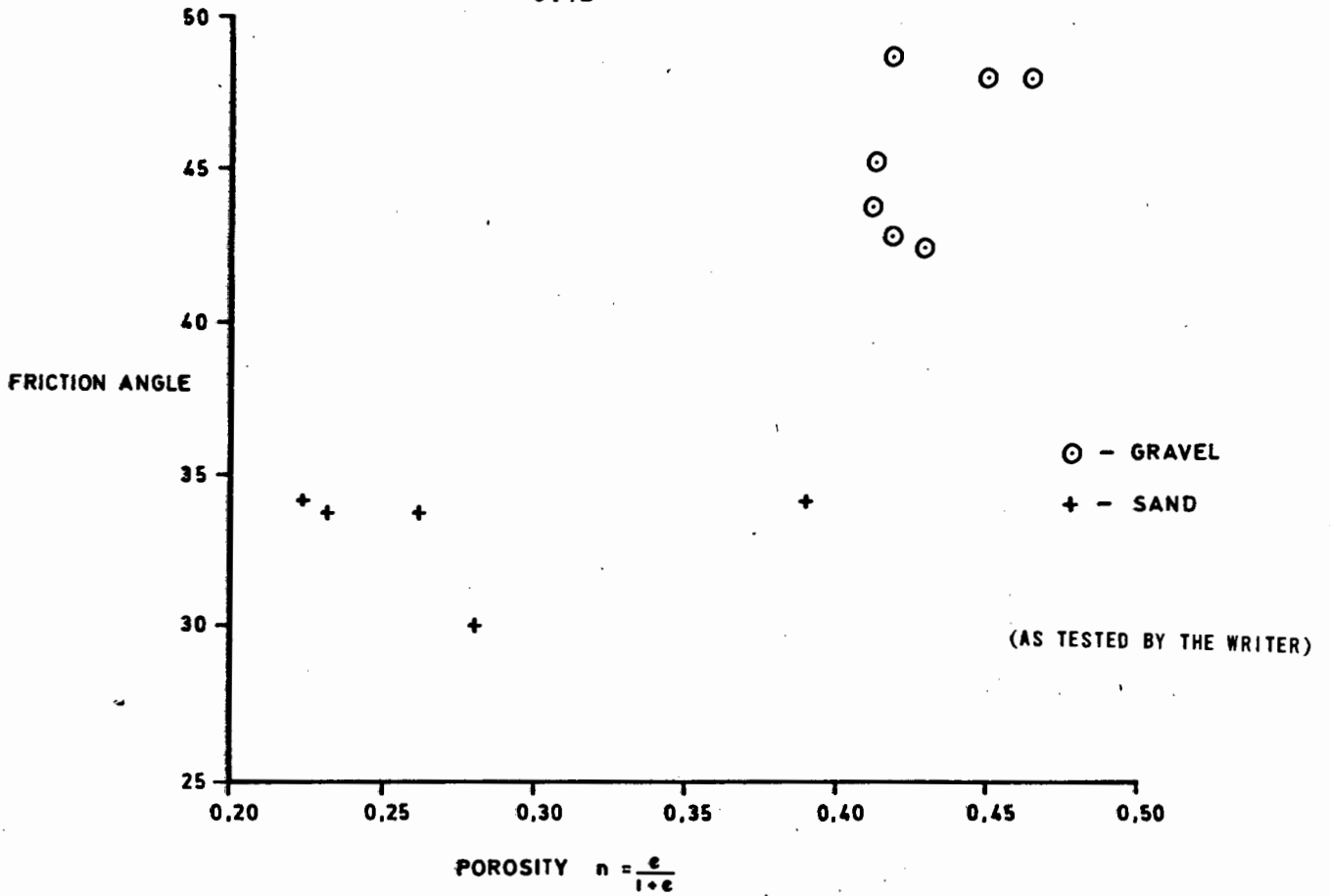


FIG. 6.6 INFLUENCE OF INITIAL POROSITY ON FRICTION ANGLE OF GRAVEL & SAND

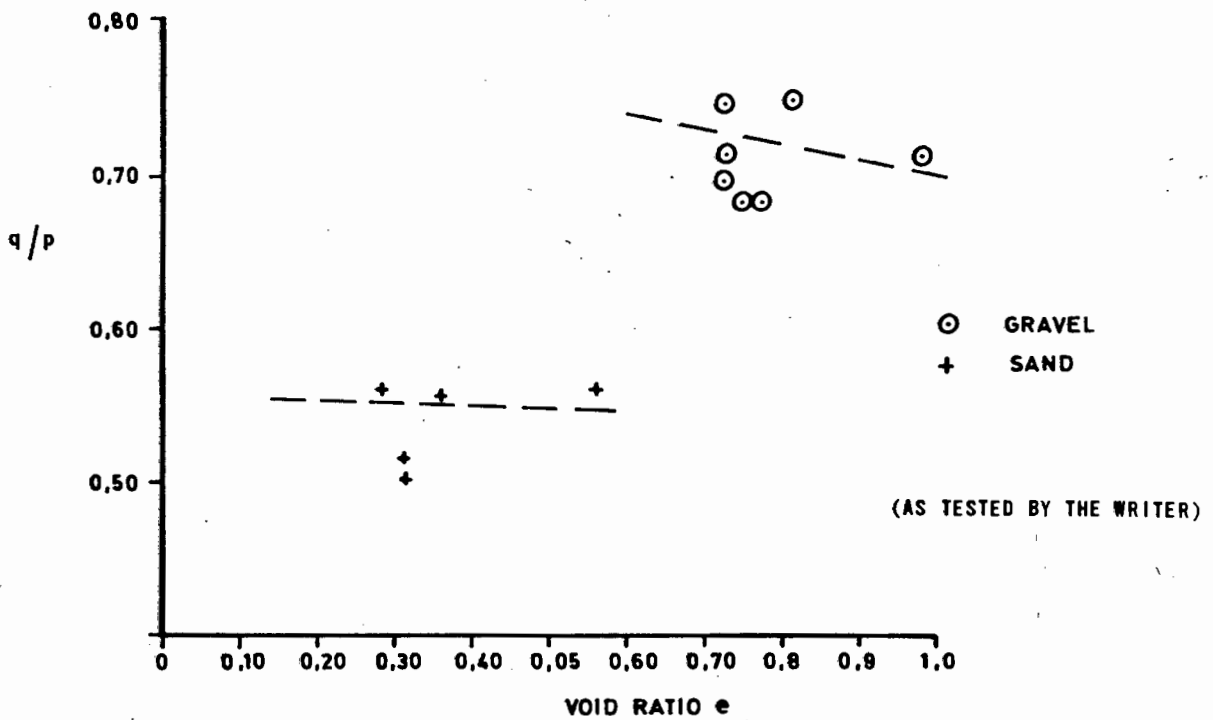


FIG. 6.7 INFLUENCE OF VOID RATIO AT FAILURE ON STRESS RATIO q/p AT FAILURE

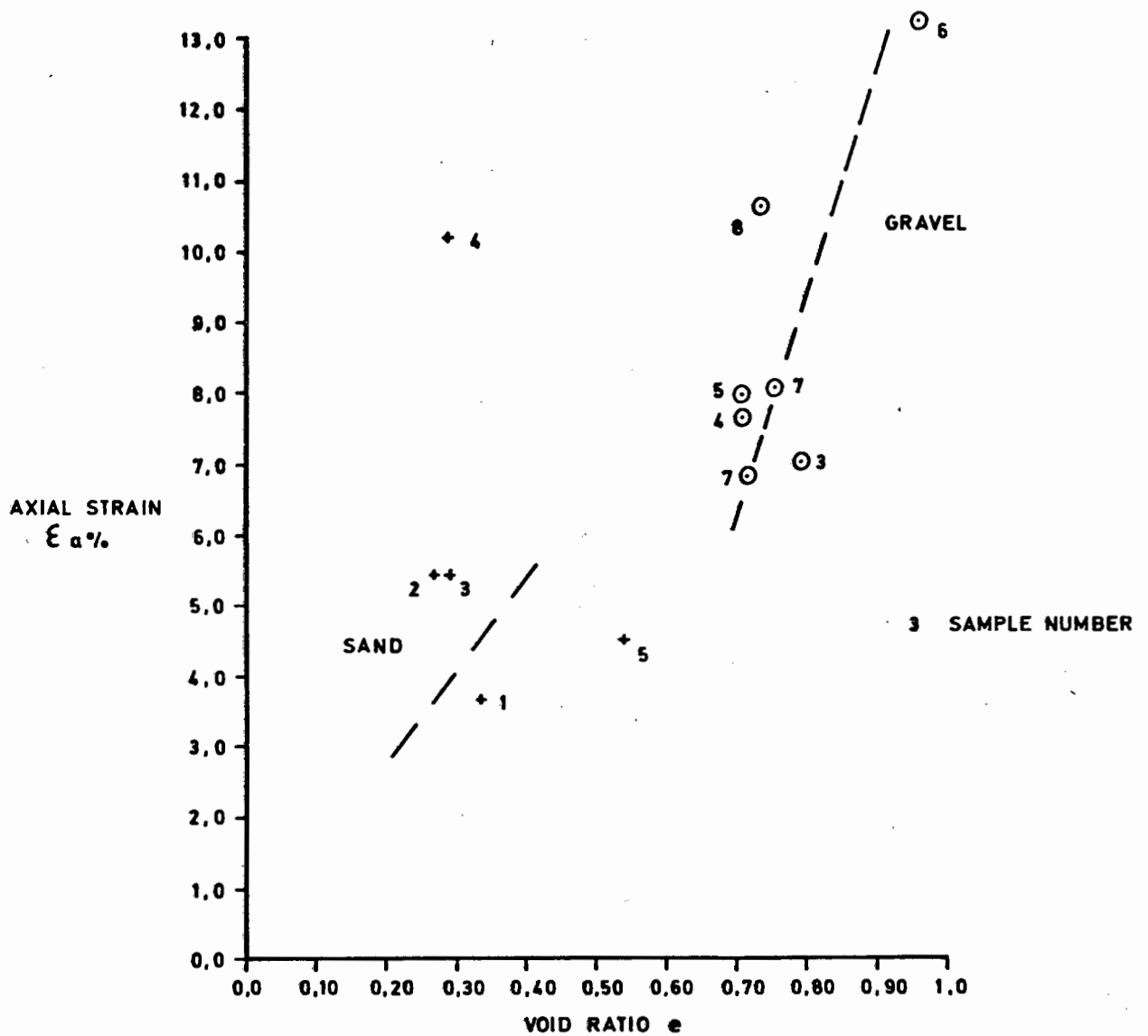


FIG. 6.8 VOID RATIO AT FAILURE v AXIAL STRAIN AT FAILURE

NOTE : THE GRAVEL HAS THE GENERAL TREND OF INCREASING e WITH LARGER AXIAL STRAINS, ALTHOUGH THIS IS NOT AT ALL CLEAR FOR THE SAND. IT SEEMS PROBABLE THAT SAMPLE 4 OF THE SAND IS IN ERROR AND SHOULD CORRESPOND TO A VOID RATIO OF AT LEAST 0,5.

(AS TESTED BY THE WRITER FOR THIS THESIS)

It is thus clear that the void ratio has a significant effect on the behaviour of sands with dense samples sustaining high stresses, but at low strains and loose samples undergoing large strains at vertical constant levels of stress.

6.6 RADIAL STRAIN

The following basic equation relates volume strains to vertical and horizontal strains (Atkinson and Bransby)

$$\epsilon_V = \epsilon_1 + \epsilon_2 + \epsilon_3 \quad 6.3$$

And for triaxial compression $\epsilon_2 = \epsilon_3$

From consideration of the above one would expect the horizontal strains ϵ_2 and ϵ_3 to occur at the same time as ϵ_1 . The laboratory tests, however show that a certain amount of axial strain will occur prior to any horizontal strain. It is admitted that the device used for measurement is somewhat crude, but the consistency of the results does indicate that the development of horizontal strain is retarded. Also, for the range of strain considered, a linear relationship exists between horizontal and vertical strain as shown in Fig 6.9. The significance of the above with regards to stone columns is that a vertical movement will occur prior to the lateral expansion required to develop the passive resistance in the pile.

6.7 RADIAL STRESS

The radial stress-strain relationship is perhaps one of the most important regarding the performance of a stone column. Results obtained were plotted with the 'y' axis forming the principal stress ratio σ_3/σ_1 and the horizontal strain plotted on the 'x' axis (Fig 6.10)

The stress ratio for the sand lies within a very narrow band compared with that of the crusher gravel, but in both cases the trend is the same with higher horizontal strains at lower stress ratios. The results obtained from the sand suggests that a

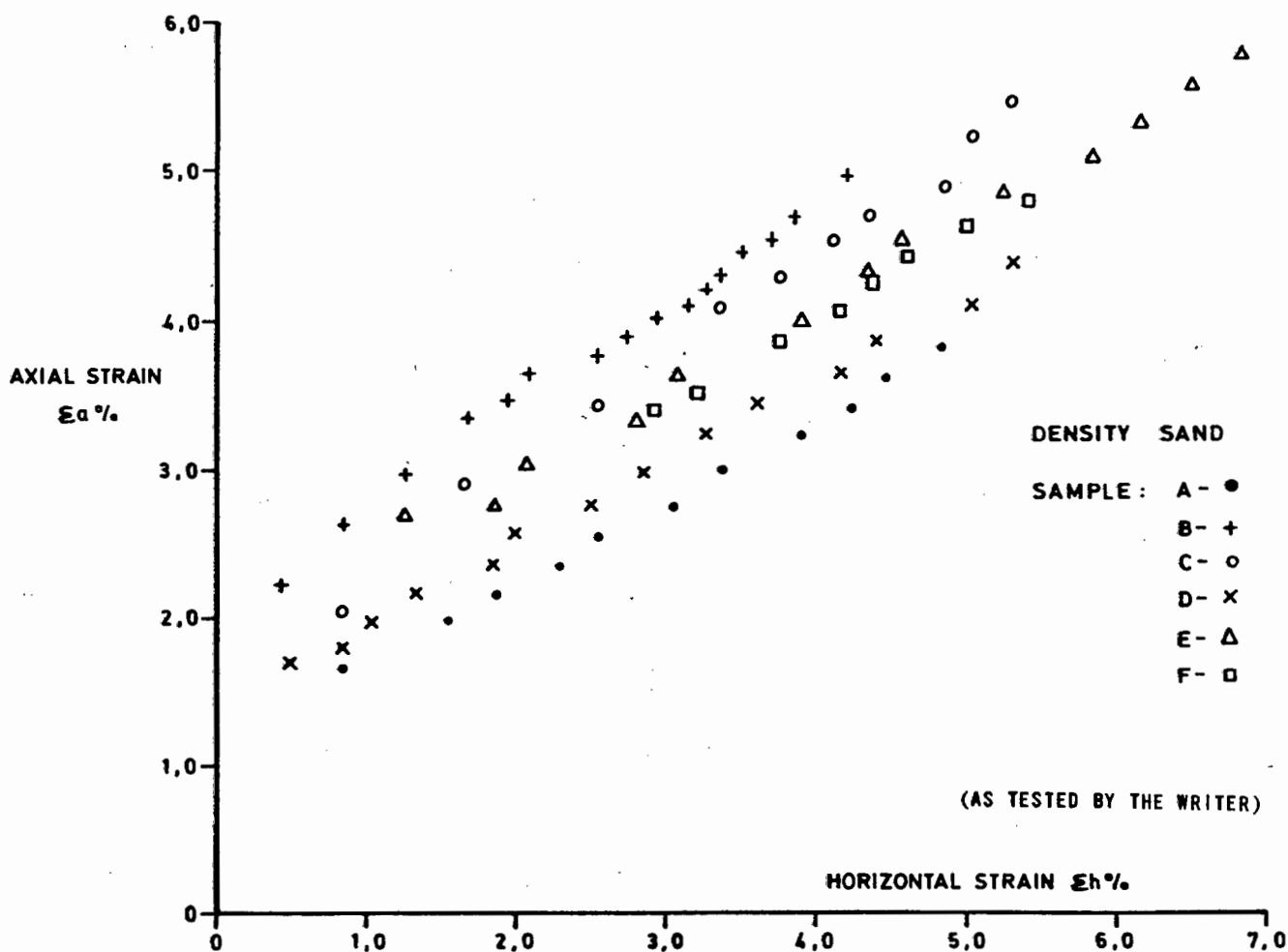
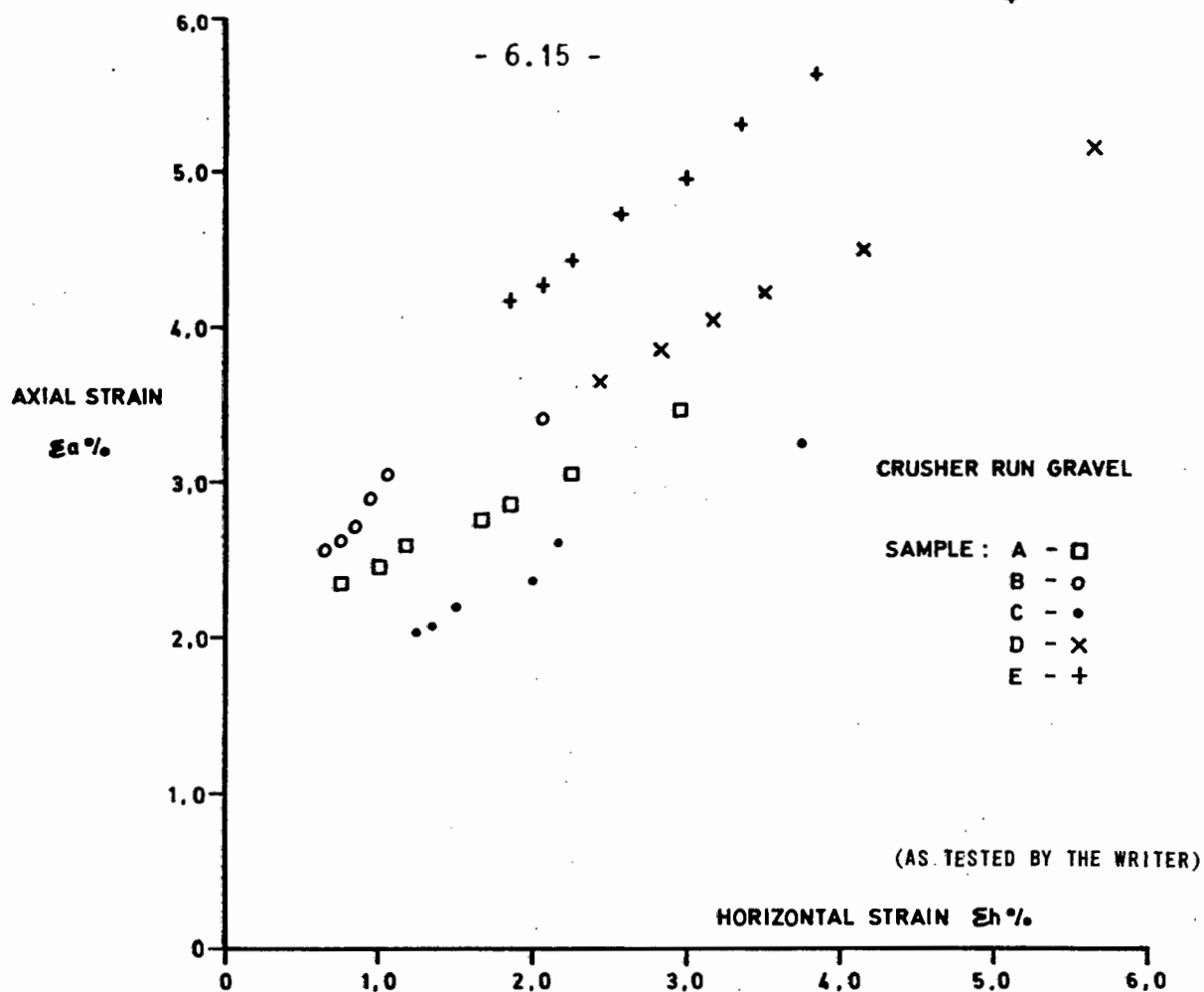
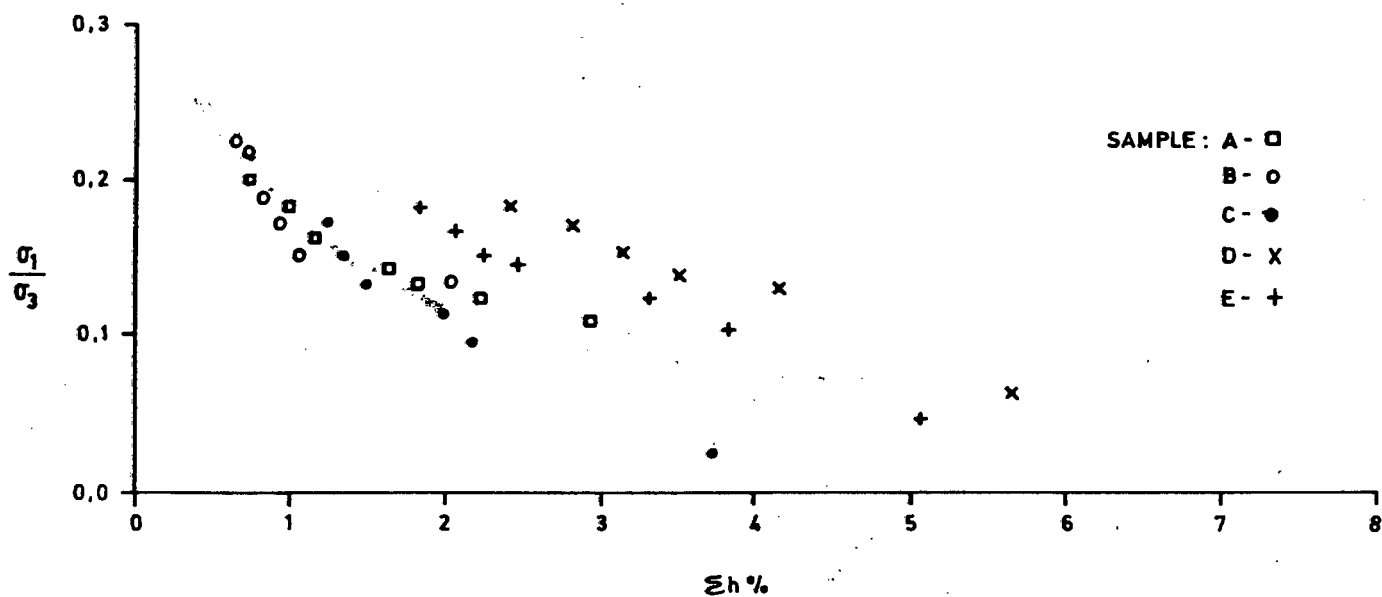
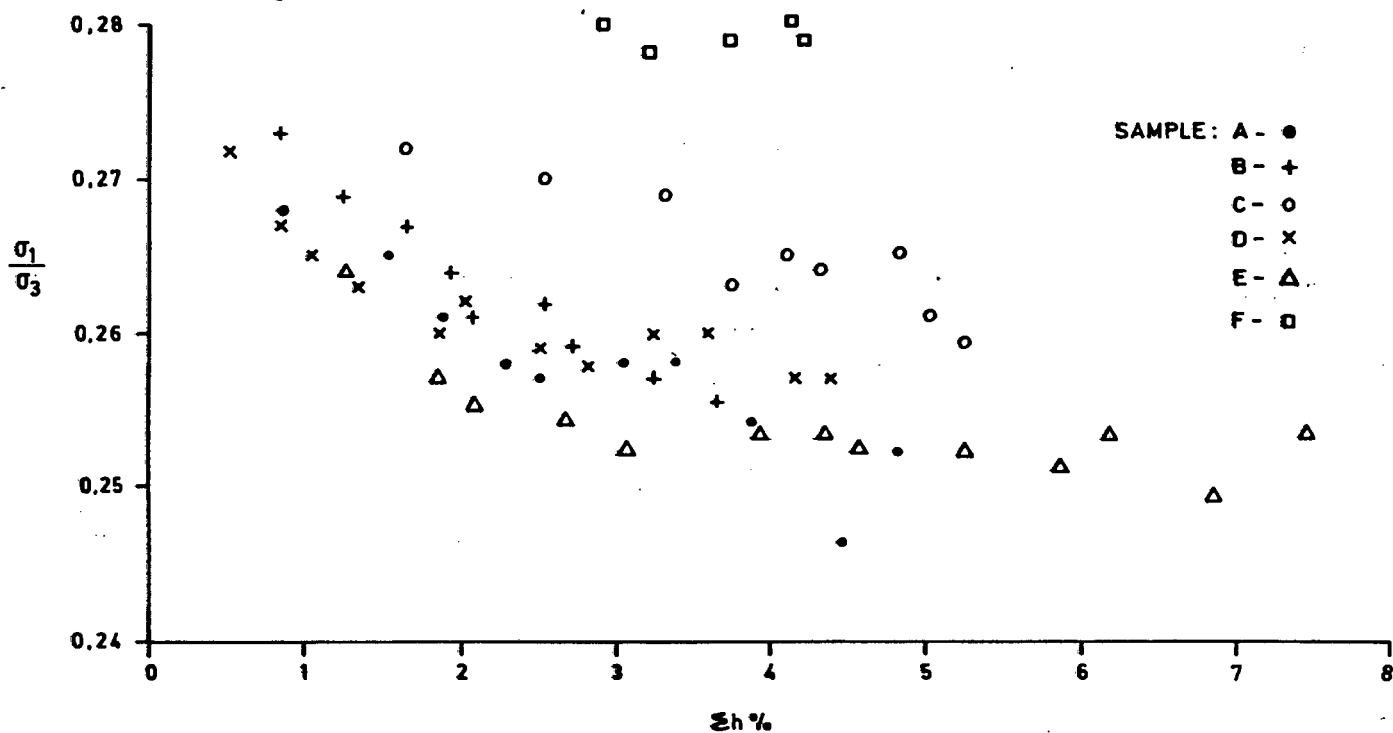


FIG. 6.9 RELATIONSHIP BETWEEN AXIAL AND HORIZONTAL STRAIN

CRUSHER RUN GRAVEL



DENSITY SAND



(AS TESTED BY THE WRITER FOR THIS THESIS)

FIG. 6.10 PRINCIPLE STRESS RATIO σ_1/σ_3 v HORIZONTAL STRAIN $\epsilon_h \%$

lower limit of stress ratio is reached, at which point increasing horizontal strain occurs for a constant stress ratio. It is to be expected that such a point is represented by a coefficient of active pressure K_a within the column, and such a point would correspond to a bulging failure for the column.

For the sand the minimum stress ratio occurs at approximately 7% radial strain, and corresponds to a K_a value of approximately 0,25. For the gravel the K_a value is much smaller, of the order of 0,05 to 0,01 at a radial strain of approximately 6%.

The implications of the differing behaviour of the two materials is that the sand requires a higher radial confining stress to prevent failure than does the gravel. This implies that in weaker soils it is preferable to use material having high friction angles for the formation of the stone columns.

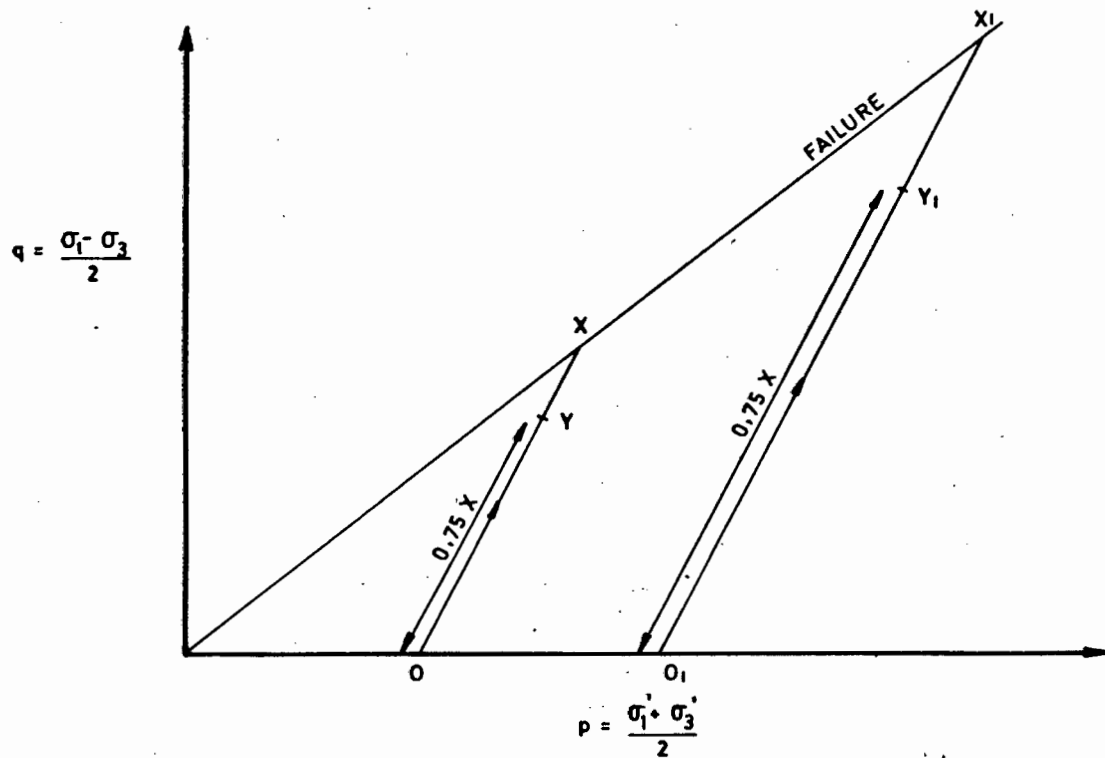
6.8

NON DIMENSIONAL RELATIONSHIPS BETWEEN STRESS AND STRAIN

All that has been mentioned to date in this chapter is basically a reaffirmation or otherwise of known soil mechanics behaviour, and presents a somewhat confused picture of stress-strain relationships as the laboratory results do not always conform with the established patterns idealized in text books.

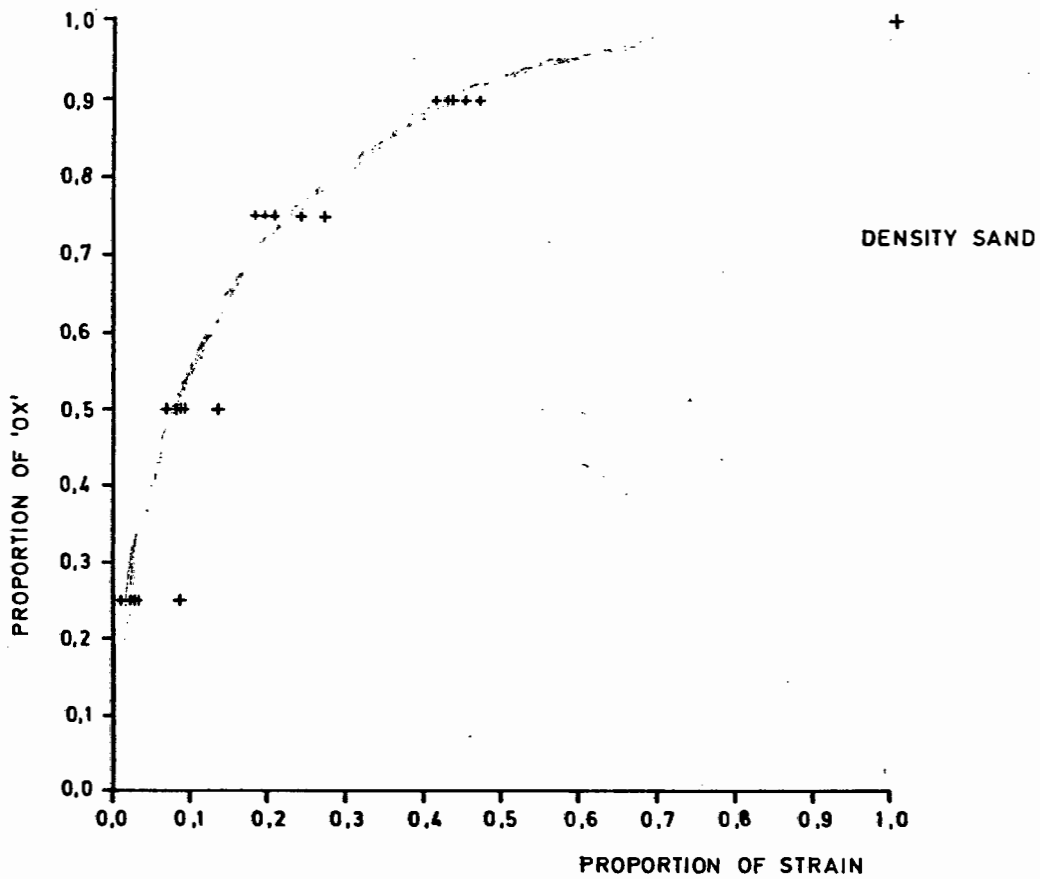
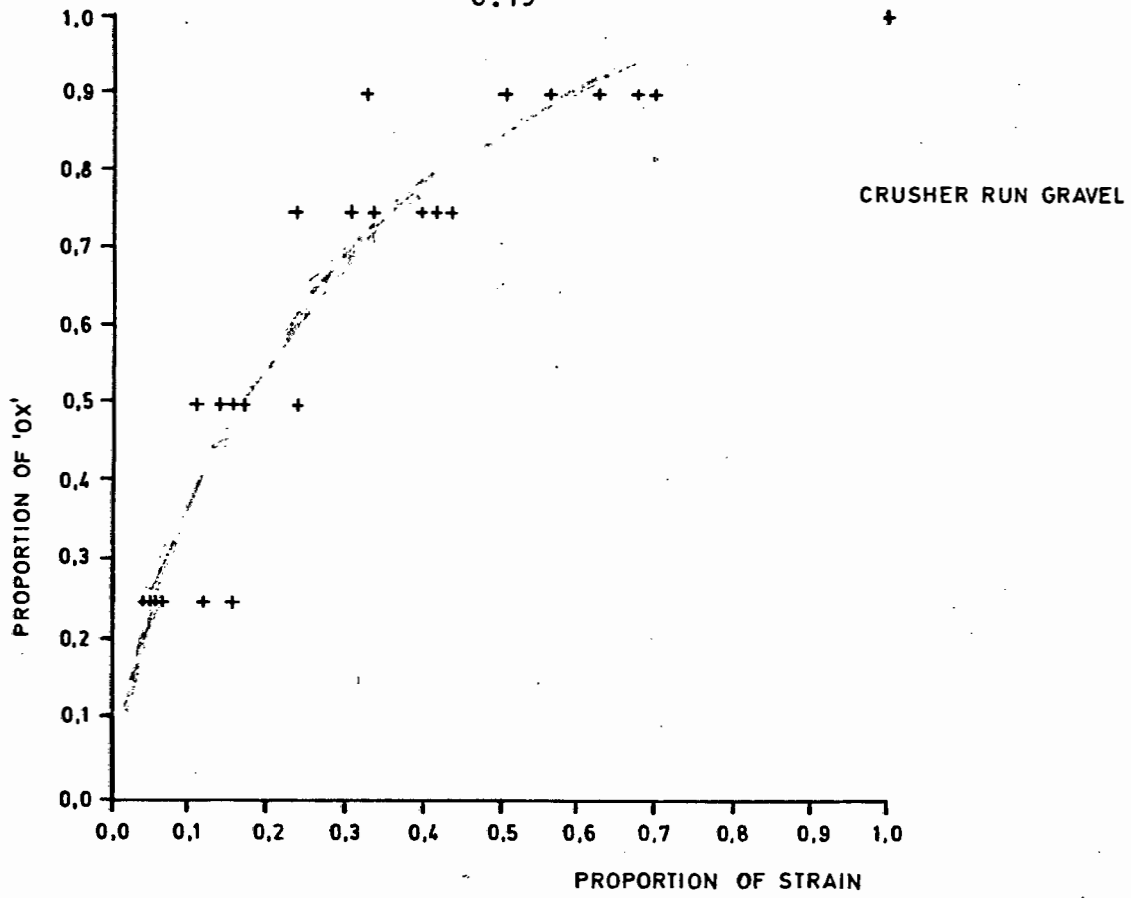
A new relationship between stress and strain is now described which produces remarkably consistent results which appear to be independent of the initial void ratio. The relationship was suggested by Sparks (1980) but has not been tested prior to this presentation. The results apply to consolidated drained tests.

It was suggested by Sparks that a relationship exists between the proportion of stress at failure and the corresponding proportion of strain. This can be visualized with reference to the idealized stress paths as shown in Fig 6.11



- PROCEDURE :
- (1) DRAW IN STRESS PATHS OX, O₁X₁, etc.
 - (2) PROPORTION OX, eg. OY AND FIND CORRESPONDING STRAIN.
 - (3) EXPRESS STRAIN AS PROPORTION OF FAILURE STRAIN.
 - (4) REPEAT FOR NEW VALUE OF OY, eg. 0.5.
 - (5) PLOT RESULTS AS SHOWN IN Fig. 6.12

FIG. 6.11 DERIVATION OF PROPORTIONAL NON DIMENSIONAL STRESS STRAIN PLOT



(AS TESTED BY THE WRITER FOR THIS THESIS)

FIG. 6.12 PROPORTIONAL NON DIMENSIONAL STRESS STRAIN RELATIONSHIP

For any stress path starting at a point 'O' on the P axis, failure occurs when the stress path reaches the point X on the failure line Kf. If one now considers various proportions of OX, such as 0,75 OX, 0,5 OX etc. and now relates the strain at such points to the strain corresponding to point 'X', one ends up with proportions of stress at failure and proportions of strain at failure. The geometry of Fig 6.11 is such that one can just as easily proportion 'q' direct.

Results obtained for the sand and gravel are shown in Fig 6.12. It can be seen that the curve fit is excellent in both cases and shows the consistency of a relationship between stress and strain which is not apparent from the conventional stress strain curves of Fig 6.2 and 6.3.

The curves can be thought of as yield lines which will be unique for differing materials. It is not a yield surface as the line represents all possible stress states, and points cannot exist above or below the line. A yield surface would act as a boundary, but would allow permissible states of stress below the surface, e.g. the Roscoe surface.

The above relationship will be incorporated in a possible design method for stone columns, details of which occur in a later chapter.

6.9

SUMMARY

1. For isotropic compression the relationship between specific volume and mean normal stress can be represented by straight lines on a $v : \ln p'$ diagram. The parameters κ and λ obtained are very small.
2. Due to particle break up under high stresses, the shape of the stress-strain curves for gravel are more irregular than the well rounded sand.

3. The greater interlocking due to the angular nature of the gravel results in higher friction angles than that of the sand.
4. The void ratio of a sample has a strong influence of the ultimate behaviour of the sample.
5. A certain amount of axial strain occurs prior to the development of any radial strain.
6. A limiting value of stress ratio σ_3/σ_1 exists at which point the horizontal strain increases indefinitely for a constant value of stress ratio.
7. A proportional representation between stress and strain at failure exists. Such a relationship is independent of void ratio.

CHAPTER 7

THE INTERACTION OF A RAFT-PILE SYSTEM

7.1

INTRODUCTION

A complex interaction occurs within a loaded raft-pile system. The rigidity of the raft affects the load distribution to the piles, which in turn, affects settlement characteristics of the system. Various methods exist with which to analyse a raft and this chapter briefly looks at some of them as well as the influence of the gravel piles on the raft design.

A complete analysis of the soil-structure interaction between the raft and piles is outside the scope of this chapter.

7.2

RIGID DESIGN METHOD

In the rigid method of raft design the assumption is made that the raft is infinitely rigid and that a deflection will not influence the shape of the pressure distribution, which will be planar. Lee (1977) has found that a raft can be considered rigid if F is less than unity where :

$$F = \frac{\pi L^4 E_s (1 - \nu_r^2)}{16(1 - \nu_s^2) E_r I_r B} \quad (7.1)$$

where B, L = width and length of the raft

E_s, ν_s = elastic parameters of the soil

E_r, ν_r = elastic parameters

I_r = flexural rigidity of the raft.

For a uniformly distributed load the method implies that the piles will carry an equal load. However, due to the influence of the gravel piles, consolidation of the clay will be greater towards the centre of the raft than at the edges and would result in a smaller stress on centre piles.

7.3

SIMPLIFIED ELASTIC METHOD

The difference in consolidation beneath the raft can be allowed for if a Winkler type analysis is used (Teng 1962). In a Winkler system the soil is considered to be an infinite number of coil springs which are not affected by each other. The spring constant is taken as the coefficient of sub-grade reaction k (Terzaghi 1955), which will vary for both the pile and clay. For such a system however, no settlement is assumed to occur outside the loaded area as the springs are not connected.

The differential equation for the deflection of a mat foundation is to be found in most works on structural analysis (Timoshenko and Woinowsky Krieger 1959, Deryck and Severn 1960, 1961) and is given by:

$$\nabla^4 w = \frac{q - kw}{D} \quad (7.2)$$

$$\text{where } \nabla^4 w = \frac{\partial^4 w}{\partial x^4} + 2 \frac{\partial^2 w}{\partial x^2 \partial y^2} + \frac{\partial^4 w}{\partial y^4}$$

q = intensity of loading

k = coefficient of sub-grade reaction

D = rigidity of mat.

The above (eqn. 7.2) readily lends itself to a solution by finite difference methods (Bowles 1977), with suitable values of k being assigned for the raft and pile respectively.

Lee (1977) argues against the use of a Winkler type solution as this leads to the maximum bending moment increasing with raft flexibility, whereas a linear elastic method predicts the observed fact that there is a decrease in maximum bending moment with increase in raft flexibility.

7.4

TRULY ELASTIC FOUNDATION

The soil is assumed to be a truly elastic material obeying Hooke's law. For such an analysis settlements will occur outside the loaded area, unlike that of a true Winkler system. An elastic analysis is ideally treated using finite element techniques

Severn (1966).

7.5 RAFT AND GRAVEL PILES.

An analysis of a raft supported by gravel piles has been undertaken by Balaam and Booker (1979), using equation 7.2 which is rewritten to give:

$$\nabla^4 w = p/D \quad (7.3)$$

where $p = q_a - q_r$, the net load distribution acting on the raft
 q_a = the pressure exerted by the applied load
 q_r = the reaction pressure exerted by the underlying columns and soil.

The analysis shows that the spacing of the piles influences the shear forces and bending moments, with larger spacings causing noticeable increases in the maximum positive bending moments, whilst the negative bending moment remains virtually constant. Also, as the pile spacing increases, the maximum shear force, which occurs at the soil pile interface, increases. There is zero shear at the centre of the pile.

Increasing the stiffness ratio E_1/E_2 of the column and clay respectively increases the rate of settlement, but also increases the shear forces and maximum bending moment.

7.6 INFLUENCE OF THE STRUCTURE

Moments and shearing forces are sensitive to the column loads and the structure, raft and supporting media should ideally be considered as a compatible system (Hain and Lee 1974, Lee and Brown 1972, Sommers 1965), but this is considered to be outside the scope of this chapter.

7.7 SUMMARY

1. Various methods exist for the analysis of a raft foundation, although opinions differ as to which method should be used.

2. The spacing of gravel piles influences the magnitude and distribution of bending moments and shear forces within the raft.
3. Shear forces and bending moments increase as the stiffness ratio E_1/E_2 increases.
4. For a complete analysis the influence of the superstructure should be considered.

CHAPTER 8

CURRENT DESIGN PRACTICE

8.1 INTRODUCTION

The use of stone columns in soft clays has extended over recent years, as has the need to form a rational design method for such columns. This chapter deals with three such methods, one uses conventional earth pressure theory whilst in another use is made of pressuremeter theory and finally, a sophisticated elastic analysis is given. Each system has its merits and demerits and will be commented on accordingly.

8.2 EARTH PRESSURE METHOD

Perhaps one of the simpler design approaches involves the use of earth pressure theory as in the design of a retaining wall (Wong 1975). It is assumed that the horizontal stress distribution within a stone column decreases linearly with depth, and the same stress distribution exists in the surrounding soil. As the foundations settle a redistribution of stress occurs as the passive resistance of the surrounding soil increases, with higher horizontal stresses being mobilized at greater depths. If it is assumed that the total horizontal force of the column is constant during the redistribution of stress, the vertical stress can be calculated for any degree of settlement as this depends upon the horizontal stress distribution of the column and the passive resistance of the soil.

If the soil - column boundary is rigid, the horizontal stress distribution in the column will decrease from a maximum value of $K_a \cdot q$ at the surface, where K_a is the coefficient of active pressure in the column and q the vertical stress on the column. However, as the columns yield more load is transferred to the lower parts. It should be noted that when equilibrium is reached the horizontal stress in the soil and column must be compatible.

If the passive pressure P_s in the soil is now considered the stress

would increase with depth as given by :

$$P_s = K_p (q_0 + \gamma ch) + 2cK_p^{\frac{1}{2}} \quad (8.1)$$

where K_p is the coefficient of passive earth pressure

γ is the bulk density

h is any depth less than H , the column depth

q_0 is the vertical stress on the soil surface

c is soil cohesion

For small settlements the maximum passive pressure in the soil should occur at the surface and be equal to :

$$K_p \cdot q_0 + 2cK_p^{\frac{1}{2}} \quad (8.2)$$

It has been suggested by Dullage (1969) and Williams (1969) that increased settlement will cause the maximum passive pressure to decrease from the surface to a depth between two and three times the column radius. For large settlements it is likely that the passive resistance will be mobilised throughout the length of the column.

Since passive stresses within the soil are in equilibrium with the active stresses in the column, then for small settlements

$$q = (K_p \cdot q_0 + 2cK_p^{\frac{1}{2}}) / K_a \quad (8.3)$$

If it is assumed that the unit total horizontal force summed over the whole column depth remains constant during stress redistribution, then for medium settlements the unit total force in the column can be equated to the horizontal force in the soil from the surface to a depth $3a$ to give:

$$q = \{ (K_p \cdot q_0 + 2cK_p^{\frac{1}{2}}) + \frac{3a}{2} K_p \gamma + (1 - \frac{3a}{2H}) \} / K_a \quad (8.4)$$

and for large settlements the horizontal forces are summed over the whole length of the column to give :

$$q = 2 \{ (K_p \cdot q_0 + 2cK_p^{\frac{1}{2}} + 3aK_p^{\frac{1}{2}}) + 3aK_p \gamma (1 - \frac{3a}{2H}) \} / K_a \quad (8.5)$$

from the above equations the following design criteria can be established .

Total safe design load P_s :

$$P_s = qA_c + q_0A_s \quad (8.6)$$

where $q = (Kpq_0 + 2cKp^{\frac{1}{2}}) / K_a$ $q_0 = \text{vertical stress}$

$A_c = \text{area of column}$

$A_s = \text{area of surrounding soil}$

$A_c + A_s = \text{total foundation area } A$

and the total ultimate load P_u :

$$P_u = qA_c + q_0A_s \quad (8.7)$$

where $q = 2\{ (Kpq_0 + 2cKp^{\frac{1}{2}}) + 3a Kp\gamma(1 - \frac{3a}{2H}) \} / K_a$

The following values of q_0 have been recommended:

$q_0 = 1.5c$ for small settlements

$q_0 = 2.5c$ for medium settlements

$q_0 = 3c$ for large settlements .

The above method as proposed by Wong is fairly simple in its application, but no indication is given as to what is a large or small settlement. Also, a design length for columns is not indicated, although a trial and error method would quickly arrive at the desired length. It is also interesting to note that the approach is in terms of total stress and no allowance has been made for the bulging of the column due to changes in stress caused by radial consolidation, i.e. an effective stress analysis.

8.3

PRESSUREMETER ANALOGY

A widely used design method is that of Hughes and Withers (1974) in which the expansion of a stone column under load has been likened to that of a pressuremeter. Model tests using radiographic techniques have clearly shown that vertical and radial displacements occur during loading, and that these rapidly diminish with depth with about four column diameters depth being strained at failure. This is summarised in Fig. 8.1 and 8.2. Also, loading of a column affects the area of clay within a cylinder up to two and a half times the diameter of the column, which means that columns

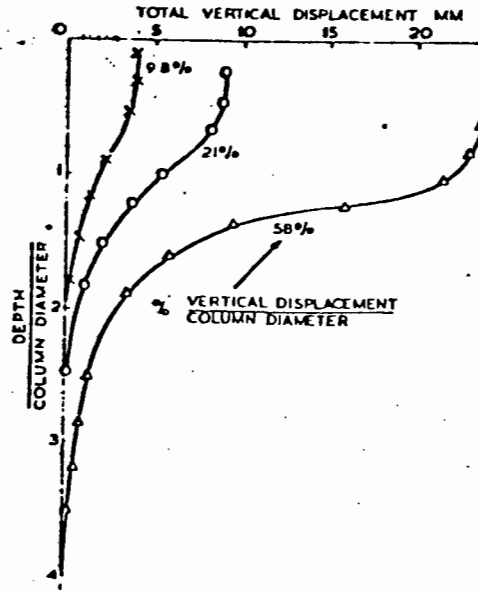


Fig. 8.1 Vertical displacement within the column against depth.

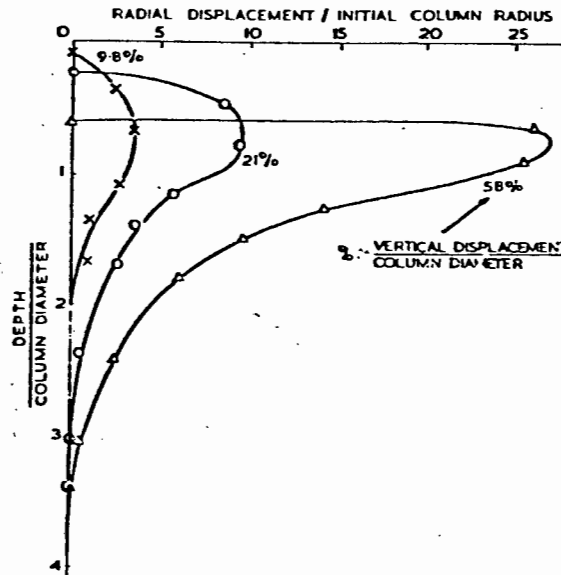


Fig. 8.2 Radial displacement at the edge of the column/initial column radius against depth.

(Hughes and Withers 1974)

greater than this distance apart can act independently.

The expansion of a stone column has been idealised as a pressuremeter (Gibson and Anderson 1961) for which the limiting radial stress σ_{rL} is

$$\sigma_{rL} = \sigma_{r0} + c \left\{ 1 + \log \frac{E}{2c(1+\mu)} \right\} \quad (8.8)$$

where σ_{r0} is the in-situ lateral stress

c is the undrained cohesion

E Elastic modulus

μ Poisson's ratio

This can be approximated to

$$\sigma_{rL} = \sigma_{r0} + 4c + u \quad (8.9)$$

where u is the initial excess pore pressure

As the column approaches failure the limiting stress in the column is

$$\sigma_v = \sigma_{rL} \frac{\{1 + \sin \phi\}}{\{1 - \sin \phi\}} \quad (8.10)$$

Substituting gives :

$$\sigma_v = \frac{\{1 + \sin \phi\}}{\{1 - \sin \phi\}} \{\sigma_{r0} + 4c + u\} \quad (8.11)$$

The values of σ_{r0} or c should be the minimum that would be expected over the critical length of the column.

Equation 8.11 gave results that agreed closely to those observed in model tests.

A comparison of various methods of calculating the radial stress suggested that triaxial tests or Camkometer results will give results which best fit in with those obtained from field trials (Hughes, Withers and Greenwood 1976). It should be noted that the Menard pressuremeter gave a limiting radial pressure which

was twice that of the Cambridge pressuremeter (Camkometer). Marsland (1977) has shown that equation 8.8 is slightly in error but this does not affect the above calculations due to the approximations made in obtaining equation 8.9. Further details concerning pressuremeters and pressuremeter theory can be found in the work of Baguelin et al (1978).

The critical column length can be found using a similar approach to that of conventional pile design as it is assumed that vertical shear stress developed along the sides of the column is equal to the average shear strength of the soil when end-bearing failure is about to occur.

$$\text{Hence } P = \bar{c}A_s + N_c c A_c \quad (8.12)$$

where P = the ultimate column load

N_c = a bearing capacity factor (usually 9 for a long column)

A_s = the surface area $\pi D L_c$ of the column sides of diameter D .

L_c = the critical length of the column

A_c = the column cross-sectional area $\pi D^2/4$

\bar{c} = average shaft cohesion

c = the cohesion at the bottom of the critical length

Settlement is calculated on the assumption that the column expands radially with settlement and retains a constant volume. The soil is divided into layers and the strain in each layer is summed to give total settlement, thus:

$$\delta = \delta_1 + \delta_2 + \delta_3 + \dots \delta_n \quad (8.13)$$

where $\delta_n = 2H \delta r_n / r$

H = thickness of soil layer considered

$\delta r_n / r$ = radial strain for layer under consideration.

Field trials carried out by Hughes indicate that the above method for calculating failure loads and settlements gives good agreement with the field trials provided the diameter of the column is correctly assessed. However, the analysis has again been based

on consideration of undrained behaviour whereas an effective stress solution would be more appropriate.

In the settlement calculation it has been assumed that the vertical strain is equal to twice the radial strain. Laboratory tests on triaxially contained sands and gravels (Ch. 6) suggest that this is not strictly correct. Also, the long term effect of drainage towards the column has not been taken into account.

8.4 ELASTIC DESIGN METHOD

Balaam and Booker (1979) have undertaken an analysis of rigid rafts supported by granular piles. In the analysis each pile with its area of influence is considered to be cylindrical and a Young's Modulus E_1 and E_2 , and Poisson's ratio ν_1 and ν_2 are assigned to the pile and the clay respectively. The five dimensionless parameters that are employed are small a/b , h/b , E_1/E_2 , ν_1 , ν_2 where h is the height of the column, 'a' is the stone column radius and 'b' the radius of the area of influence which extends into the clay.

A finite element analysis showed that:

- i) The vertical displacement was near uniform on any horizontal plane and varied linearly from a maximum value at the surface to zero at the base.
- ii) Shear stresses developed along the substratum were small.
- iii) Surface vertical displacement, horizontal displacement and contact stresses are insensitive to the base condition.

The analysis also showed that the initial contact stresses between the rigid raft and soil is uniform over both the pile and soil, and that the stress state in the pile is triaxial.

A parametric study was undertaken to determine the effects of the dimensionless parameters on the stresses and strains in the cylinders

considered. The parameter h/b was not studied as a smooth base was assumed. The findings are listed below, and reference should be made to the series of graphs which have been reproduced directly from Balaam and Booker's paper.

The effect the introduction of piles has on the reduction of settlement can be seen from Fig. 8.3. As the stiffness of the column increases relative to the clay the settlement relative to that of an area not treated by gravel piles decreases. This thus shows the effectiveness of gravel piles in soft clays to reduce settlements.

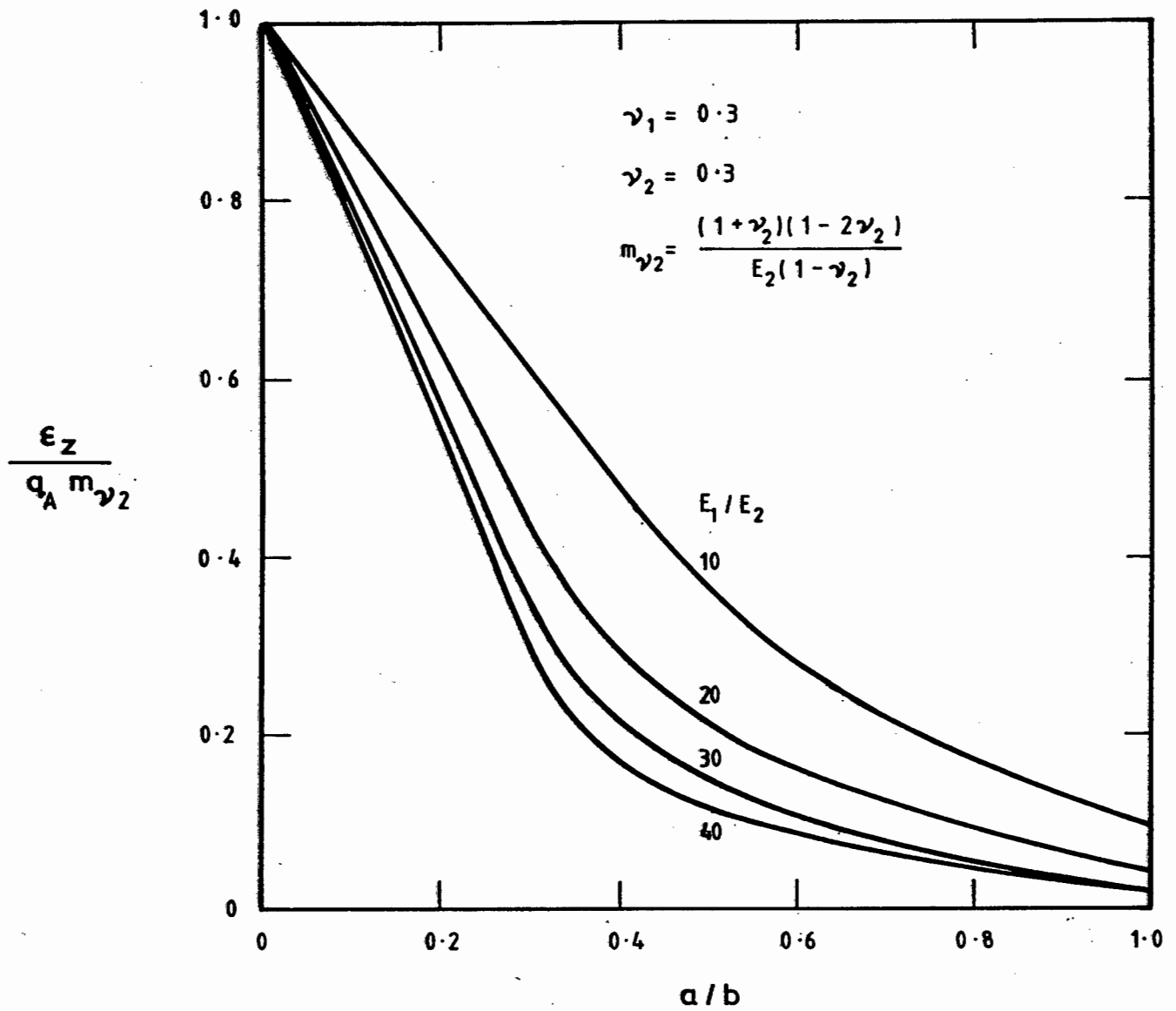
A correction factor for Fig. 8.3 is shown in Fig. 8.4 for varying values of the parameter ν_2 . It can be seen that for a constant E_1 / E_2 ratio, increasing the value of Poisson's ratio of the clay results in a decrease in vertical strain. The effect of consolidation upon the vertical strain can now be seen as the value of ν_2 changes from a fully saturated condition of $\nu_2 = 0,5$ to a lower value and hence increases strain within the pile.

Fig. 8.5 shows that for a constant b/a ratio and a constant value of q , a stiffer column results in a greater stress on the column. This suggests that columns are more efficient if the raft is rigid as more load is carried by the columns.

Upon initial loading, the clay, which is undrained, may be effectively stiffer than the column. However, as pore pressures dissipate the relative stiffnesses change and the contact stress on the columns exceeds that of the clay. This is shown in Fig. 8.6. It should be noted that moment and shear distributions within the raft would change accordingly.

The time dependent behaviour of the raft is also analysed using a finite element method applied to Biot's equations for consolidation. The stone columns are assumed to be infinitely permeable, with a soil permeability being Kh . A time factor T_h is defined in terms of the radial coefficient of consolidation c_r where

$$c_r = \frac{Kh E_2 (1 - \nu_2)}{\gamma_w (1 + \nu_2)(1 - 2\nu_2)} \quad (8.14)$$



**FIG. 8.3 VERTICAL STRAIN OF PILE - SOIL UNIT
WITH VARYING SPACING**

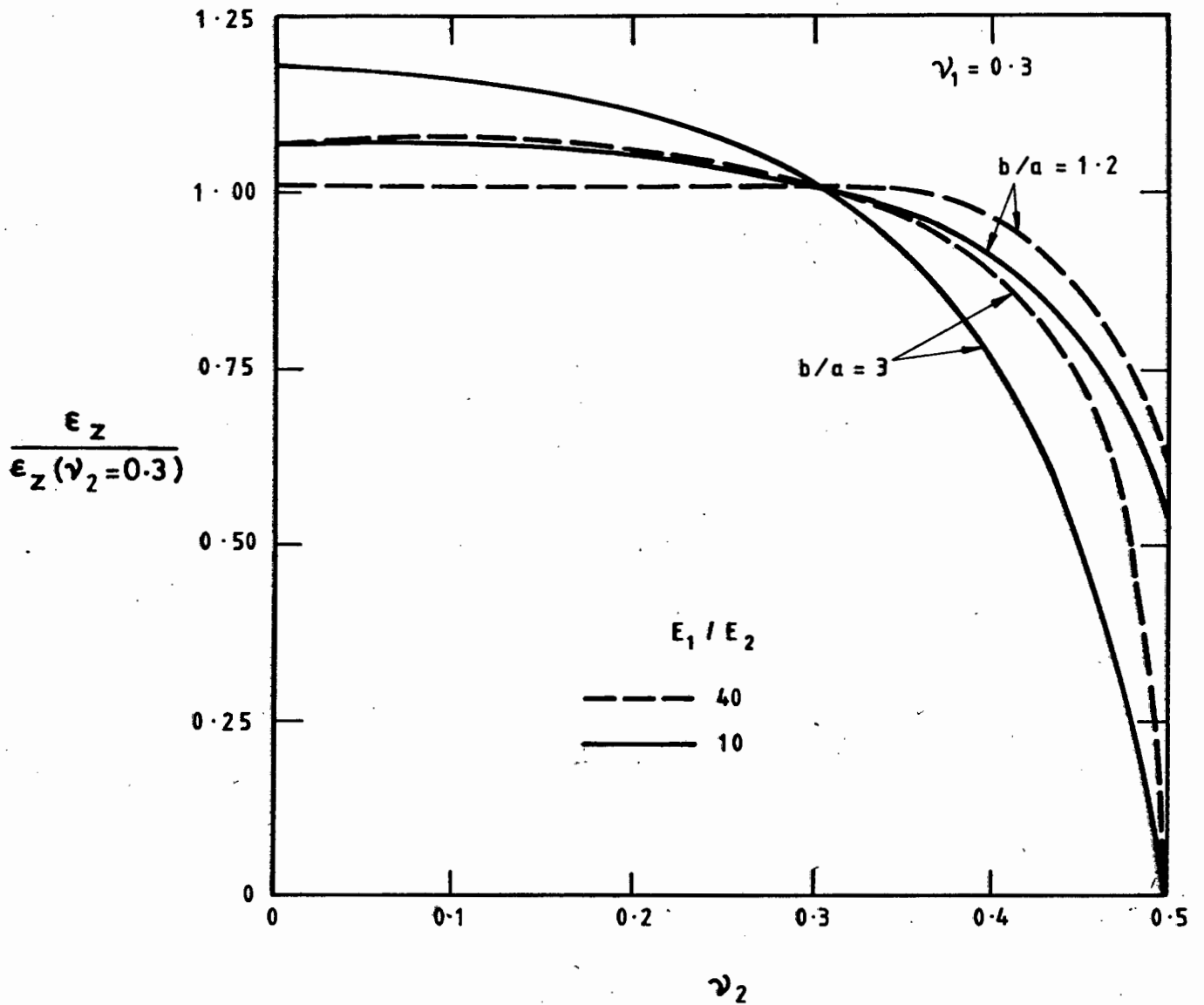


FIG. 8.4 RATIO OF STRAINS FOR CALCULATING SETTLEMENTS FOR THE COMPLETE RANGE OF POISSONS RATIOS ν_2

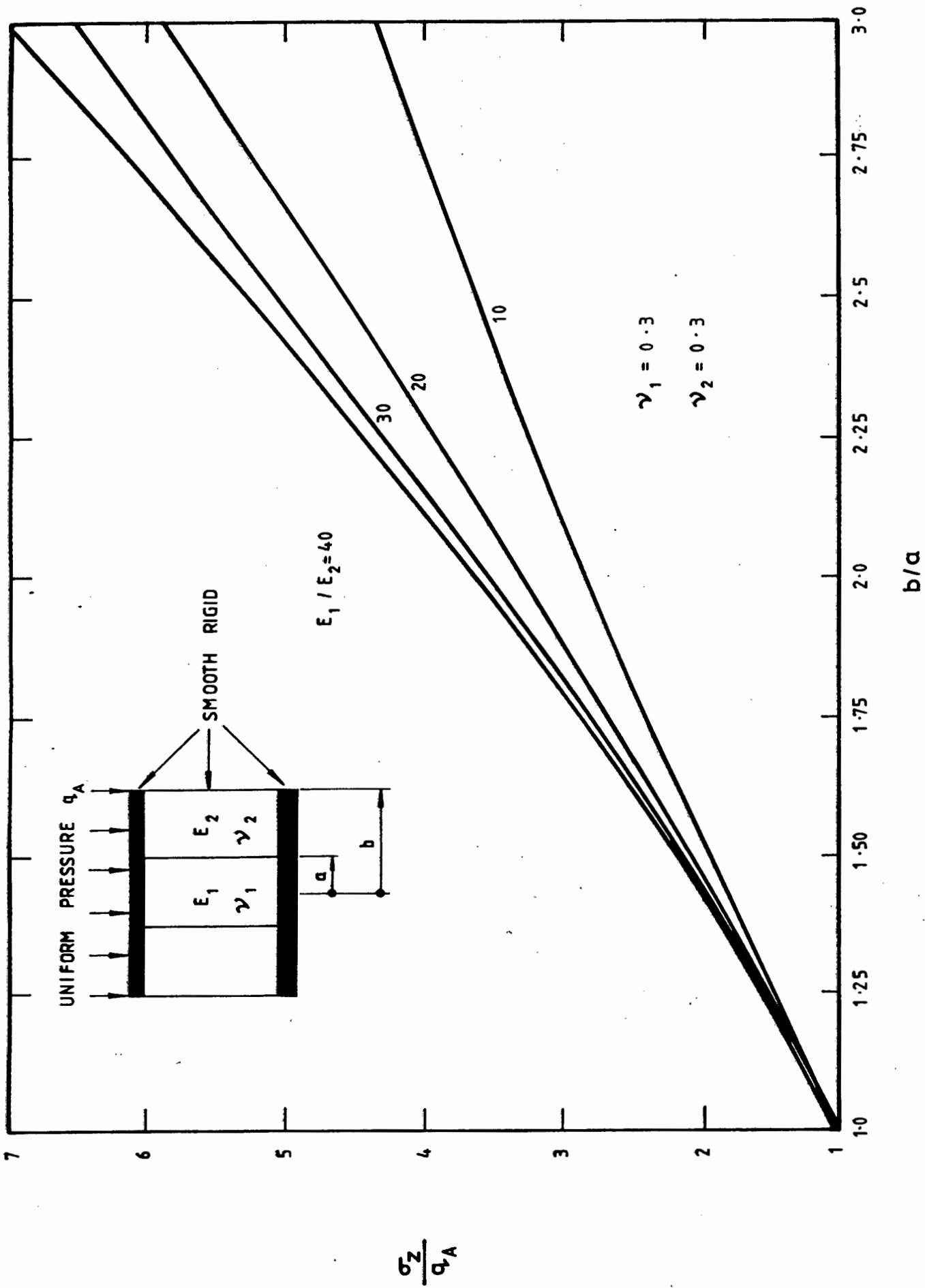
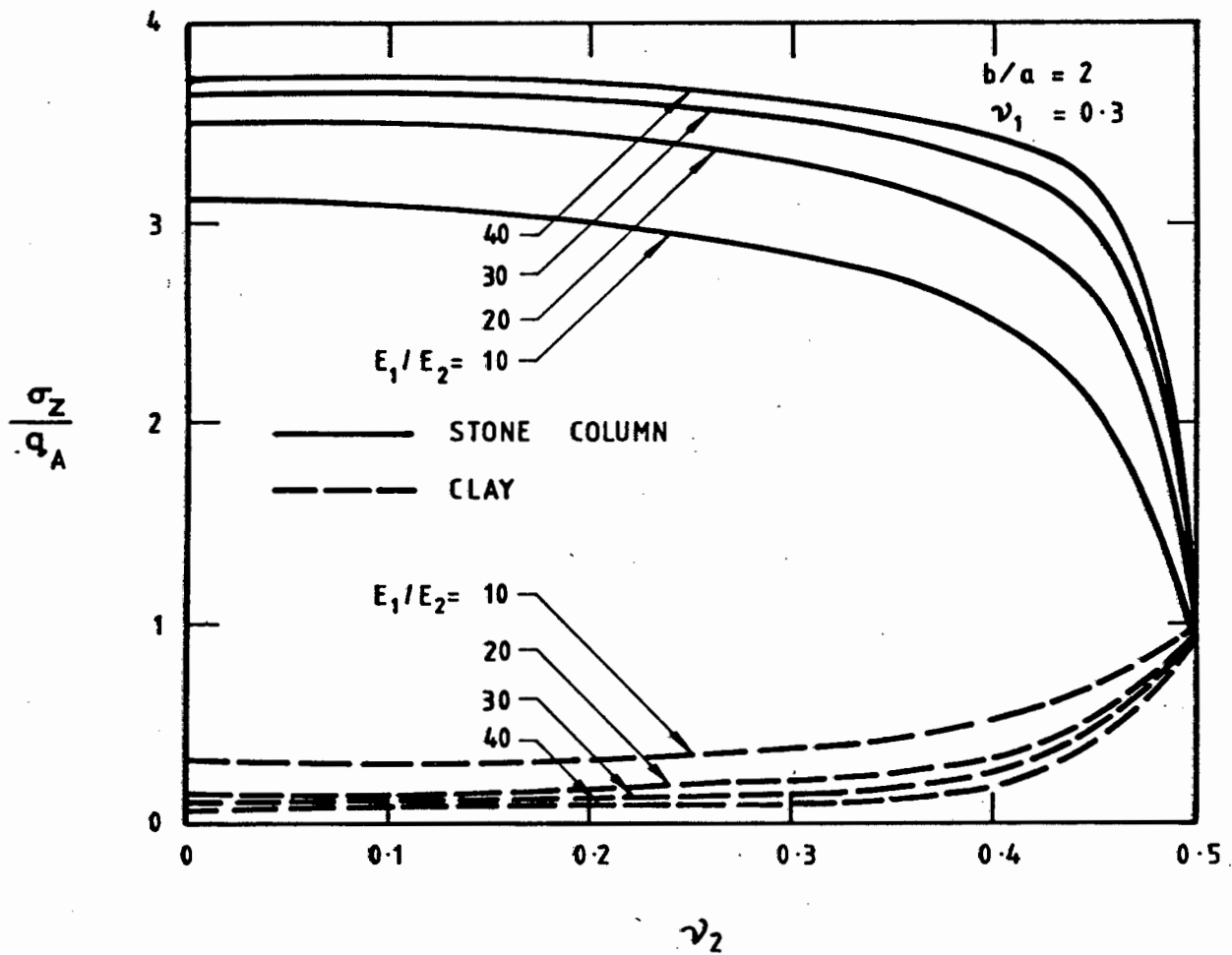


FIG. 8.5 VARIATION OF VERTICAL STRESS IN STONE COLUMN WITH b/a



**FIG. 8.6 VARIATION OF VERTICAL STRESSES WITH
POISSON RATIO OF CLAY**

and the degree of settlement U_s is given by :

$$U_s = \frac{S_t - S_i}{S_f - S_i} \quad (8.15)$$

where S_t = settlement of raft at time t

S_i = initial settlement of raft

S_f = total final settlement of raft

This is compared with the average degree of pore pressure dissipation U_p of Barron's curves, Fig 8.7 to 8.11, which are again reproduced directly from Balaam and Booker and show rates of consolidation for various d_e/d and E_1/E_2 ratios. Differences occur in the results obtained by Barron due to his solutions not accounting for the differences in stiffness of the column and clay. The reader is referred to the source reference of Balaam and Booker for further details.

8.5

SUMMARY

1. Three design approaches have been outlined which vary in complexity from a simple earth pressure approach to an analysis using pressuremeter theory, and finally an elastic analysis using numerical and analytical techniques.
2. The earth pressure method is simple in its approach but does not take time dependent behaviour into account. The radial stress - strain behaviour of the pile is not analysed so making settlement predictions difficult.
3. The use of pressuremeter theory provides a realistic approach to column design, but only relates to undrained conditions. A realistic value for the ultimate load of a column can thus be made with results comparing well with monitored field trials. Settlements, however, are again based on undrained conditions.
4. The elastic analysis has provided a useful set of graphs which predict column behaviour when various dimensionless parameters are changed. A sensitivity analysis can

therefore be quickly undertaken. The analysis does however, deal with linear elastic methods and a suggested improvement is to use a non-linear analysis (Duncan and Chang 1970).

5. From a consideration of the three design methods a realistic design should be obtained if the pressure-meter and elastic design methods are used in conjunction.

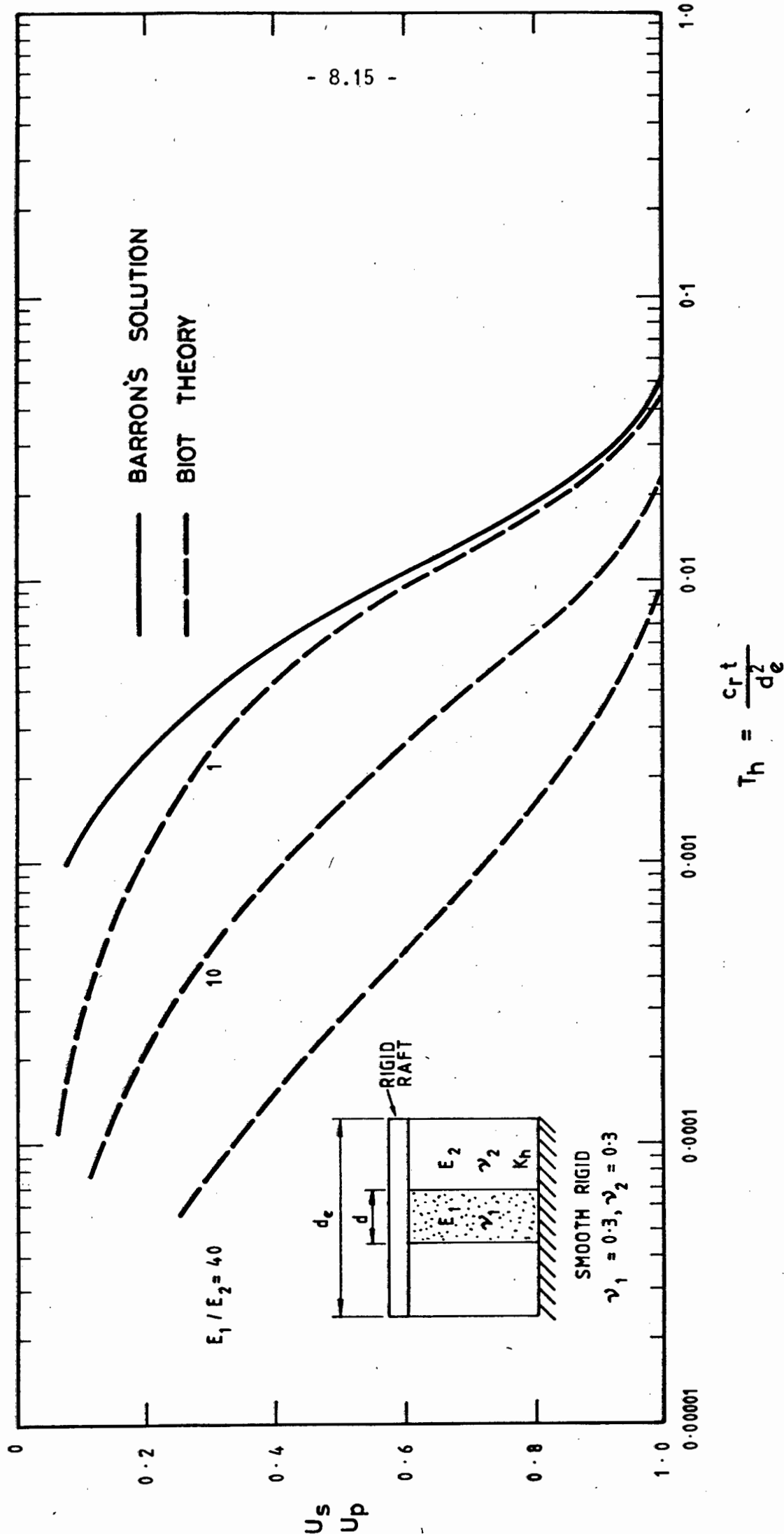


FIG. 8.7 RATE OF SETTLEMENT OF RIGID RAFT ; $d_e / d = 1.5$

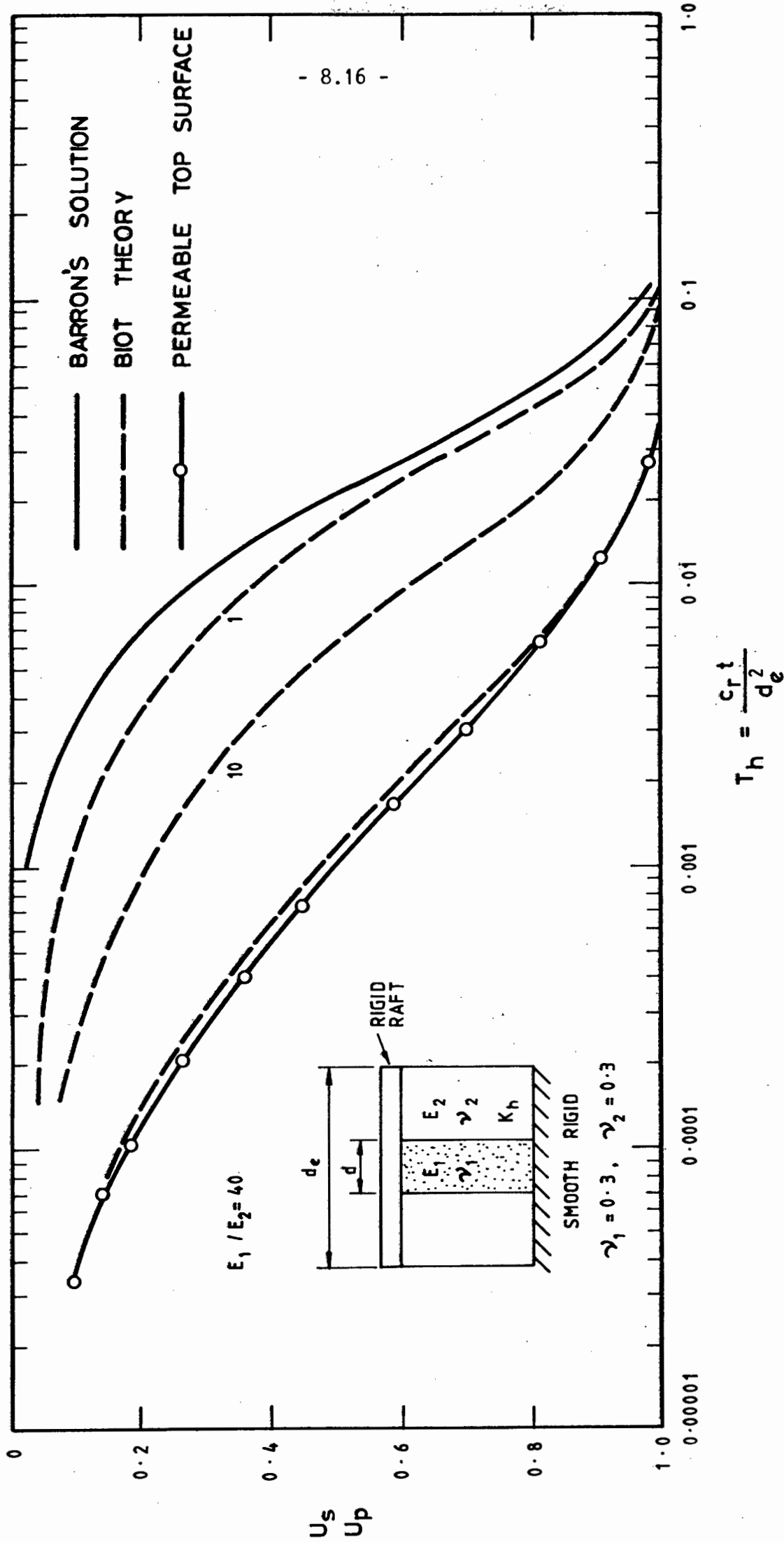


FIG. 8.8 RATE OF SETTLEMENT OF RIGID RAFT: $d_e / d = 2$

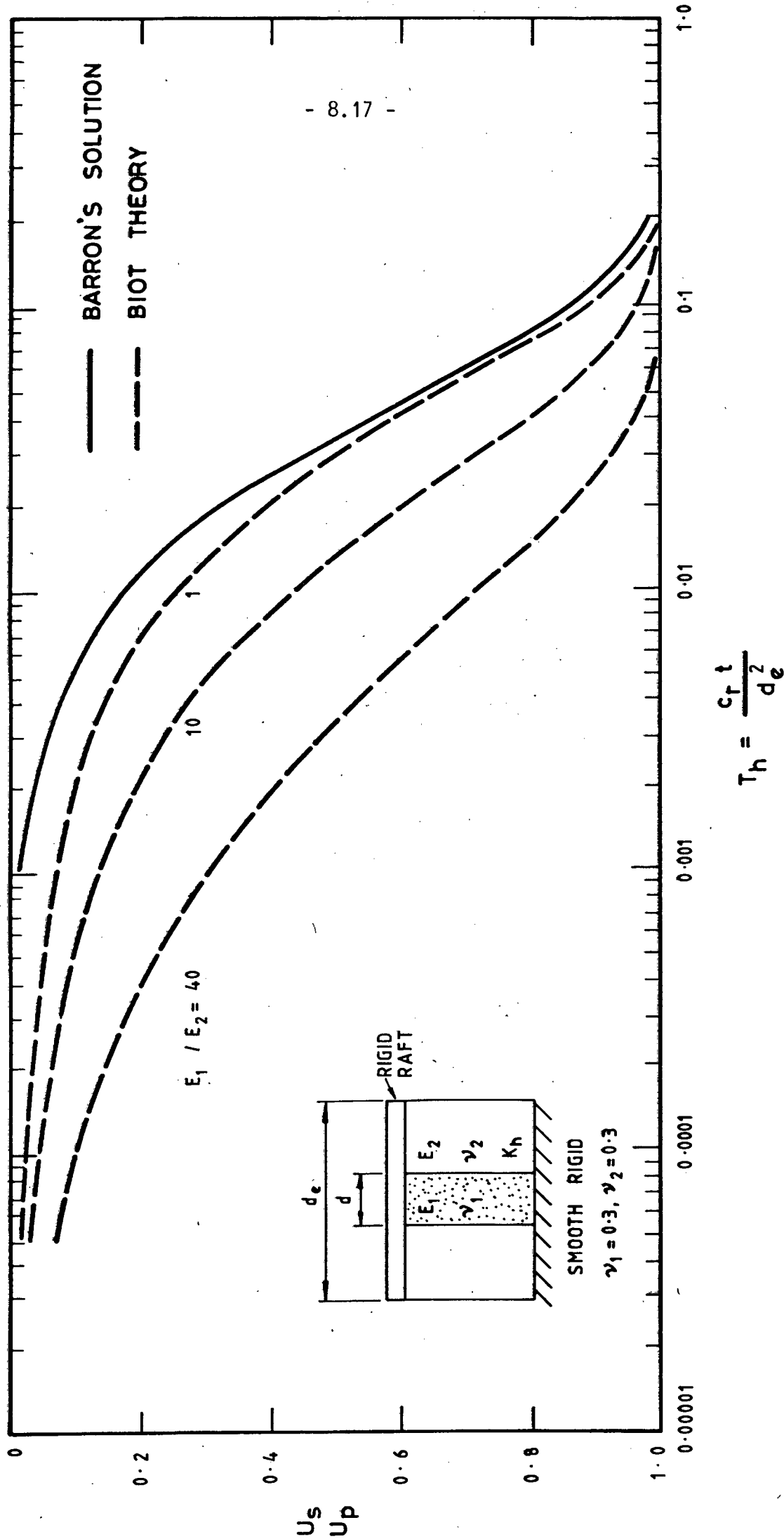


FIG. 8.9 RATE OF SETTLEMENT OF RIGID RAFT: $d_e / d = 2.5$

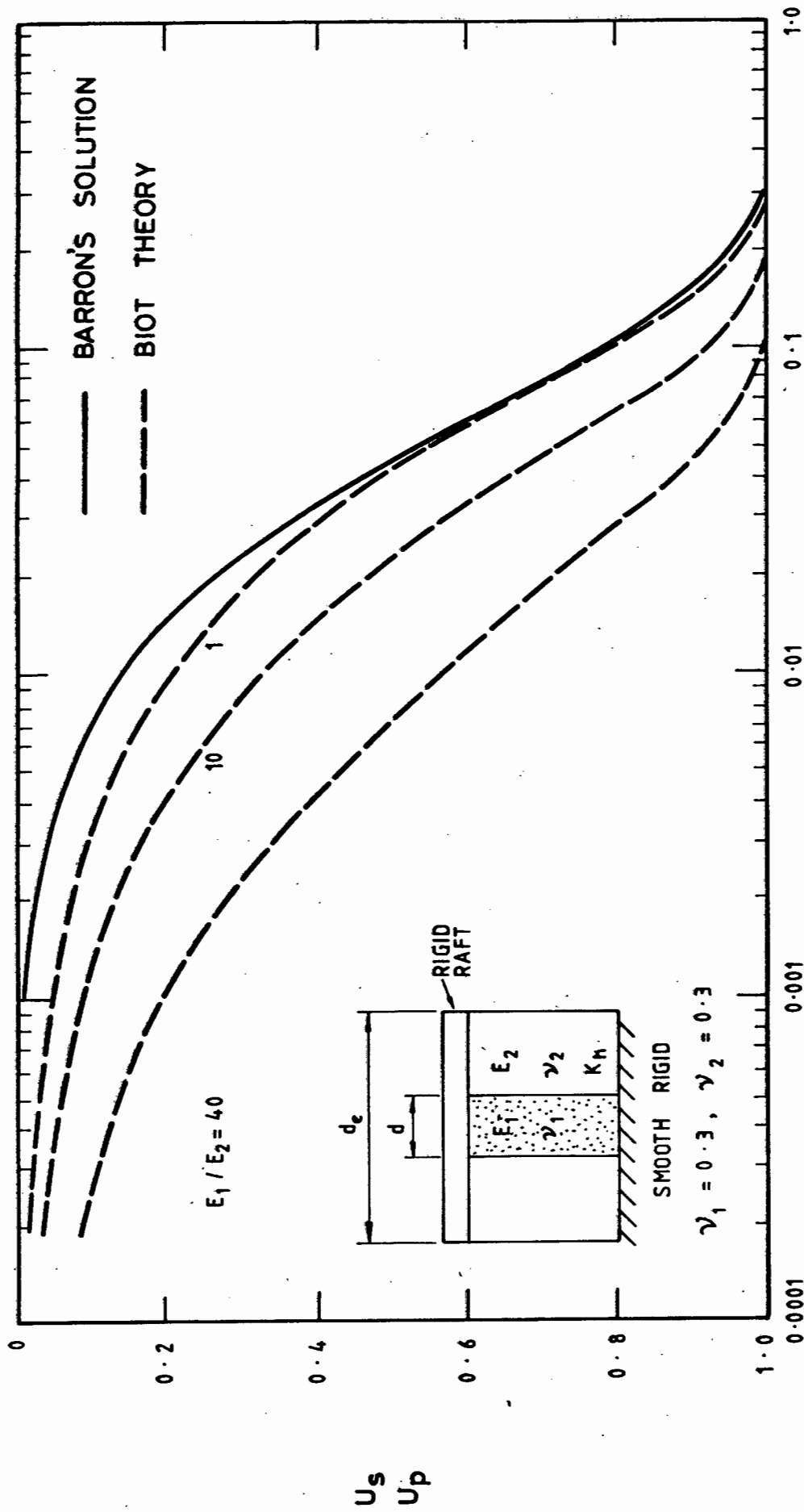


FIG. 8.10 RATE OF SETTLEMENT OF RIGID RAFT ; $d_e / d = 3$

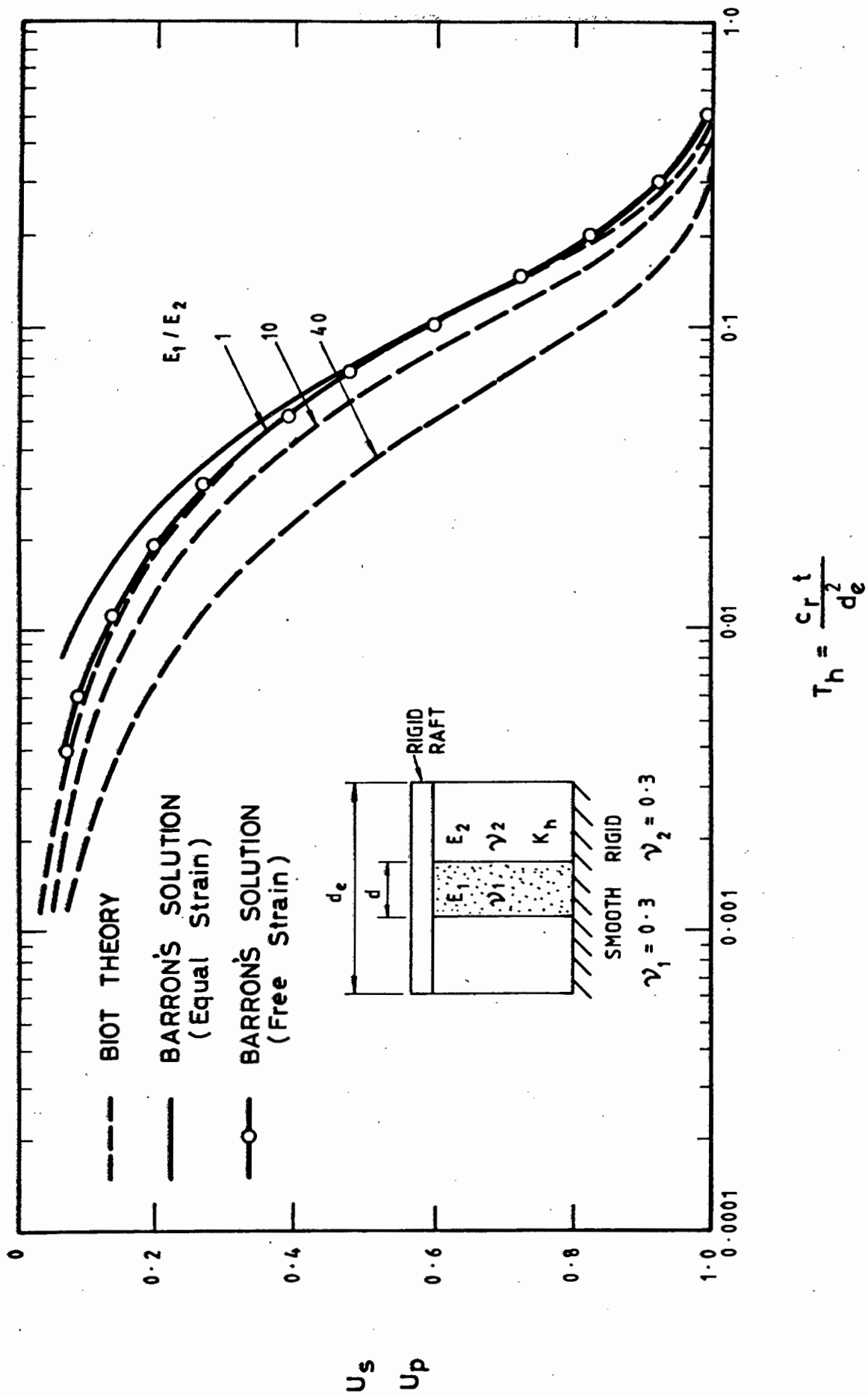


FIG. 8.11 RATE OF SETTLEMENT OF RIGID RAFT; $d_e / d = 5$

CHAPTER 9

ALTERNATIVE DESIGN METHOD BASED UPON MODEL TESTS.

9.1

INTRODUCTION

The laboratory testing as described in Ch. 6 has been consolidated to establish a design method. It is accepted that the relationships established in Ch. 6 are not always perfect, but nevertheless the design method as proposed in this chapter gives results which are in close agreement with other design methods, backed up by field trials. A direct comparison cannot be made as the materials differ but the general trend suggests the validity of the proposed method.

9.2

ULTIMATE COLUMN LOAD.

The ultimate column load has been predicted using the relationship between the stress ratio q/p and void ratio as previously illustrated in Fig. 6.7. Unfortunately the curve is not well defined, but there is a trend of increasing void ratio at failure as the q/p ratio decreases.

For calculating the column load the assumption is made that the pile has a fixed void ratio once placed in the ground due to densification on placement. The maximum q/p ratio can now be read from the graph. During laboratory testing the writer found difficulty in achieving a specific volume less than 1,70, so this value was taken as the placement void ratio and corresponded to a q/p ratio of approximately 0,70.

It is known that the ultimate load is governed by the radial restraint offered by the surrounding soil, providing end bearing failure does not occur. However, this is unlikely if the pile is sufficiently long. The limiting radial stress is therefore required and can be obtained directly by the use of a pressure-meter or indirectly from triaxial tests as it has been found that it is approximately equal to six times the cohesion.

To test the validity of the proposed method comparisons were made with the work of Hughes et al (1976) where various design methods were compared with the results of a load test carried out on a pile.

From the work of Hughes a value of σ_3 was taken as 120 kN/m². Thus:

$$\frac{q}{p} = \frac{\sigma_1 - \sigma_3}{\sigma_1 + \sigma_3} \quad \text{where } \sigma_3 = 120 \text{ kN/m}^2 \quad (9.1)$$

$$\text{i.e. } \sigma_1 = 680 \text{ kN/m}^2$$

For a 0,660 m diameter column this gives a failure load of 232 kN. This compares with a failure load of 170 kN as predicted by Hughes, with a maximum axial stress of 500 kN/m².

By substituting into eqn. 9.1 this corresponds to a q/p ratio of 0,61. Also, the angle of internal friction of the material used by Hughes was taken as 38° compared with 45° for the material used by the writer. The results obtained therefore appear to be in reasonable agreement when it is considered that higher stresses can be sustained by material with higher friction angles.

Hughes found that upon excavation of the trial column the diameter averaged 730 mm, not 660 mm. This would thus correspond to a failure load of 284 kN compared with that of 220 kN for the field column.

9.3 LOAD SETTLEMENT RELATIONSHIP.

The load settlement relationship can now be calculated from the results of the laboratory tests as summarised in Fig. 6.8 which relates the failure strain to void ratio and Fig. 6.12, the non-dimensional stress-strain curve. Figs. 6.7, 6.8 and 6.12 are shown schematically in Fig. 9.1.

Using the specific volume of 1,70 the failure strain as given by Fig. 6.8 is approximately 7%. Again, using the work of Hughes

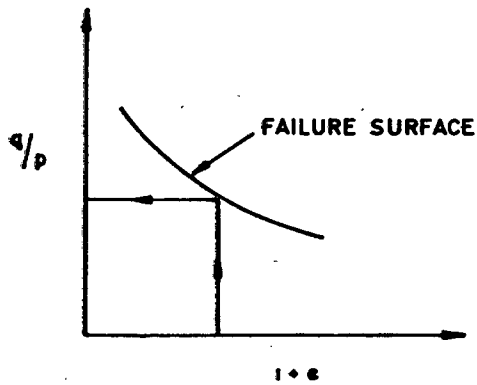


(FIG. 6.7)

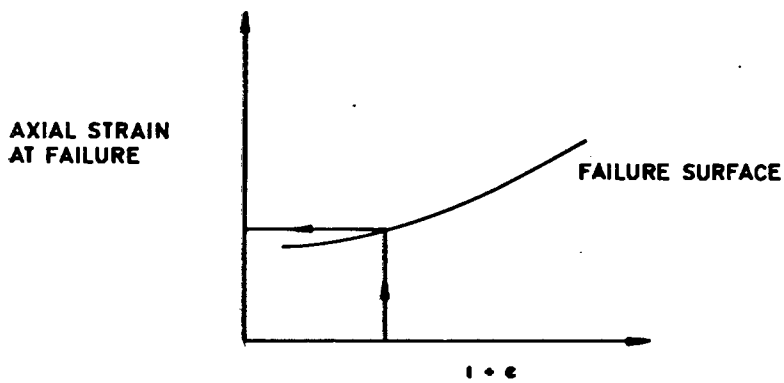


(FIG. 6.12)

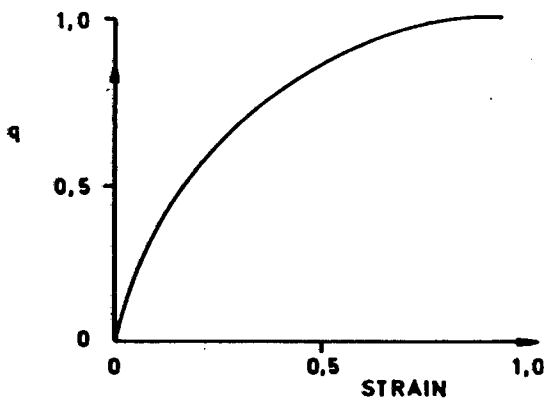


(FIG. 6.12)

**FIG. 9.1 SCHEMATIC REPRESENTATION OF CURVES USED IN DERIVING
LOAD-SETTLEMENT RELATIONSHIP**

TABLE 9.1

Axial stress σ_1 kN/m ²	$q = \frac{\sigma_1 - \sigma_3}{2}$	q%	Axial strain ϵ_a %	Column load kN 0,66m 0,73m	Settlement mm
680	280	100	100	232	490
650	265	93	68	222	333
600	240	84	50	205	245
550	215	75	40	188	196
500	190	67	30	171	147
450	165	58	23	154	113
400	140	49	16	137	78
300	90	32	8	103	39
200	40	14	3	68	15

the column length used for settlement calculations is taken as 7,0 m. The total anticipated settlement is therefore 490mm.

With reference to Fig. 6.12 the maximum value of strain ϵ_a can be equated with the 490 mm, and proportioned accordingly, as can the value of q : since $q = (\sigma_1 - \sigma_3)/2$ and $\sigma_3 = 50$ kN. A complete load settlement curve can thus be drawn by varying the value of axial stress σ_1 as listed in Table 9.1.

The load settlement curves for both a 660 mm and 730 mm pile are shown in Fig. 9.2. As can be seen there is good agreement with the results obtained using the above method and that obtained by Hughes and that of the field trial. It should be borne in mind that the results do not represent a direct comparison as the material used is not the same. However, the results do indicate the validity of the above as a design method.

9.4

TIME - SETTLEMENT RELATIONSHIP.

The previous sections of this chapter have dealt with the ultimate load and load settlement characteristics of a gravel pile using the results obtained from model tests. Similarly, the testing as detailed in Ch. 6 combined with the consolidation theory of Ch. 3 can be used to establish a time - settlement relationship. The relevant diagrams from Ch. 6 are Figs. 6.9, showing the relationship between radial and vertical stress and Fig. 6.10, which relates the principle stress ratio σ_3/σ_1 to the horizontal strain. These are again shown schematically in Fig. 9.3.

From a knowledge of the initial horizontal stress σ_3' and by using the consolidation theory as previously outlined, a new value of σ_3' can be found at any time interval Δt , since σ_3' changes due to pore pressure dissipation. By using Fig. 6.10 the radial strain in the pile can readily be established.

Similarly from Fig. 6.9, for a known value of radial strain the vertical strain can be found. The strains can readily be converted to absolute measurements as both the column radius and effective length are known. From the above it follows that, for a known

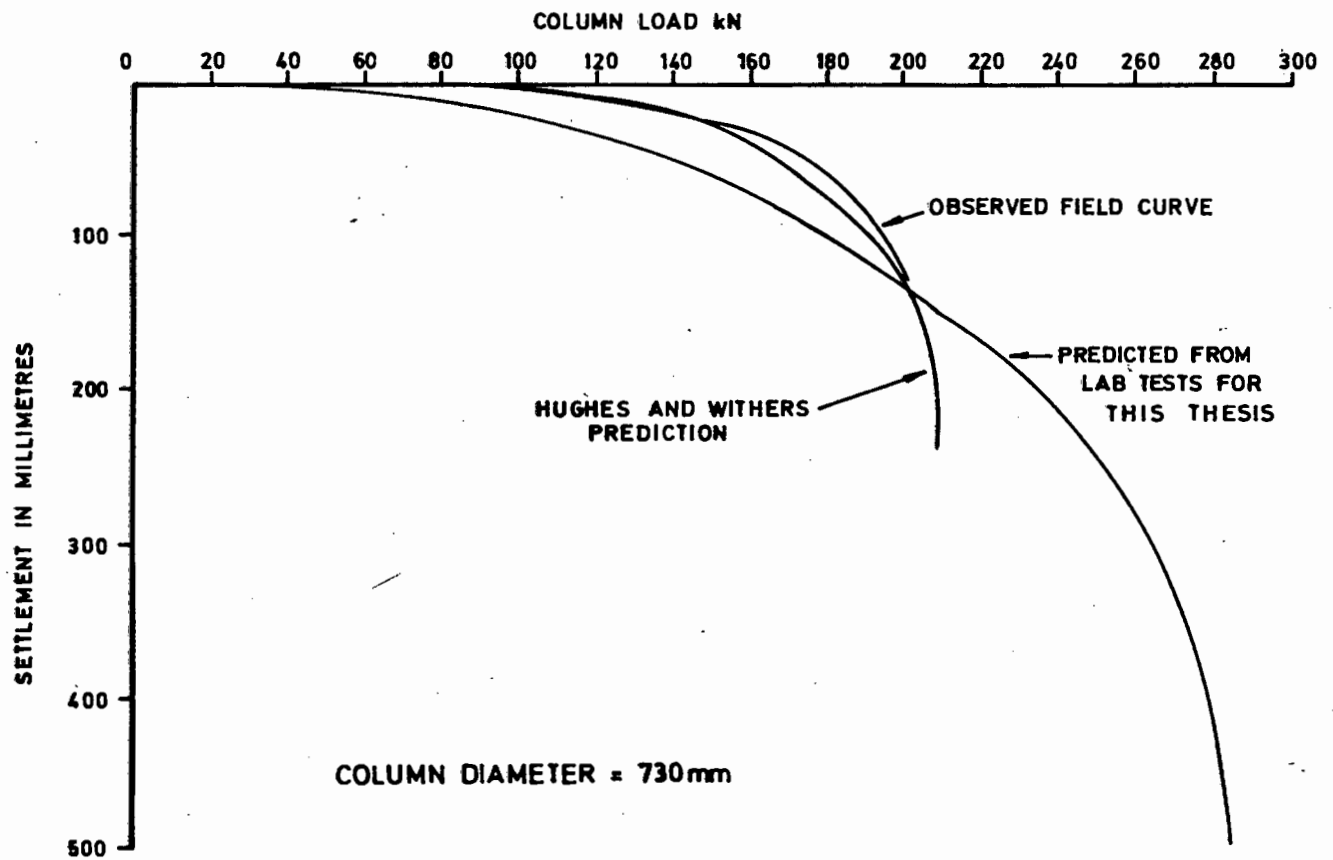
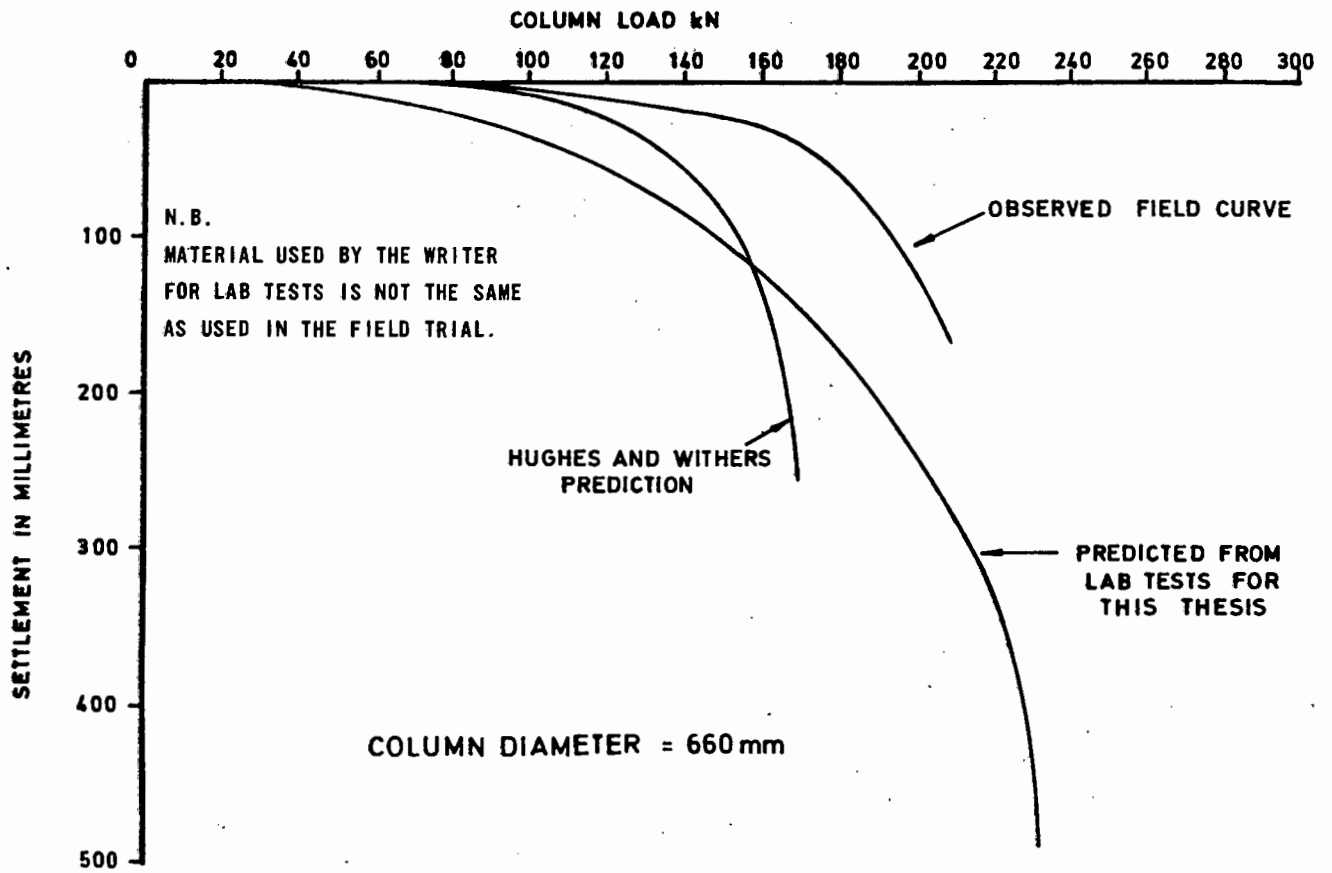
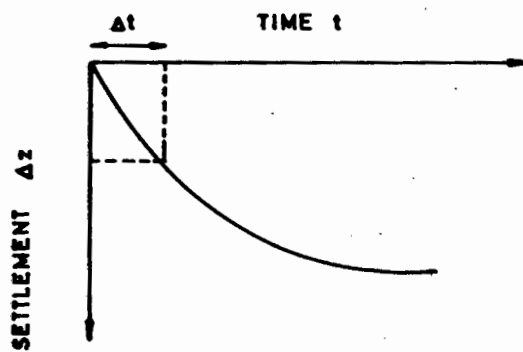
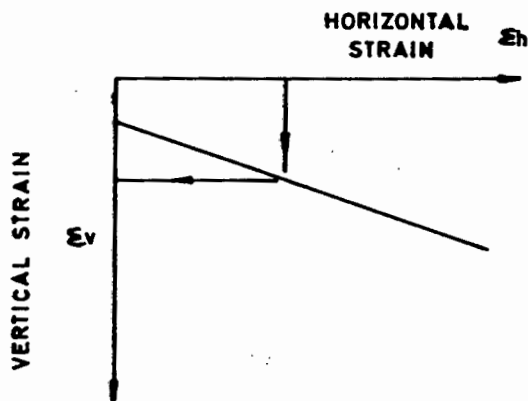
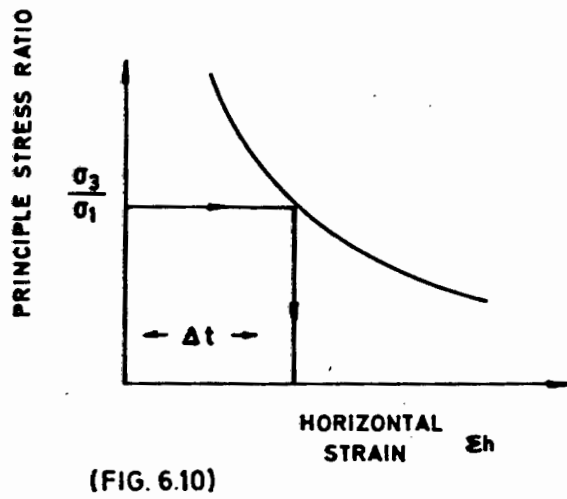


FIG. 9.2 LOAD-SETTLEMENT CHARACTERISTICS OF A STONE COLUMN



$$\Delta z = \epsilon_v \times L$$

WHERE L = LENGTH OF PILE

FIG. 9.3 ESTABLISHMENT OF LOAD SETTLEMENT CURVE

time interval Δt the vertical settlement Δz is known, so enabling a time settlement curve to be drawn. The sequential method to follow is shown in Fig. 9.3.

The initial radial stress r_o can again be found by the use of a pressuremeter or from the approximation :

$$r_o = 2c \quad \text{where } c \text{ is the cohesion.}$$

At time $t > 0$ the horizontal stress σ_3 will be given by:

$$r_o > \sigma_3 \leq r_L \quad \text{where } r_L \text{ is the limiting radial stress.}$$

A comparison of results cannot be made with the work of Hughes as the consolidation characteristics of the clay are not given. As previously stated, it is recommended that the average degree of pore pressure dissipation be obtained using Barron's curves.

9.5

DESIGN METHOD USING CAM-CLAY THEORY.

Although outside the scope of this thesis it is evident that the Cam-clay theory can be used to establish volumetric strains as shown in eqn. 5.7 as all of the parameters are measurable. However, uncertainty exists as to the measurement of λ and κ for sands, so at present this method is not seriously considered. The reader is referred to the work of Schofield and Wroth (1968) and Atkinson and Bransby (1978) for a fuller description of the theory.

9.6

SUMMARY

1. The ultimate column load can be predicted by model tests if the limiting lateral stress is known.
2. The load settlement relationship can be established using model tests and the non-dimensional stress-strain curve.
3. Time - settlement relationships can similarly be established

3. from model tests and using consolidation theory.
4. It is possible that the volume changes within a pile can be established using Cam-clay theory.

CHAPTER 10

CONCLUSION

10.1 INTRODUCTION

This chapter summarises the main points of the thesis and considers whether the objectives outlined in Ch. 1 have been achieved. Also, the writer discusses interests developed during the course of the work and knowledge gained from the study.

10.2 ACHIEVEMENT OF OBJECTIVES

The aim of the thesis was to give a basic understanding of stress-strain behaviour of gravel piles and to examine various methods used in their design. Also, it was hoped that a new design method could be formulated.

The stress-strain behaviour of piles basically depends upon the stress-strain properties of sands as detailed in Ch. 4, where it is clear that the behaviour is predominantly influenced by the void ratio of the material. This has again been demonstrated in Ch. 6 in tests carried out in the laboratory. The difference in behaviour between angular and smooth material is also demonstrated ; one being the obvious one of the difference in measured friction angle. This alone shows the preference of using more angular material for a gravel pile.

Current design methods have been discussed in Ch. 8 and include the little known work of Balaam and Booker. The writer considers this work to be invaluable as it quickly allows a design to be formulated using the various graphs presented, as well as checking sensitivity of the design parameters.

A new design method has been formulated which differs from those detailed in Ch. 8 and is based primarily upon laboratory work involving the stress-strain behaviour of sand. It is believed that this method gives a better understanding of pile behaviour

than some of the other design methods.

The writer thus feels that the objectives of the thesis have been achieved and it is hoped that this work can serve as a concise guide to column behaviour.

10.3 DEVELOPED INTERESTS.

During the course of the work three main interests were developed by the writer, viz. three dimensional consolidation, critical state theory and stress-strain behaviour of sands.

The finite difference method of solving the three dimensional consolidation equations was found to be a very powerful and adaptable technique as it can be used for any boundary condition. Obviously, it can be used for one and two dimensional problems with relative ease and the writer would consider such use for practical examples rather than confining the use for academic interest. A positive aspect of the finite difference method is that hand computations can be used and one need not have access to large computers as for finite element methods. However, the writer can personally testify to the time consuming nature of the method.

The critical state theory for soils is only briefly mentioned although the writer found it an extremely stimulating approach to soil mechanics as it enables various relationships between stresses, strains and void ratio to be combined in a unifying theory. This is an area in which the writer wishes to undertake further research and to apply the method to more commonplace soil problems.

The stress-strain properties of sand were found to be particularly intriguing. A tremendous amount of work has been written on the behaviour of sands, but these are nearly all related to laboratory conditions. Whilst this is of academic interest it has been found difficult to relate such laboratory results to conditions in the field. It is hoped that the non-dimensional approach will overcome some of these problems as the curve

produced appears to be independent of void ratio. Laboratory tests can thus be undertaken on disturbed samples and a general stress-strain curve obtained. If this can be related to in situ void ratio (relative density) this could thus serve as a method of settlement prediction.

REFERENCES

- Anon. (1964) "The bulk sugar terminal, Maydon Wharf, Durban."
Public Works of South Africa. Feb.
- Anon (1964) "World's biggest sugar silo taking place in Durban".
Construction in Southern Africa. March.
- Anon (1965) "Consolidation of cohesive soils at Teesport."
Civ. Eng. & Public Works Review. Oct.
- Atkinson, J.H. & Bransby, P.L. (1978) "The mechanics of soils. An
introduction to critical state soil mechanics".
McGraw-Hill Book Co. London.
- Baguelin, F., Jézéquel, J.F., & Shields, D.H. (1978) "The pressuremeter
and foundation engineering." Trans Tech Publications.
- Balaam, N.P. & Booker, J.R. (1979) "Analysis of rigid rafts supported by
granular piles". Research Report No. R339, School of
Civ. Eng. University of Sydney.
- Barron, R.A. (1948) "Consolidation of fine-drained soils by drain wells."
Transaction, ASCE, Vol. 113, Paper No. 2346.
- Barron, R.A. (1972) "Rate of settlement under two and three dimensional
conditions" - Discussion. Géotechnique, Vol. 22.
- Basore, C.E. & Biotano, J.D. (1969) "Sand densification by piles and vibro-
flotation". Journal of the Soil Mechanics and Foundations
Division. ASCE, Vol. 95, No. SM6.

References marked with an asterix * were not available to the writer.

- Biot, M.A. (1941) "General theory of three dimensional consolidation".
Journal of Applied Physics, Vol. 12, No.2.
- Bishop, A.W. (1950) "Measurement of the shear strength of soils " -
Discussion. Géotechnique, Vol. 2, No. 1 .
- Bishop, A.W. & Henkel, D.J. (1962) "The measurement of soil properties
in the triaxial test ". Edward Arnold, London.
- Bishop, A.W. (1966) "Strength of soils as engineering materials".
Sixth Rankine Lecture. Géotechnique, Vol. 16.
- Bishop, A.W. (1971) "Shear strength parameters for undisturbed and
remoulded soil specimens." Roscoe Memorial Symposium,
Cambridge.
- Bowles, J.E. (1977) "Foundation analysis and design." McGraw-Hill
Kogakusha Ltd., Tokyo.
- Bratchell, G.E., Leggatt, A.J. & Simons, N.E. (1975) "The performance of
two large oil tanks founded on compacted gravel at Fawley,
Southampton, Hampshire." Proc. Conf. Settlement of
Structures, Cambridge. London, Pentech Press.
- Broms, B.B. & Boman, P. (1979) "Stabilisation of soil with lime columns".
Ground Engineering. Vol. 12, No. 4.
- Brown, R.E. & Glenn, A.J. (1976) "Vibroflotation and Terra-probe comparison".
Journal of the Geotechnical Engineering Division. ASCE,
Vol. 102, No. GT10.
- * Carillo, N. (1942) "Simple two and three dimensional cases in the theory of
consolidation of soils ". Journal of Maths and Physics.
Vol. 21, No. 1.
- * Castro, G. (1969) "Liquifaction of sands". Thesis presented to Harvard University
in partial fulfillment of the degree of Doctor of Philosophy.

Cementation (1977) "Vibroflotation". Company brochure. Rickmansworth, United Kingdom.

Christian, J.T. (1977) "Two and three dimensional consolidation". Numerical Methods in Geotechnical Engineering. McGraw-Hill, New York.

Christie, I.F. (1959) "Design and construction of vertical drains to accelerate the consolidation of soils." Civ. Eng. and Pub. Works Rev. 54.

Cornforth, D.H. (1964) "Some experiments on the influence of strain conditions on the strength of sand." Géotechnique, Vol. 14, No. 2.

Cryer, C.W. (1963) "A comparison of the three dimensional consolidation theories of Biot and Terzaghi". Quarterly Journal of Applied Mechanics and Applied Maths. Vol. XVI, Part 4.

Davis, E.H. & Poulos, H.G. (1972) "Rate of settlement under two and three dimensional conditions". Géotechnique, Vol. 22, No. 1.

Deryck, N. & Severn, R.T. (1960) "Stresses in foundation rafts". Proc. Inst. of Civ. Eng. London. Jan. Part 1, Vol. 15.

Deryck, N. & Severn, R.T. (1961) "Stresses in foundation rafts". Proc. Inst. Civ. Eng. London. Oct. Part 2, Vol. 20.

Desai, C.S. & Christian, J.T. (1977) " Numerical methods in geotechnical engineering ." McGraw-Hill, New York.

* Dullage, C.R. (1969) "An investigation into the feasibility of small scale tests on granular piles in clay ". M.Sc. Thesis, University of Wales.

Duncan, J.M. & Chang, C.Y. (1970) "Non-linear analysis of stress and strain in soils ." Journal of the Soil Mech. & Fndtn. Div. ASCE. Vol. 96, No. SM5.

- Gibson, R.E. & Lumb, P. (1953) "Numerical solution of some problems in the consolidation of clay ". Proc. of the Inst. Civ. Eng. Part 1, Vol. 2.
- Gibson, R.E. & Anderson, W.F. (1961) "In-situ measurements of soil properties with the pressuremeter". Civ. Eng. and Pub. Works Rev. Vol. 56.
- Gibson, R.E. & McNamee, J. (1963) "A three dimensional problem of the consolidation of a semi-infite clay stratum. " Quarterly Journal of Applied Mechanics and Applied Maths. Vol. XVI, Part 2.
- Green, G.E. & Bishop, A.W. (1969) "A note on the drained strength of sand under generalised strain conditions ". Géotechnique, Vol. 19, No. 1.
- Greenwood, D.A. (1965) "Strengthening sand ". Consulting Engineer, Oct.
- Greenwood, D.A. (1976) "Discussion". Ground Treatment by Deep Compaction. I.C.E. London.
- Grimes, A.S. & Cantley, W.G. (1965) "A twenty storey office block in Nigeria founded on loose sand ". The Structural Engineer, No. 2, Vol. 43.
- Hain, S.J. & Lee, I.K. (1976) "The analysis of flexible raft-pile group interaction." Géotechnique, Vol. 26.
- * Horne, M.R. (1965) "The behaviour of an assembly of rotund, rigid cohesionless particles ". Parts 1 and 2. Proc. R. Soc. A 286.
- Hughes, J.M.O. & Withers, N.J. (1974) "Reinforcing of soft cohesive soils with stone columns." Ground Engineering, Vol. 7, No. 3.

- Hughes, J.M.O., Withers, N.J. & Greenwood, D.A. (1976) "A field trial of the reinforcing effect of a stone column in soil". Ground Treatment by Deep Compaction. I.C.E. London.
- James, H.W. (1973) "Densification of sand for a dry dock by Terra-probe". Journal of the Soil Mech. and Fndtn. Div. Vol. 99, No. SM 6.
- Jones, D.L. (1978) "Bearing capacity and settlement of gravel piles in clay.- A preliminary study." University of Cape Town.
- Keller, J. (1967) Company brochure. Frankfurt/Main; Johann Keller.
- Kondner, R.L. (1963) "Hyperbolic stress-strain response : Cohesive soils ." Journal of the Soil Mech. and Fndtn. Div. ASCE, Vol. 89 No. SM 1.
- Kruger, J.J., Coupe, P.S., Guyot, C., Morizot, J.C. (1980) "The dynamic substitution method." International Conference on Compaction. Paris.
- Lade, P.V. (1978) "Prediction of undrained behaviour of sand ". Journal of the Geotechnical Engineering Div. ASCE, Vol. 104, No. GT 6.
- Lamb, T.W. (1967) "The stress path method. " Journal of the Soil Mech. and Fndtn. Div. ASCE, Vol. 93, No. SM 6.
- Lamb, T.W. & Whitman, R.V. (1969) "Soil mechanics". John Wiley & Sons Inc., New York.
- Lee, I.K. & Brown, P.T. (1972) "Structure foundation interaction analysis ". Journal of the Structural Div. ASCE, Vol. 98, No. ST 11.
- Lee, I.K. (1977) "Interaction analysis of rafts and raft pile systems ". International symposium on soil structure interaction, India.

- Mandel, J. (1957) "Consolidation des sols." Géotechnique Vol. 3.
- Marsland, A. & Randolph, M.F. (1977) "Comparisons of the results from pressuremeter tests and large in situ plate tests in London clay ". Géotechnique, Vol. 27, No. 2
- Mckenna, J.M., Eyre, W.A., & Wolstenholme, D.R. (1976) "Performance of an embankment supported by stone columns in soft ground ". Ground Treatment by Deep Compaction, I.C.E. London.
- Menard, L. (1979) "Report on trials at Gold Monument ". (unpublished report) . Techniques, Louis Menard, Longjumeau, France.
- Mitchell, J.K. (1970) "In place treatment of foundation soils. " Journal of the Soil Mech & Fndtn. Div., ASCE, No. SM 1.
- Murray, R.T. (1974) "Two dimensional analysis of settlement by computer programme ". TRRL Report, LR 617.
- Murray, R.T. (1976) "Settlement of embankments ". Proc. Settlement and Stability of Earth Embankments on Soft Fdtns. TRRL, Supplementary Report 399.
- * Parry, R.H.G. (1956) "Strength and deformation of clay". Ph.d Thesis Imperial College of Science and Technology, University of London.
- Parry, R.H.G. (1960) "Triaxial compression and extension tests on remoulded saturated clay ". Géotechnique, Vol. 10.
- Prevost, J.H. (1979) "Mathematical modelling of soil stress-strain-strength behaviour." Third International Conference on Numerical Methods in Geo-mechanics. Aachen.
- * Rendulic, L. (1936) "Porenziffer und Porewasser Druck in Tonen ." Der Bauingenier. 17 No. 51/53.

- Richart, F.E. (1957) "Review of the theories for sand drains ".
The Journal of Soil Mech. and Fndtn. Div. ASCE,
Vol. 83, No. SM 3.
- Roscoe, K.H. (1970) "The influence of strains in soil mechanics".
Tenth Rankine Lecture, Géotechnique, Vol. 20, No. 2.
- Ross, A.D. (1954) "Numerical solution of some problems in the consolidation
of clay ". Correspondence. Proc. Inst. of Civ. Eng.
Part 1, Vol. 3.
- Rowe, P.W. (1962) "The stress dilatancy relation for static equilibrium
of an assembly of particles in contact ". Proc. R. Soc.
A. 264.
- Rowe, P.W. a (1969) "Osborne Reynolds and dilatancy ." Géotechnique,
Vol. 19, No. 1.
- Rowe, P.W. b (1969) "The relation between shear strength of sands in
triaxial compression, plane strain and direct shear. "
Géotechnique, Vol. 19, No. 1.
- Schofield, A.N. & Wroth, C.P. (1968) "Critical state soil mechanics ".
McGraw-Hill Book Co., London.
- Severn, R.T. (1966) "The solution of foundation mat problems by finite
element methods." Structural Engineer, London.
Vol. 44, No. 6.
- Sommer, H. (1965) "A method for the calculation of settlements, contact
pressures and bending moments in a foundation including
the influence of the flexural rigidity of the superstructure."
Proc. of the Sixth Int. Conf. on Soil Mech. and Fndtn.
Vol. 2.
- Sparks, A.D.W. (1980) "Personal communication ." University of Cape Town.

- Taylor, D.W. (1948) " Fundamentals of soil mechanics." John Wiley,
New York.
- Teng, W.C. (1962) "Foundation design." Prentice-Hall Inc., Englewood
Cliffs, N.J.
- Terzaghi, K. (1925) "Erdvaumechanick auf bodenphysikalischer Grundlage."
Deuticke, Vienna.
- Terzaghi , K. (1944) "Theoretical soil mechanics." John Wiley and Sons
New York.
- Terzaghi , K. (1955) "Evaluation of coefficients of subgrade reaction."
Géotechnique, Vol. 5 No. 4.
- Terzaghi , K. & Peck, R.B. (1967) "Soil mechanics in engineering practice."
Second Edition. John Wiley, New York.
- Timoshenko, S.P. & Woinowsky-Krieger, S (1959) "Theory of plates and shells"
McGraw-Hill Kogakusha Ltd., Tokyo, Japan.
- Vesic, A.S. & Clough, G.W. (1968) "Behaviour of granular materials under
high stresses ". Journal of the Soil Mech. and Fndtn. Div.
ASCE, Vol. 94, No. SM 3.
- Webb, D.L. & Hall, R.I. (1969) "Effects of vibroflotation on clayey sands ".
Journal of the Soil Mech. and Fndtn. Div. ASCE, Vol. 95
No. SM 6.
- * Williams, J.D.G. (1969) "Small scale tests on granular piles in soft clays."
B.Sc. Thesis, University of Wales.
- Wong, H.Y. (1975) "Vibroflotation - its effect on weak cohesive soils."
Civil Engineering. April.

APPENDIX

The following is a list of courses successfully completed by the writer:

Course No.	Title	Credit	Year
CE 506	Properties of Concrete	4	1976
CE 515	Surface structures	5	1976
CE 525	Coastal Engineering	5	1977
CE 529	Potential Theory and Groundwater Flow	5	1977
CE 500	Geotechnical Site Investigation	5	1978
CE 534	Advanced Soil Mechanics	5	1978
CE 535	Engineering Economy	3	1979

Note: Course CE 529 Potential Theory and Groundwater Flow did not have an examination but was assessed by means of a project .

Examination papers for the above are enclosed.

UNIVERSITY OF CAPE TOWN
DEPARTMENT OF CIVIL ENGINEERING

FINAL EXAMINATION DECEMBER 1978

COURSE CE 500 - ADVANCED SOIL MECHANICS

MINIMUM REQUIREMENTS FOR COURSE :

Part A - This written examination (Time: 3 hours 20 minutes)

Part B - A short project. (Draft Mini-regulations for Foundation Design)

Part C - A longer project (On approved subject of candidate's choice)

PART A - Written Examination

WORK IN S.I. UNITS. A choice of questions is permitted. Attempt as many questions as you wish, but note that full marks for this paper will correspond to 100 marks. The marks, and an approximate guide to the time which might be required for each question, are indicated after each question.

WHEN ANSWERING A QUESTION, PROVIDE THE FORMULA WHICH IS BEING USED; STATE THE SOURCE (WITH AUTHOR) OF ANY METHOD OR OF ANY QUOTATION AND PROVIDE ANY SKETCHES WHICH ARE NECESSARY FOR A READER TO UNDERSTAND YOUR ANSWER.

IF VALUES MUST BE ASSUMED FOR CALCULATIONS, STATE YOUR ASSUMED VALUES. LIST ANY IMPORTANT ASSUMPTIONS OF CONCEPT USED IN YOUR ANSWER.

MARKS WILL BE ALLOCATED TO THE LOGICAL LAYOUT OF YOUR ANSWERS.

FOR CALCULATIONS : Assume specific weight of water = 10 kN/m^3 .

CONVERSIONS : The following approximations can be used for converting other units to the SI units :

(Note that kg is not acceptable as a weight unit in S.I. units, but in certain old references the weight of a kilogram mass was used as a weight unit).

APPROXIMATIONS : ONLY FOR THE APPROXIMATE CONVERSION OF EXISTING VALUES IN TABLES

Atmosphere $\approx 1 \text{ kg(wt)/cm}^2 \approx 1 \text{ ton/ft}^2 (107 \text{ kN/m}^2) \approx 100 \text{ kN/m}^2$

$\approx 33 \text{ ft of water} \approx 10 \text{ m of water} \approx 100 \text{ kPa}$

$\approx 15 \text{ lb/in}^2 \approx 1 \text{ bar} \approx 2,2 \text{ kip/ft}^2 \approx 2200 \text{ lb/ft}^2$

1 foot $\approx 0,305 \text{ m}$

1 kN $\approx 224,8 \text{ pounds}$

1 m $\approx 3,281 \text{ ft}$

1 m $\approx 1,094 \text{ yards}$

1 inch = $0,0254 \text{ m}$

1 kip = 1000 pounds

1 kg(wt) = $2,2 \text{ pounds}$

1 kg(wt) $\approx 10 \text{ newtons (approximately)}$

USE SI UNITS IN YOUR CALCULATIONS

Marks per question:

Q1	20 marks
Q2	32 marks
Q3	20 marks
Q4	25 marks

Q5	15 marks
Q6	30 marks
Q7	20 marks
Q8	20 marks.

Question 1.

Figure 1 shows a non-circular trial slip surface which has been drawn through a rockfill dam with a clay core.

The factor of safety F for this slip surface must be found for the partial pool case shown in Figure 1. In this particular example, the calculations may be simplified by assuming that $c = 75 \text{ kN/m}^2$ and $\phi = 0$ for the clay core. Because a $\phi = 0$ analysis is being made within the clay core, it will not be necessary to calculate the pore water pressures within the clay core.

The angle of internal friction for the compacted cohesionless rockfill is $\phi' = 43^\circ$, except at the interface with the horizontal rock base where the value of ϕ' is 37° .

Note that the zones AB, CD and EF are in the compacted rockfill ($\phi' = 43^\circ$, $c = 0$). The portion BC is within the clay core. The portion DE is along an interface between the rockfill and the rock sub-base ($\phi' = 37^\circ$, $c = 0$).

(20 marks, 40 minutes)

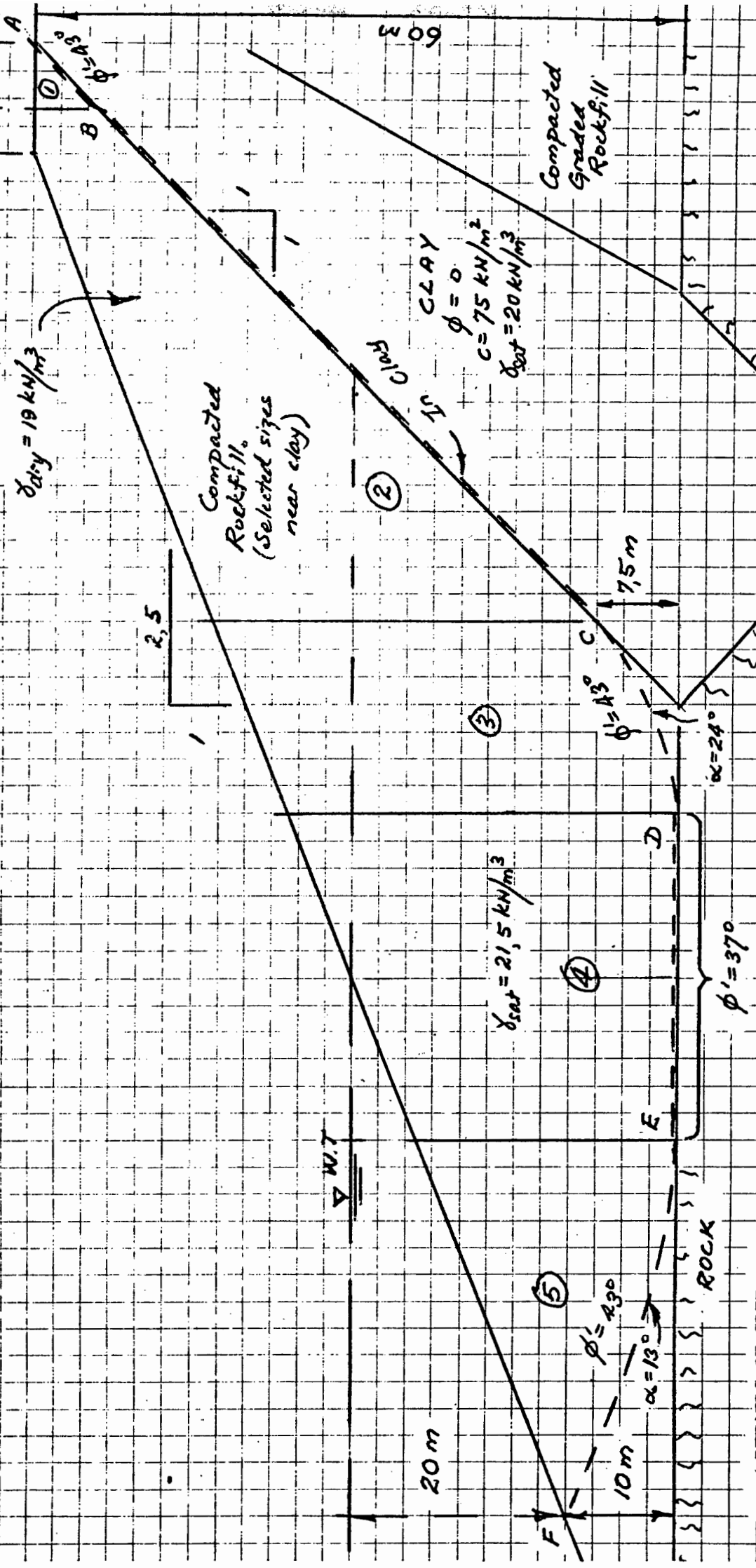


FIGURE 1

Non-circular slip surface.

DETAILS OF SLIP

- AB in rockfill $\phi' = 43^\circ$
- BC in clay $\phi = 0, c = 75 \text{ kN/m}^2$
- CD in rockfill $\phi' = 43^\circ$
- DE rock interface $\phi' = 37^\circ$
- EF in rockfill $\phi' = 43^\circ$

Question 2.

Two identical beams XY and YZ are hinged together at the point Y and are attached to an elastic foundation supporting medium, as shown in Figure 2.

Each beam has a constant EI value throughout its length. The ends X and Z of the beams are free to deflect up or down with the supporting medium.

The value of $\frac{kh^4}{EI}$ for the system is 3.0; where k is the coefficient of subgrade reaction, and h is the nodal distance (See Fig.2).

- a) Consider the load system and the nodal points shown in Figure 2. Using finite difference approximations, derive a suitable set of equations from which the deflections at the nodes may be calculated.

Tabulate this set of equations in such a manner that the deflections at the seven nodes in Figure 2 are the only unknowns in the equations.

For this part of the question, the solution of the tabulated equations is not required.

(15 marks, 30 minutes)

- b) By some simple direct method [other than by solving the equations in part (a) above], estimate the anticipated average settlement of the foundation system shown in Figure 2. Express your answer in terms of units of qh^4/EI .

(5 marks, 10 minutes)

- c) Use the concept of symmetry and reduce the number of equations and unknowns in part (a). Hence solve these equations by approximate methods or by direct methods to estimate the maximum and minimum settlements. (It is suggested that this portion be left to near the end of the examination).

(12 marks, 25 minutes)

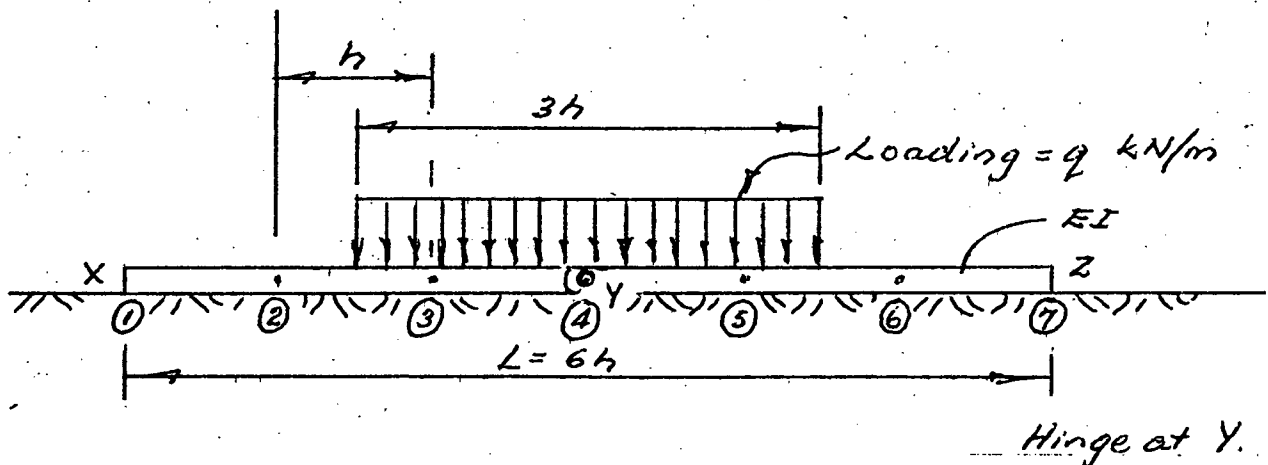


Figure 2

Question 3.

In this question, use the notation and sign conventions used by W.D. Means (i.e. in his book 'Stress and Strain', Springer 1976, p 130 - 180).

- a) A geological deposit is homogeneously deformed from the undeformed shape shown in Figure 3a(i) to the deformed shape shown in the section in Figure 3a(ii)

Fig 3a(i)
Undeformed
Shape

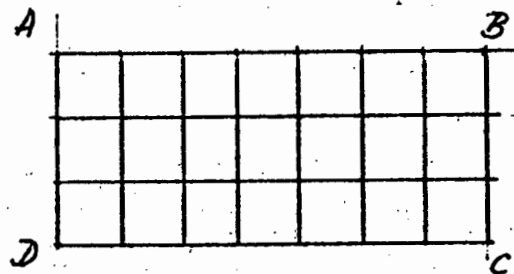
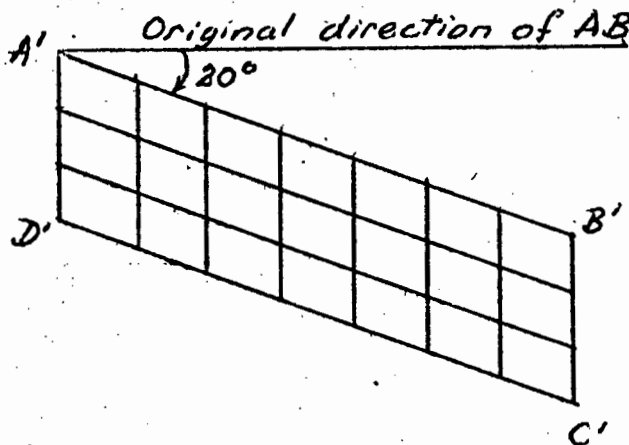


Fig 3a(ii)
Deformed
Shape.



The original length of line AB (which was originally horizontal) has increased by 20 percent to the length A'B'. The original length AD has decreased by 15 percent to its new length A'D'. A'D' and AD are both vertical.

Calculate for each set (i.e. AB, AD) of the original grid lines:

- i) The elongation ϵ
- ii) The stretch S
- iii) The quadratic elongation λ
- iv) The natural strain $\bar{\epsilon}$
- v) The angular shear ψ
- vi) The shear strain γ

- 3 b) On page 146 of his book, W.D. Means states:

Simple shear "is a deformation involving a non-zero strain component and a non-zero rotational component. It consists of a biaxial strain plus a rotation of the λ_1 and λ_3 axes about the λ_2 axis of unchanged length, such that one of the circular sections has the same orientation before and after deformation".

With the aid of sketches explain the above statement, and in particular describe what is meant by 'non-zero strain component', 'non-zero rotational component', ' λ_1 and λ_3 axes', and 'circular sections'.

- c) The Mohr Circle for Stress is a graphical representation of the following equations:

$$\sigma_n = \frac{1}{2}(\sigma_1 + \sigma_2) + \frac{1}{2}(\sigma_1 - \sigma_2) \cos 2\theta \quad (1)$$

and

$$\sigma_t = \frac{1}{2}(\sigma_1 - \sigma_2) \sin 2\theta \quad (2)$$

Whereas the Mohr Circle for Infinitesimal Strain is based on the following equations:

$$\epsilon = \frac{1}{2}(\epsilon_1 + \epsilon_2) + \frac{1}{2}(\epsilon_1 - \epsilon_2) \cos 2\theta \quad (3)$$

and

$$\frac{\gamma}{2} = \frac{1}{2}(\epsilon_1 - \epsilon_2) \sin 2\theta \quad (4)$$

However the Mohr Circle for Finite Strain is a graphical analogy of the following equations:

$$\lambda' = \frac{1}{2}(\lambda'_1 + \lambda'_2) + \frac{1}{2}(\lambda'_1 - \lambda'_2) \cos 2\theta' \quad (5)$$

and

$$\gamma' = -\frac{1}{2}(\lambda'_1 - \lambda'_2) \sin 2\theta' \quad (6)$$

With the aid of sketches and formulae, briefly, define the symbols used in the equations (3), (4), (5) and (6) above.

- 3 d) Figure 3d(i) shows portion of an undeformed section of a cylindrical gravel pile surrounded laterally by a soft compressible soil. This portion of the pile eventually shortens under vertical applied loading, and its diameter is increased as shown in Figure 3d(ii).

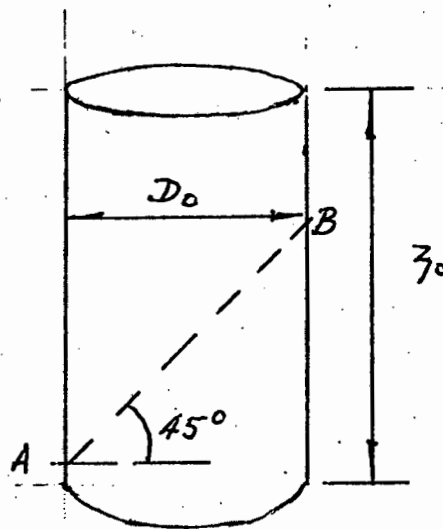


Fig 3 d(i)
Undeformed Portion
of Gravel Pile

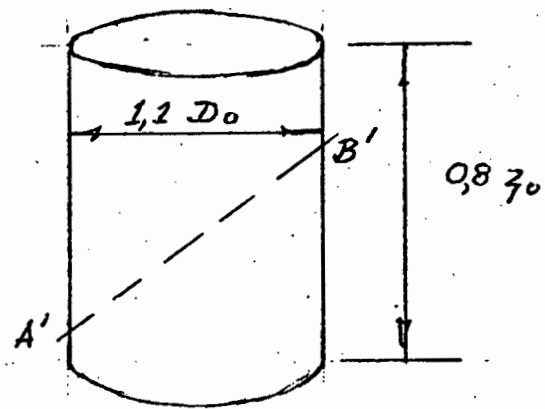


Fig 3 d(ii)
Deformed Portion
of Gravel Pile

- (i) Has the gravel material in the pile shown compressive or dilatant behaviour during the above deformation process ?
- (ii) Construct a Mohr Circle for Finite Strain for the above problem. Hence determine the elongation ϵ and the shear strain γ which has occurred along the line AB which was originally at 45° to the horizontal. For the line AB, this shear strain γ corresponds to an angular shear ψ . Draw a sketch to show the meaning of ψ in this case (for the line AB or A'B').

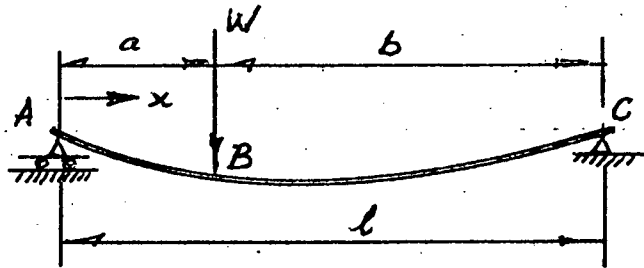
(20 marks, 40 minutes)

Question 4.

A continuous uniform elastic beam DE is supported by the footings A, B and C as shown in Figure 4(a). Two equal static vertical loads W_1 and W_2 are applied to the beam DE at the points F and G.

It is known that the settlement of the footings are nonlinear functions of the loads applied to the footings. Typical load settlement curves for the footings are shown in Figure 4(a).

- a) Estimate the final settlements (cm) of the footings A, B and C. An iterative, or other method may be used. For your guidance, the following deflection formulae may be useful:

Deflections

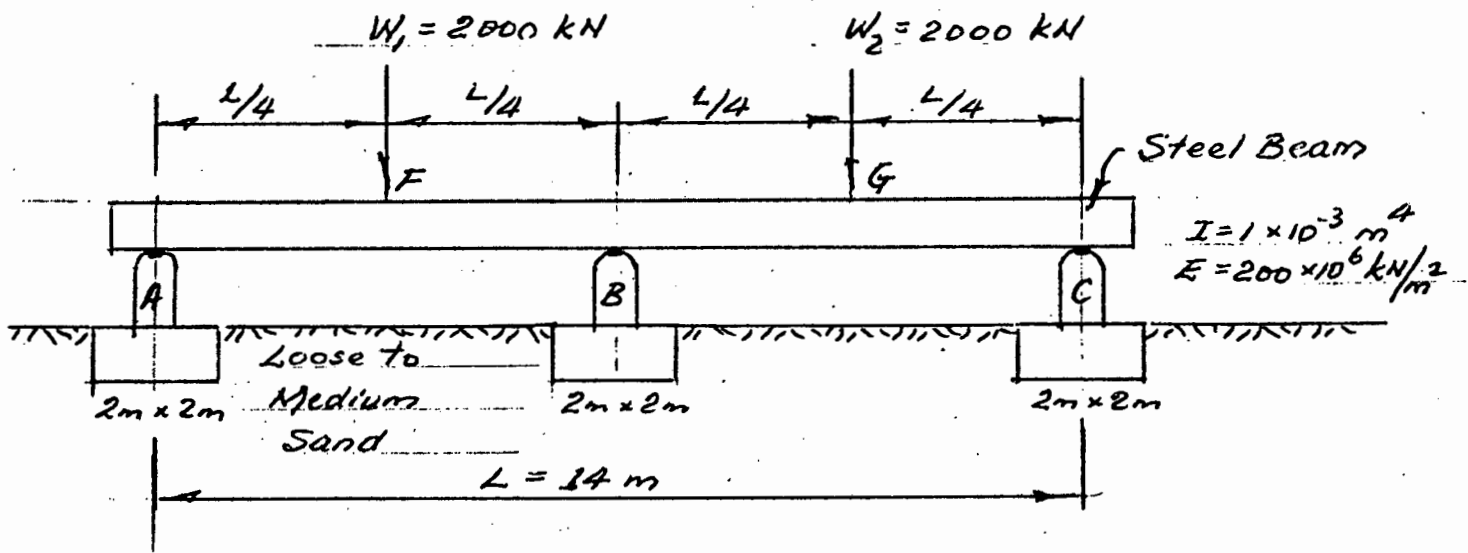
$$(A \text{ to } B); \quad y = -\frac{Wbx}{6EI\ell} \left[2\ell(\ell - x) - b^2 - (\ell - x)^2 \right]$$

$$(B \text{ to } C); \quad y = -\frac{Wa(\ell - x)}{6EI\ell} \left[2\ell b - b^2 - (\ell - x)^2 \right]$$

(15 marks, 30 minutes)

- b) Hence draw a flow chart for a suggested method of deflection analysis for problems of the type shown in Figure 4(a) for the general case in which the static loads, W_1 and W_2 might not be equal, and might be at other positions on the beam.

(10 marks, 20 minutes)



For footings A, B and C :-

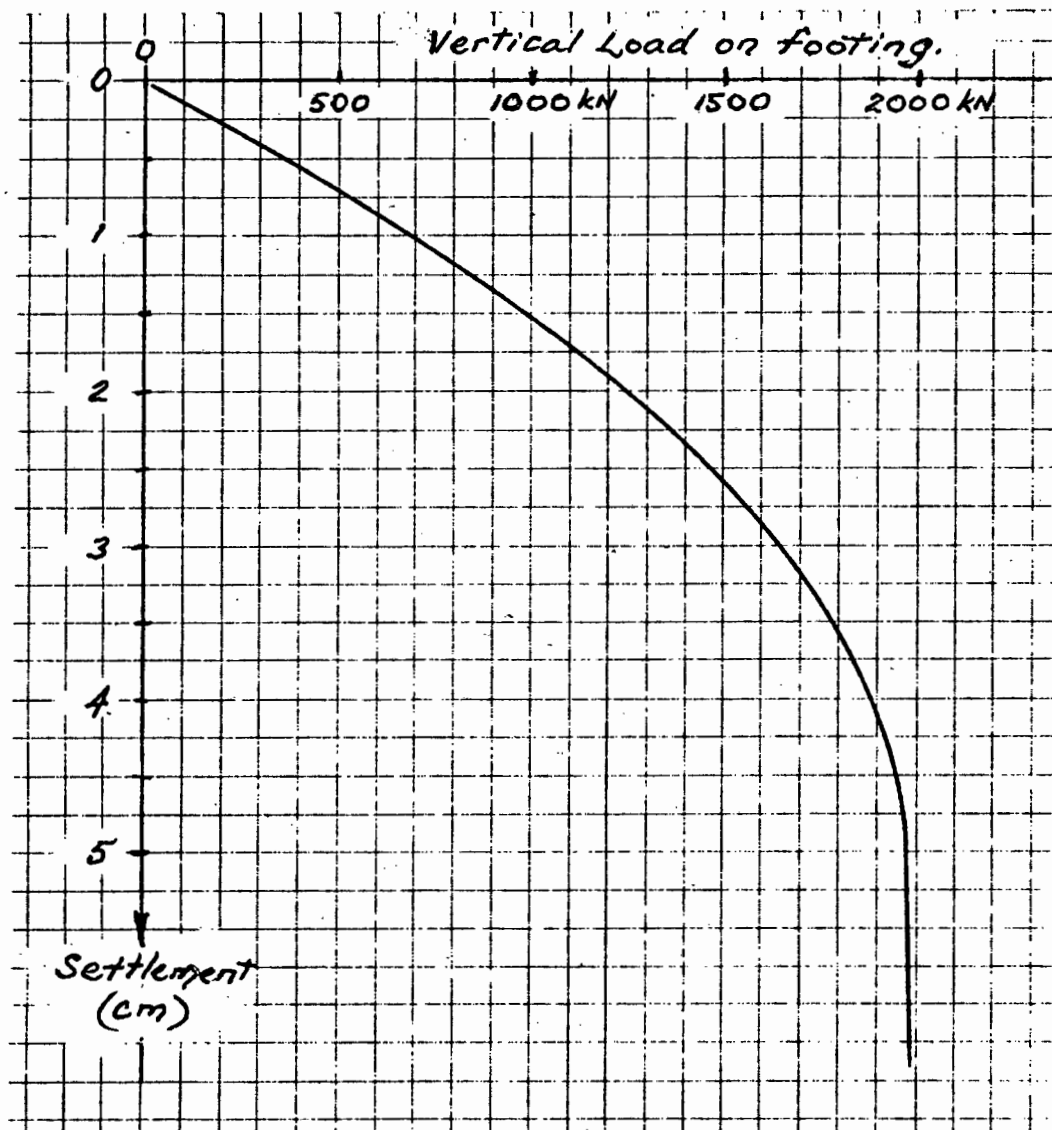


Figure 4(a)

QUESTION 5

p 10.

Two vertical column loads $V_A = 600 \text{ kN}$ and $V_B = 900 \text{ kN}$ are to be carried by a strap footing (i.e. a cantilever or pumphandle footing).

The plan sections of the column are each $0,5 \text{ m} \times 0,5 \text{ m}$. Unfortunately the property boundary line must coincide with the outer surface of the column A, and all footings must be constructed within the property. (See Figure 5).

The allowable soil pressure is 100 kN/m^3 for both footings. The strap beam must not bear on the soil surface.

- Determine suitable plan dimensions for the two footings.
- Plot the shear force and bending moment diagrams for the region between the centres of the two columns (i.e. in the strap beam.).

(15 marks , 30 minutes)

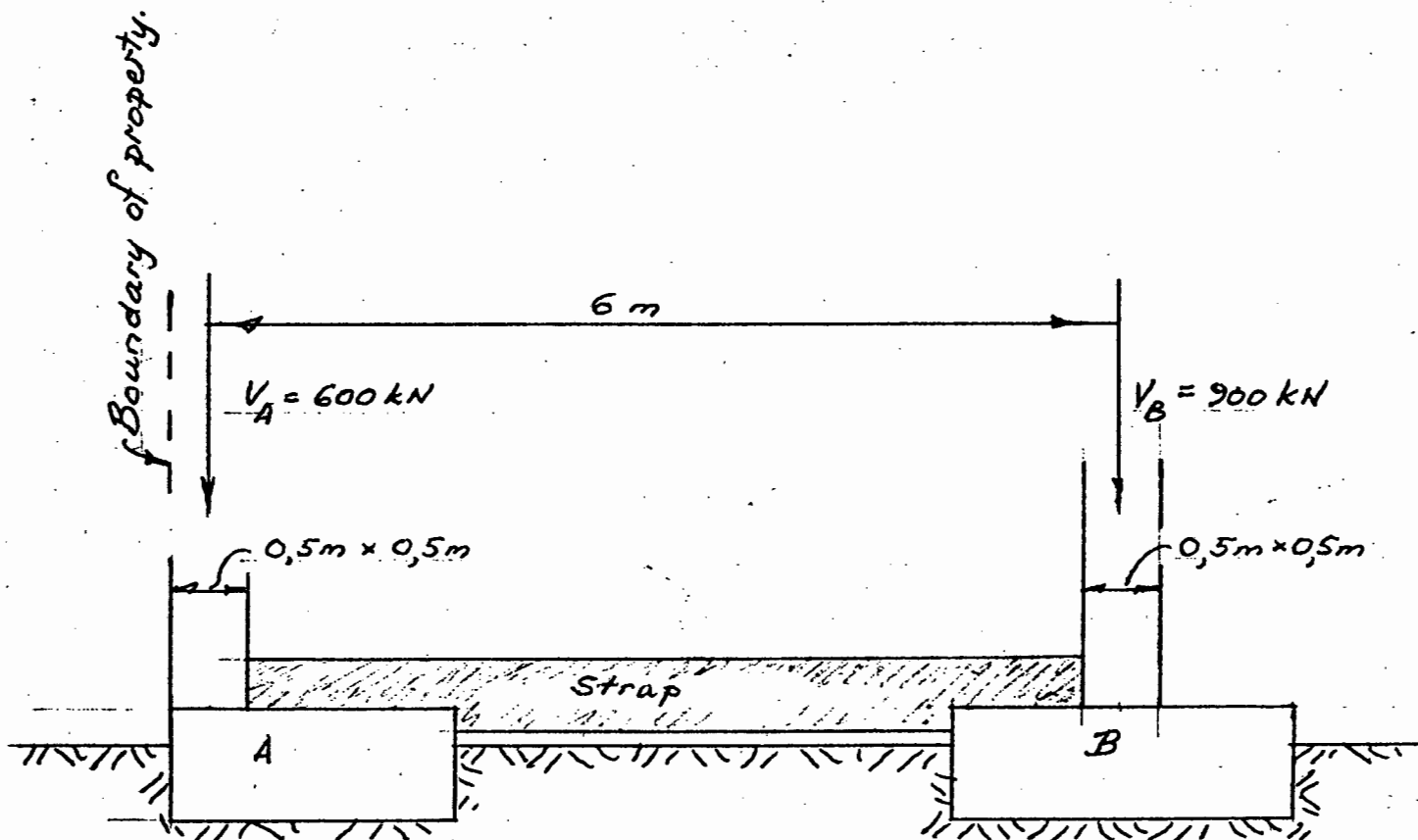
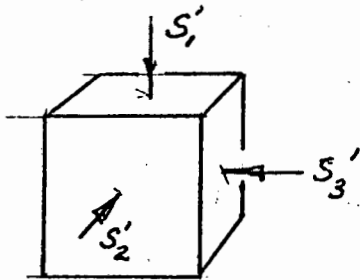


FIGURE 5 . The soil may be assumed to be very compressible when compared with the rigidity of the foundation structure.

QUESTION 6

- a) In your own words, and with the aid of sketches briefly explain (in two pages) the concept of 'unordered principal stress space' and in particular introduce the concept of 'failure surfaces i.e. failure envelopes' by discussing the results of different types of tests.
- b) A cohesionless granular material has a maximum failure value of internal friction angle of $\phi' = 39^\circ$



An element of this material is subjected to the principal effective stresses S'_1 , S'_2 and S'_3 .

It is known that

$$S'_2 = 200 \text{ kN/m}^2 \text{ (compressive)}$$

$$S'_3 = 100 \text{ kN/m}^2 \text{ (compressive)}$$

Find all the compressive or tensile values of S'_1 which are required to cause shear failure in the above element using :

- i) the Mohr-Coulomb theory
- ii) the Extended Tresca theory
- iii) the Extended von Mises theory

- c) In his lecture at the Roscoe Memorial Symposium, Prof. Bishop seems to have reservations about the validity of the strict definition of critical state as used by the Cambridge workers.

Briefly state the reasons for, and the nature of, Bishop's reservations. (Quote page numbers and sources where necessary).

- d) In Figure 1.4(a) on page 10 of the above paper by Bishop it is often desirable to measure distances from the central point O' .

Prove that the displacement from O' to any point X on Figure 1.4(a) is

$$\frac{1}{\sqrt{3}} [(S_1 - S_2)^2 + (S_2 - S_3)^2 + (S_3 - S_1)^2]^{1/2} \quad \text{where } (S_1, S_2, S_3) \text{ are the principal stress co-ordinates of the stress point X.}$$

(30 marks, 60 minutes)

QUESTION 7

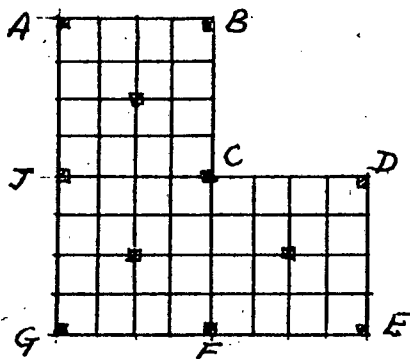
In Geotechnique (September 1977), Dr V.F.B de Mello presented a paper entitled 'Reflections on design decisions of practical significance to embankment dams'.

Using your own words, list the most significant aspects and findings in his paper (quote page numbers and Figure numbers where necessary).

(20 marks, 40 minutes)

QUESTION 8

Briefly (2 to 3 pages) describe how finite difference equations may be used to find the deflected shape and the bending moments, shear forces, and twisting moments in a raft foundation which has the following plan view :



Raft foundation carries applied column loads at positions shown.

PLAN VIEW

If possible provide your answer in flow chart form, or list the various steps. Provide the necessary formulae, and quote your references.

(20 marks, 40 minutes)

UNIVERSITY OF CAPE TOWN

DEPARTMENT OF CIVIL ENGINEERING

M.Sc. IN CIVIL ENGINEERING

UNIVERSITY EXAMINATION : JULY 1977

CE 525 : Coastal Hydraulics

All Questions may be attempted

Time : 3 hours

Constants

Sea water density = 1025 kg/m^3

Sea water weight = 10 kN/m^3

1. A beach site has an average underwater slope of 1 in 50, and the beach material is a coarse quartz sand of relative density 2,65 and average size 1,35 mm, the shoreline being essentially straight.

Two conditions of wave attack are being considered :-

(A) swell of 10 second period with a deep water wave height of 1,6 m approaching the beach with wave crests parallel to the shore line.

(B) as in (A) above, but with a deep water wave incidence of 35° , (angle between wave crest and contour)

For case (A) make the following calculations :-

- (a) the wave length and wave celerity in deep water.
- (b) the water depth at which the wave begins to be affected by the presence of the sea bed.
- (c) the wavelength, celerity and height for water depths at 10 m intervals between $d=80 \text{ m}$ and $d=10 \text{ m}$, and at 1 m intervals between $d=10 \text{ m}$ and $d=1 \text{ m}$.
- (d) the water depth in which the wave breaks, the breaker type, and the wave height at breaking. Ignore the effect of wave set up or down.
- (e) the deep water energy flow.
- (f) the wave height and energy flow in a water depth of 1 m.
- (g) the water depth in which the sand is on the point of moving.
- (h) the water depth in the which the sand is in motion but has no net drift.

For case (B) make the following calculations :-

- (i) the water depths in which the angle of incidence becomes 30° , 20° , 10° and 5° , and the wave heights at these depths.
 - (j) the water depth and wave height under breaking conditions. (assume the depth at breaking is 80 per cent of the value obtained for parallel waves)
 - (k) the thrust on the mass of water in the surf zone, per metre length along the shore.(N)
 - (l) an estimate of the bulk sand volume flow rate in m^3/s in the alongshore direction.
2. A cylindrical pipe is laid on the sea bed across a harbour entrance in 10 m of water, the pipe diameter being 0,3 m, and the axis of the pipe is parallel to the local wave crests. If the local wave length is 50 m, estimate the wave period, and find the peak magnitudes of the velocity and acceleration force components per metre length of pipe. Estimate the peak resultant force in the inshore direction, and the timing of this in relation to the passage of the wave crest. The wave height is 2 m, take $C_D = 1,2$ and $C_M = 2,16$
3. (a) A steady wind of speed 15 m/s blows over a fetch for a period of 8 hours, producing a significant wave height of 1,8 m at the downwind end of the fetch. Estimate the fetch length in km and the wave period. Check whether the wind duration is sufficient for this condition to be stable and also check whether this is the fully arisen sea for this wind speed.
- (b) In a zero damage design calculation for the armour protection of a rubble mound breakwater, 3 tonne and 5 tonne dolosse are specified for the trunk and head respectively, the slope of the breakwater face being $\cot \theta = 2$. Estimate the block masses and block heights if tetrapods had been used in the same design. If the design wave height was 3 m, and a storm causes damage of the order 20-30 per cent to the tetrapod scheme, estimate the storm wave height. (concrete density = 2245 kg/m^3)
- (c) An incoming swell has crests parallel to a straight beach with a deep water wave height of 2 m. Estimate the horizontal force (per metre along the beach) acting on the beach inside the refraction zone, due to the dynamic action of the waves.
- (d) In an area where the sea bed is horizontal, and the water depth is 3 m, a wave has a period of 7 s, a wavelength of 38 m, and a wave height of 1,5 m. Estimate the drift velocity at bed level, and indicate the direction. Compare this velocity with the maximum orbital velocity at the same level, and indicate the influence on bed drift of a strong onshore wind.
- (e) A storm at sea generates waves with a period range of 8 to 16 seconds. The resulting swell travels towards a harbour 500 km away. Estimate the time interval between the arrival of the shortest and longest waves, assuming deep water throughout.

UNIVERSITY OF CAPE TOWN
DEPARTMENT OF CIVIL ENGINEERING
UNIVERSITY EXAMINATION JUNE 1978

CE 534 GEOTECHNICAL SITE INVESTIGATION

Time allowed : 3 hours

There is a potential of 199 marks
180 marks will be regarded as 100%

Section 1 is to be handed in at the
end of 1½ hours. After this time the
examination will be OPEN BOOK.

PART A : CLOSED BOOK

1. Answer all questions on the attached sheets, in the space provided. If additional space is required the answer is to be completed in an Examination Answer Book where the answer must be clearly numbered.

[106]

PART B : OPEN BOOK

2. Your firm has been commissioned by the Cape Provincial Administration to submit a memorandum detailing and justifying the geotechnical site investigations and specific geotechnical tests that should be undertaken preparatory to the design and construction of a large new hospital to be sited some 5 km north of Muizenberg.

The proposed structures include an eight-storey hospital block covering a ground area of 20 000 m² (for which two underground basement levels are to be provided), a 30 m water tower, parking areas, nurses and doctors quarters and two playing fields.

At the existing site poorly vegetated sand dune remnants can be seen. Although the land is not directly affected by flooding from any river, pools of water are observed to lie over many portions of the site throughout the winter.

Tabulate (Use both sides of the Examination Answer Book pages to use the full width).

- (a) The investigations and tests you propose. (Specify the number of tests and proposed depth, where appropriate).
- (b) A brief description of what the work entails

...../2(c)

2. (c) The purpose of investigation or test.
- (d) The implications of not having the correct information.
- (e) The approximate cost of each investigation or test (State times and assumed rates where appropriate).

e.g. Civil Engineer 10 hrs @ R 15-00 per hr R 150-00
Technician 20 hrs @ R 10-00 per hr R 200-00
Labourers 40 hrs @ R 2-00 per hr R 80-00
Drilling rig
(including operators) 40 hrs @ R 20-00 per hr R 800-00

Note: Some tests can be quoted on time taken or depth - either will be acceptable.

In the absence of known rates reasonable assumptions must be made and stated.

[40]

3. (a) Show by means of annotated sketches 3 situations in which the determination of the shear strength of the soil mass is essential for adequate design. In each case show the assumed failure surface. (3)
- (b) Give 3 field methods that can be used to determine quantitative values for in-situ shear strength (3)
- (c) Briefly explain the physical basis of each of the three tests described above in (b) and how the results are interpreted. (6)
- (d) Explain what is meant by "effective stress" as applied to partially saturated soils. Give a Mohr circle representation of your explanation. (4)

[16]

4. (a) A stereo-pair of black and white photographs is available for for an area composed of two different soil types (the one being TMS (Table Mountain Series) and the other being Cretaceous (as found in the Swartkops River Valley near Port Elizabeth).

What clues would you look for in the photographs to delineate the soil boundaries. Where possible be specific.

(10)

- (b) Tabulate the steps you would take in the preparation of an engineering soils map of a remote area of the northern Cape. Assume that the map you will produce will be used in road route selection.

(10)

[20]

5. (a) Explain what is meant by a spectral signature and hence explain how multispectral scan data may be used in the preparation of maps delineating specific soil and vegetation types.

(10)

- (b) Explain why thermal imaging of ground scenes at ambient temperatures is generally done in the 8 to 14 μm range, whereas fire detection is done at the shorter wavelengths of 3 to 5 μm .

(2)

- (c) Explain briefly what the following terms mean :

pixel
density slicing
spatial rectification of imagery

(3)

- (d) What portion of the electromagnetic spectrum is specifically useful for imaging the vigour of vegetation?

(1)

What natural phenomenon makes this possible.

(1)

[17]

UNIVERSITY OF CAPE TOWN

DEPARTMENT OF CIVIL ENGINEERING

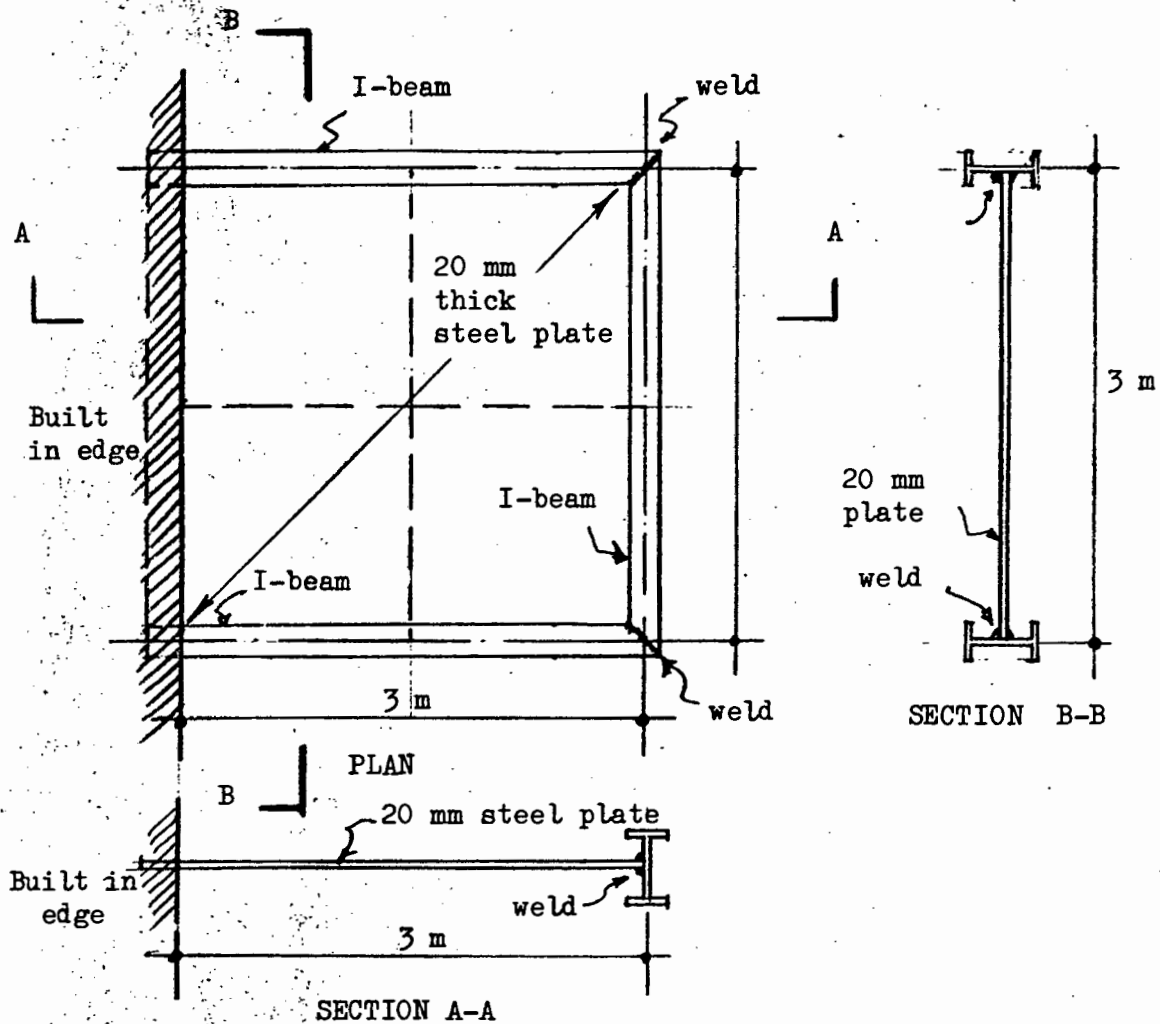
UNIVERSITY EXAMINATION - 21st AUGUST, 1976

COURSE CE 515: SURFACE STRUCTURES

Time allowed: 3 hours

Answer both questions

1.



A 20 mm thick plate is welded to a rigid framework on three sides and the plate and beams are built into a substantial concrete wall on the other side as shown.

The properties of the steel beams and the plate are given below.

The plate is subjected to a uniformly distributed load of 10 kN/m^2 .

Show all the steps necessary to analyse this structure for displacements and bending moments.

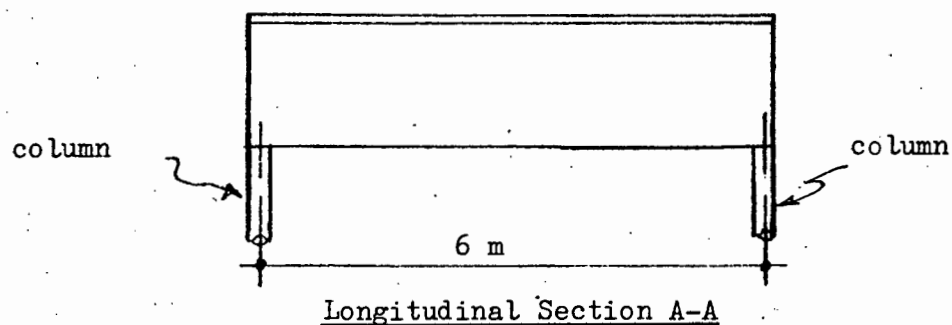
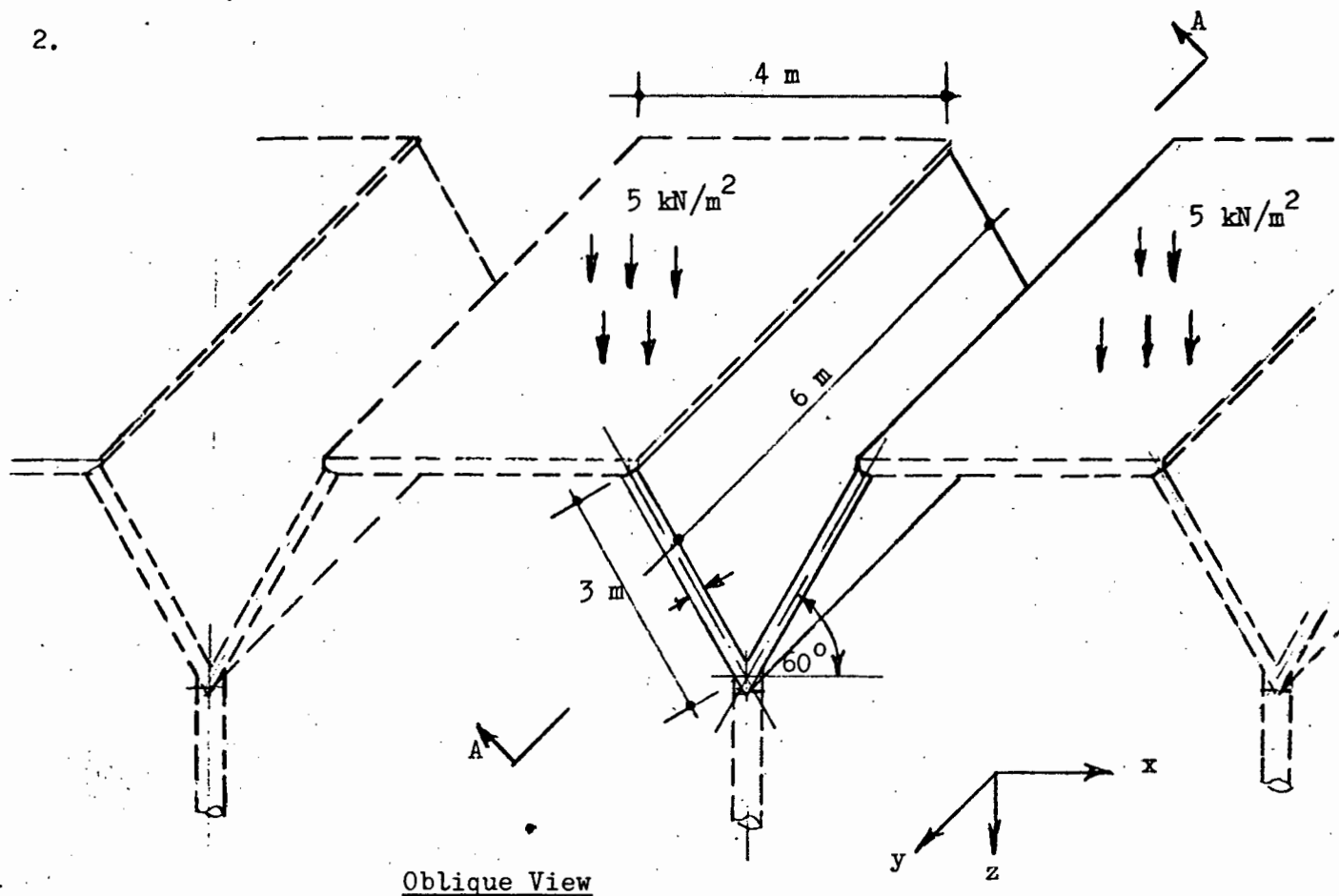
(Hint: Demonstrate the method with a coarse grid as shown).

Section Properties:

Beams: $E = 200 \text{ GPa}$ $I = 1,7 \times 10^{-3} \text{ m}^4$
 $G = 80 \text{ GPa}$ $J = 0,05 \times 10^{-3} \text{ m}^4$
 $A = 22 \times 10^{-3} \text{ m}^2$

Plate: $E = 200 \text{ GPa}$
 $\nu = 0,3$
 $h = 20 \text{ mm}$

2.



Show what steps are required to determine the displacements, stresses and bending moments in the V-shaped portion only of the roof structure shown.

The horizontal slabs are subjected to a uniformly distributed load of 5 kN/m^2 .

Note: (1) There is no moment connection between the horizontal slabs and the V-shaped sections.

(2) All slabs are 100 mm thick.

$$[H] = \frac{E}{ab(1-\nu^2)} \begin{bmatrix} -b & -va & 0 & va & b & 0 & 0 & 0 \\ -vb & -a & 0 & a & vb & 0 & 0 & 0 \\ (-ca-db)(-cb-da)(ca+db) & (-cb+da)(-ca+db)(cb+da) & (ca-db) & (cb-da) & 0 & -va & -b & va \\ 0 & -va & -b & va & 0 & 0 & b & 0 \\ 0 & -a & -vb & a & 0 & 0 & vb & 0 \\ (-ca+db)(-cb-da)(ca-db) & (-cb+da)(-ca-db)(cb+da) & (ca+db) & (cb-da) & -b & 0 & 0 & 0 \\ -vb & 0 & 0 & 0 & b & -va & 0 & va \\ -vb & 0 & 0 & 0 & vb & -a & 0 & a \\ (-ca-db)(-cb+da)(ca+db) & (-cb-da)(-ca+db)(cb-da) & (ca-db) & (cb+da) & 0 & 0 & -b & 0 \\ 0 & 0 & -b & 0 & 0 & -va & b & va \\ 0 & 0 & -vb & 0 & 0 & -a & vb & a \\ (-ca+db)(-cb+da)(ca-db) & (-cb-da)(-ca-db)(cb-da) & (ca+db) & (cb+da) & 0 & 0 & -vb & 0 \end{bmatrix}$$

Where $c = \frac{1-\nu}{4}$ and $d = \frac{\nu}{2}$

Stress/Displacement Matrix for Plane Stress Rectangular Elements

Finally the element stiffness matrix for in-plane forces becomes:-

(See over)

UNIVERSITY OF CAPE TOWN

DEPARTMENT OF CIVIL ENGINEERING

UNIVERSITY EXAMINATION: JUNE 1976

COURSE CE 506 - PROPERTIES OF CONCRETE

Time allowed: 3 hours

5th June, 1976

Part A consists of fifteen multiple-choice questions. Each question is followed by five suggested answers; select the one which is best in each case and circle one of (a), (b), (c), (d) or (e) for each question. This portion of the examination paper must NOT be removed from the Examination Room and must be handed in for marking.

Part B consists of five questions. Answer all questions.

PART A - Multiple-Choice Section (All questions of equal value)

Question A1: In controlling the quality of concrete produced for a project, a test is needed which:

- (a) gives the true strength of the material;
- (b) gives, for variations in testing procedures, the least variation in results;
- (c) gives the true strength of the specimen;
- (d) gives a clearly defined stress pattern;
- (e) is easy to carry out.

Question A2: In design of concrete mixes according to CP 110 Concrete Structures Code, the target strength chosen is directly related to:

- (a) the design strength f_{cu} ;
- (b) the design strength f_{cu} plus 1,65 times the standard deviation ' σ '.
- (c) the design strength f_{cu} plus the standard deviation ' σ ';
- (d) the design strength f_{cu} plus the coefficient of variation ' v ';
- (e) the design strength f_{cu} plus 1,65 times the coefficient of variation ' v '.

Question A3: The most important aspect of sampling from a pre-mixed concrete truck is to:

- (a) protect the sample from wind and sun;
- (b) obtain a representative sample in order to carry out further tests;
- (c) ensure that the concrete is properly mixed;
- (d) check the workability and slump;
- (e) obtain a sufficient quantity of concrete to carry out further tests.

/Question A4:

- Question A4: For a water/cement ratio of 0,6 by weight the use of rounded river gravel in place of crushed aggregate of cubic shape and rough texture will:
- (a) show little difference in compressive strength but increase flexural strength;
 - (b) increase compressive strength by about 10% and also increase flexural strength;
 - (c) decrease compressive strength by about 10% but increase flexural strength;
 - (d) increase compressive strength slightly but lower flexural strength;
 - (e) decrease slightly, both compressive and flexural strengths.
- Question A5: The Unit Water Method of Mix Design, described in lectures, suggests that the grading of the combined aggregate be made finer than the recommended grading when:
- (a) the maximum aggregate size is larger;
 - (b) the maximum aggregate size is smaller;
 - (c) the coarse aggregate is crushed material;
 - (d) the cement content is higher;
 - (e) the cement content is lower.
- Question A6: An increase in the proportion of aggregate material in the sieve range 2,00 mm to 9,5 mm (No. 8 to 3/8") will tend to:
- (a) make the concrete harsh and liable to honeycomb;
 - (b) make the finishability of the concrete better;
 - (c) improve the economy of the mix;
 - (d) increase the amount of water required;
 - (e) reduce the amount of water required.
- Question A7: The addition of an air entraining agent to a concrete mix usually leads to:
- (a) a more economical mix;
 - (b) a stronger concrete;
 - (c) a decrease in the required sand percentage;
 - (d) a decrease in cement content;
 - (e) a denser concrete because of improved workability.

/Question A8:

- Question A8: In the Unit Water Method of Mix Design, described in lectures, the estimated water content for a particular slump is fixed by:
- (a) the maximum size of the aggregate;
 - (b) the grading of the aggregate;
 - (c) the shape of the aggregate;
 - (d) (a) and (b) above;
 - (e) (a) and (c) above.
- Question A9: Capillary water in hydrated cement paste is:
- (a) water held in areas of restricted adsorption of the gel structure;
 - (b) water occupying space beyond the range of surface forces of the solid phase of the gel structure.
 - (c) water existing in cavities and channels up to 100 times greater than the size of gel pores;
 - (d) both (b) and (c) above;
 - (e) water chemically combined such that it is part of the solid matter in the hardened paste.
- Question A10: Plastic shrinkage of concrete is caused by:
- (a) removal of capillary and gel pore water;
 - (b) the absorption of mixing water by porous or dry aggregates;
 - (c) sedimentation and settling of solids in the concrete mix;
 - (d) bleeding of free water to the top surface of the concrete where it is often lost by evaporation or drainage;
 - (e) all of (b), (c) and (d) above.
- Question A11: The secant elastic modulus of concrete is increased by:
- (a) increased water:cement ratio and increased paste content;
 - (b) constant water:cement ratio and increased paste content;
 - (c) increased water:cement ratio and decreased water content;
 - (d) constant water:cement ratio and air entrainment;
 - (e) decreased water:cement ratio and decreased paste content;
- Question A13: Decreasing the water/cement ratio influences the ultrasonic pulse velocity because:
- (a) poor compaction leads to voids;
 - (b) a decrease in the density causes the pulse velocity to increase;
 - (c) an increase in strength (due to a lowering of the water cement ratio) causes the pulse velocity to increase;
 - (d) an increase in the density causes the pulse velocity to increase;
 - (e) an excess of paste causes the pulse velocity to decrease.

/Question A14:

Question A14: Rapid Hardening Portland cement can be manufactured by:

- (a) more finely grinding the Portland cement;
- (b) changing the ratio of $C_2S:C_3S$;
- (c) intergrinding some high alumina cement with the Portland cement;
- (d) both (a) and (b) above;
- (e) all of (a), (b) and (c) above.

Question A15: Excessive bleeding of concrete can be corrected by:

- (a) adding more cement;
- (b) adding crusher dust or other fine material;
- (c) by air entrainment;
- (d) both of (a) and (b) above;
- (e) all of (a), (b) and (c) above

[Total 20 marks]

DEPARTMENT OF CIVIL ENGINEERING

UNIVERSITY OF CAPE TOWN

CE 535

ENGINEERING ECONOMY

FINAL EXAMINATION

1979

3 HOURS

OPEN BOOK

ANSWER ALL QUESTIONS

CALCULATORS MAY BE USED

- (1) You have two mutually exclusive investment opportunities, both of which have a life of 3 years with no salvage value. Both cost R120,000 and produce revenues as shown in Table 1. Bob, one of your analysts, has calculated the NPV at your cost of capital (10%) and selects B on the grounds of a higher NPV. Andy, another analyst, has selected A on the grounds of a higher IRR.

- (a) Are they correct?
- (b) If so, why do they differ?
- (c) What is your recommendation.

TABLE 1.1

	<u>INVESTMENT</u>	<u>INVESTMENT</u>
	<u>A</u>	<u>B</u>
Cost	120,000	120,000
Revenue Year 1	100,000	10,000
Year 2	50,000	60,000
Year 3	10,000	110,000

(12 MARKS)

- (2) Your Swazi client has negotiated a E6,000,000 interest free loan to construct a teaching complex and has appointed you to head the project management team. An architect has been appointed to design the facility and you are to provide him with a budget figure within which to work.

You expect the design phase to take 9 months, documentation and tendering 3 months and construction 12 months. The lending authority will make payment against your interim valuations as the work progresses, but will under no circumstances disburse more than the value of the loan.

- (a) Make and motivate all necessary assumptions.
- (b) Calculate the design budget figure on the basis that the architect's knowledge of costs is probably 3 months old.

(12 MARKS)

- (3) A major employer is proposing to introduce the escalation formula described in Appendix 1.

Critically examine:

- (a) The differences between the proposed formula and other existing formulae.
- (b) The proposed indices, their applicability and desirability.
- (c) The proposed coefficients.
- (d) The proposals potential for accuracy relative to other formulae.
- (e) The need and desirability for a major employer to develop his own formula.

(20 MARKS)

- (4) The life of an item of equipment may be described in any of the following ways:

- Ownership life.
- Physical life.
- Primary service life.
- Accounting life.
- Tax life.
- Economic life.
- Useful life.

Define each period with particular regard to the manner in which the period is assessed and/or the factors which serve to terminate the period.

(12 MARKS)

- (5) A proposal has been made that a new piece of equipment be purchased this year. Characteristics of the purchase plan are given in Table 5.1. Calculate the before tax IRR. (use $i = 12$ and 15). If the effective tax rate is 40% and if wear and tear allowances are granted on a straight line basis over 5 years, calculate the after tax IRR. (use $i = 7$ and 10).

TABLE 5.1

20,28
18,16.

P	=	R50,000
SV	=	0
n	=	5 years
Expected income	=	28,000 - 1,000k (k = 1, 2, 3, 4, 5)
Expected disbursements	=	9,500 + 500k

(12 MARKS)

- (6) One phase of a meat-packing operation requires the use of separate machines for the following functions: pressing, slicing, weighing, and wrapping. All machines under consideration are expected to have a life of six years with no salvage value. Their first cost and annual costs are given in Table 6.1.
- (a) If different machines can be selected from different manufacturers and if the company's Minimum Attractive Rate of Return is 20% , determine which separate machine should be selected for each function (identify them as Pressing 1, Pressing 2, Slicing 1, etc.)
- (b) For the machines selected in part (a), determine the total investment and operating cost for the entire operation.

Another alternative is one large machine to do the pressing and slicing and another large machine to do the weighing and wrapping. The machine that will do the pressing and slicing (identified as Pressing-Slicing 3) will cost R29,000 and will have an annual operating cost of R9,000. The machine that will do the weighing and wrapping (identified as Weighing-Wrapping 3) will cost R26,000 and will have an annual operating cost of R18,000.

- (c) Which machines should be selected for the entire operation?
- (d) Determine the total investment and operating cost for the entire operation.
- (e) If a single machine is to perform all four functions (identified as Machine 4) having an initial cost of R45,000 and an annual operation cost of R32,000 is available - which machine(s) should be selected?

TABLE 6.1

	<u>SUPPLIER 1</u>		<u>SUPPLIER 2</u>	
	<u>First cost</u>	<u>Annual cost</u>	<u>First cost</u>	<u>Annual cost</u>
Pressing	R5,000	R13,000	R10,000	R11,000
Slicing	4,000	10,000	17,000	4,000
Weighing	12,000	15,000	15,000	13,000
Wrapping	3,000	9,000	11,000	7,000

(20 MARKS)

- (7) The Cash Flow approach to capital consumption cost recognises an outflow (C) at the end of year 0 and an inflow (C_L) at the end of the assets life (A yrs). The annual capital consumption cost thus becomes $C \cdot (A/P \ i) - C_L \cdot (A/F \ i)$

Establish the relationship between this expression and expressions which provide for a sinking fund plus profit on initial capital or which provide for capital recovery plus interest on residual value.

(12 MARKS)

CONTRACT PRICE ADJUSTMENT SCHEDULEFOR USE WITHGENERAL CONDITIONS OF CONTRACT 1972 AS AMENDED (1978)

Note: further proposed amendments indicated by ruling in margin.

1. In accordance with Sub-clause 70(2) of the General Conditions of Contract, the value of each certificate issued in terms of Clause 62 of the General Conditions of Contract shall be increased or decreased by the amount obtained by multiplying "Ac", defined in Clause 2.0 hereof, by the Contract Price Adjustment Factor determined according to the formula:

$$(1 - x) \left\{ a \frac{Lt}{Lo} + b \frac{Pt}{Po} + c \frac{Mt}{Mo} + d \frac{Ft}{Fo} + e \frac{SMt}{SMo} - 1 \right\}$$

in which the symbols have the following meanings:

- 1.1 "x" shall be the proportion of the "Ac" which is not subject to adjustment. Unless otherwise stated in the Appendix to the Tender, this portion shall be 0,35.
- 1.2 "a", "b", "c", "d", and "e" shall be the co-efficients determined by the Engineer and stated in the Appendix to the Tender, which are deemed, irrespective of the actual constituents of the work, to represent the proportionate value of, respectively, labour, plant, materials other than special materials, fuels and lubricants, and special materials specified in terms of sub clause 70 (3) of the General Conditions of Contract in the appendix to the tender. The arithmetical sum of "a", "b", "c", "d" and "e" shall in all cases be unity.
- 1.3 "L" shall be the Labour Index and shall be the "Wage Rate Index - Civil Engineering (Weighted Average for all Provinces)" published by the Department of Statistics.
- 1.4 "P" shall be the Plant Index and shall be the weighted average of the Price Indices of "Construction Machinery (excluding trucks)" and of "Trucks", as published by the Department of Statistics. The weighting ratio shall be determined by the Engineer and stated in the Appendix to the Tender. Unless otherwise stated in the Appendix the Tender, the ratio shall be "Construction Machinery (excluding trucks)" to "Trucks" 2:1.
- 1.5 "M" shall be the Materials Index and shall be the "Wholesale Price Index of Materials used in Building and Construction", as published by the Department of Statistics.
- 1.6 "F" shall be the Fuel Index and shall be the "Wholesale Price Index of Selected Materials - Diesel Oil Witwatersrand", as published by the Department of Statistics.

- 1.7 "SM" shall be the sum of the costs of all the Special Materials used in the works calculated by multiplying the agreed rate or price of each material by the nett quality of material measured up to the date of price change or during the period to which the payment certificate relates.
- 1.8 The suffix "o" denotes the basic indices applicable to the base month, which shall be the month in which falls the closing date for the Tender.
- 1.9 The suffix "t" denotes the current indices applicable to the month in which the work was performed in accordance with the contract, as indicated in the relevant certificate.
- 1.10 If any index relevant to any particular certificate is not known at the time the certificate is valued, the value of such index shall be estimated.
2. For the purposes of calculating the adjustment to the value of the relevant certificates, the amount "Ac" shall be determined by the formula:

$$Ac = T - S - D - E - Ap$$

in which the symbols have the following meanings:

- 2.1 "T" shall be the total value of Preliminary and General Items, work done and materials on site as certified in the certificate under consideration before the deduction of any retention monies, penalties or repayment of advances and before any adjustments made in terms of this Schedule.
- 2.2 "S" shall be the aggregate of (i), (ii), (iii) and (iv) referred to below and included in "T":
- (i) the amounts actually expended and substituted for any P.C. amounts;
 - (ii) the value of any work done by nominated Sub-contractors;
 - (iii) the value of any work done against provisional sums;
 - (iv) the value of any extra or additional work

where special arrangements for price adjustments in respect of those amounts were made and recorded at the time the work was ordered.

- 2.3 "D" shall be the value of work included in "T" done at new rates fixed in terms of Sub-clause 52 (1) and (2) of the General Conditions of Contract, where those rates are not based on labour, plant or materials costs in force at the time of tendering. Such values arising from new rates shall be shown separately and escalated on the same formula as above, but with the new relevant base date, which shall be the date on which such new rates were tendered.

- 2.4 "E" shall be the amount paid for any work executed at cost plus percentage allowances as set out in Sub-clause 52(4) of the General Conditions of Contract.
- 2.5 "Ap" shall be the sum of "Ac" amounts determined in terms of 2.0 hereof for all certificates preceding in time the certificate under consideration.
3. The costs of special materials are to be determined thus:
 - 3.1 The base price or rate is to be listed by the tenderer in Annexure G.
 - 3.2 The term "cost to the contractor on site" shall mean the merchants selling price on a 30 day basis, less the normal trade discount, if any, allowed to the Building and Civil Engineering industries. The Contractor shall consult with the Employer prior to ordering materials listed in Annexure G and make every effort to secure such materials to the best advantage of the employer.
 - 3.3 Claims for cost increases to the base price shall be supported by invoices, quotations, etc., and certificates signed by the Contractor's auditor, all at the Contractor's expense.
4. Save only for additional work or variations ordered to be carried out after the due date for completion, the Contract Adjustment Factor to be applied to certificates relating to work done or materials supplied after the due date for completion, shall be half the factor calculated by inserting in the formula referred to in 1.0, the indices, Lt, Pt, Mt, Ft, and SMt applicable at the due date for completion.
5. Any claim resulting from the application of the above formula shall be calculated monthly and submitted monthly, but in any event the last claim shall be submitted not later than thirty days after the agreement of the final measurements.

ANNEXURE "G"

SPECIAL MATERIALS - "SM"

(REF. SUB-CLAUSE 70(3) OF THE CONDITIONS OF CONTRACT)

<p style="text-align: center;">Materials</p> <p>(Examples given below. Include only items representing the major materials content of the particular contract)</p>	<p><u>Cost price/unit (on site)</u> (Note: If necessary due to inadequate space, a price list of the detailed sizes, etc., for the respective items as reflected hereunder is to be submitted with tenders).</p>
<p>Cement Sand Stone Brick Mild Steel Reinforcement High Tensile Steel Reinforcement Mesh Reinforcement Q.C. Steel Centering Holding down bolts Bitumen road surfacing products Salt glazed pipes and fittings Concrete pipes Mild Steel pipes and fittings Fencing materials</p>	

DATE: _____

SIGNATURE OF TENDERER